Experimental Investigations on Superconducting Niobium Cavities at Highest Radiofrequency Fields

Dissertation

zur Erlangung des Doktorgrades
des Fachbereichs Physik
der Universität Hamburg

vorgelegt von

Lutz Lilje
aus Wittingen

Hamburg

2001

Gutachter der Dissertation	Prof. Dr. P. Schmüser Prof. Dr. J. Kötzler
Gutachter der Disputation	Prof. Dr. P. Schmüser Dr. Dieter Proch
Datum der Disputation	14. August 2001
Dekan des Fachbereichs Physik und Vorsitzender des Promotionsausschusses	Prof. Dr. F.-W. Büßer

Abstract

In order to increase the maximum accelerating gradient in superconducting niobium cavities, electrolytic polishing was applied to 1.3 GHz single cell and nine-cell cavities. A facility for the electropolishing was set up in collaboration with CERN.

Tests on single-cell cavities have shown that electropolishing increases the maximum accelerating gradient significantly as compared to the standard etching treatment. Preliminary results on high temperature heat treatments of electropolished cavities are shown. Electropolishing of nine-cell cavities was carried out in collaboration with KEK. One nine-cell cavity improved the accelerating gradient from 22 MV/m after standard etch to 32 MV/m after electropolishing.

A low temperature 'in-situ' bakeout at 120°C for 48 hours was found to be necessary to reduce the degradation of the quality factor at accelerating fields above 25 MV/m. The detailed nature of this process is yet to be understood. Some models were investigated to describe this behaviour.

Zusammenfassung

Im Rahmen dieser Arbeit wurde das Verfahren der Elektropolitur auf ein- und neunzellige 1,3 Ghz Niobresonatoren angewandt, um die maximal erreichbare Beschleunigungsfeldstärke zu erhöhen. Ein Aufbau zur Elektropolitur von einzelligen Resonatoren wurde in Zusammenarbeit mit dem CERN in Betrieb genommen.

Messungen von einzelligen Resonatoren haben gezeigt, daß der Beschleunigungsgradient in elektropolierten Resonatoren deutlich über dem mit der Standardbehandlung gebeizten Resonatoren liegt. Vorläufige Ergebnisse zur Hochtemperaturbehandlung von elektropolierten Resonatoren werden gezeigt. Neunzellige TESLA-Resonatoren wurden in Zusammenarbeit mit dem KEK elektropoliert. Ein neunzelliger Resonator verbesserte sich von einem Beschleunigungsgradienten von 22 MV/m nach der Standardbeizung auf 32 MV/m nach der Elektropolitur.

Es hat sich gezeigt, daß ein Niedertemperaturheizverfahren bei 120°C für 48 Stunden notwendig ist, um den Abfall der unbelasteten Güte bei Beschleunigungsgradienten von mehr als 25 MV/m zu verhindern. Dieser Prozess ist bisher noch nicht verstanden. Verschiedene Modelle werden betrachtet, um dieses Verhalten zu erklären.

Contents

Introduction

Superconducting radiofrequency resonators for particle acceleration have become a standard component for particle accelerators. Particle bunches with high currents are accelerated with high efficiency as the power dissipated in the cavity walls is very low. The available radiofrequency power is nearly completely converted to particle energy. This high efficiency of superconducting accelerating cavities is used in continuous particle beam accelerators as CEBAF as well as in high current applications as in CESR.

The high quality factor and the small dissipation in the wall allow for cavities with large volume as accelerating structures and low frequencies as compared to high gradient normalconducting copper structures. The optimum accelerating gradient for a continuous wave operation for superconducting cavities is between 10 - 15 MV/m. For gradients of more than 20 MV/m it is necessary to go to a pulsed operation to reduce the cryogenic losses which scale with the square of the accelerating gradient. Still, long pulses of about a millisecond with low radiofrequency peak power are possible. This has to be compared with very short pulses in the order of microseconds for copper accelerating structures. The effect of wakefields which can influence the beam quality is also reduced by the large apertures of low frequency cavities. The alignment tolerances for superconducting structures are more relaxed than for the higher frequency normalconducting cavities. A low beam emittance can be preserved in a linac. This makes a superconducting linac the ideal driver for a free electron laser.

The TESLA[1]-Collaboration aims for the realization of a linear collider in the TeV energy range. In this project particle beams of electrons and positrons are accelerated with superconducting cavities made from niobium to energies of 250 GeV and brought to head-on collision. An X-ray free electron laser is integrated in the design of the accelerator. A pulsed high frequency field at 1.3 GHz is used for particle acceleration. By now, such cavities routinely achieve gradients of 25 MV/m which is the gradient to safely drive the beam in TESLA to the desired 0.5 TeV center-of-mass energy.

[1]TESLA stands for "TeV Energy Superconducting Linear Accelerator". Details in [Brinkmann et al. 1997] and [Brinkmann et al. 2001].

In an energy upgrade scenario for TESLA even higher gradients of 35 MV/m with an Q_0 of 5×10^9 are aimed for. For high electromagnetic cavity surface fields the condition and the preparation of the surface is of utmost importance. In the last years it became obvious that the standard chemical etching is not a suitable method for achieving gradients above 30 MV/m in cavities with a large inner surface. Electrolytic polishing of the niobium surface solves this problem by producing very glossy and nearly defect-free surfaces in niobium cavities.

For high surface electromagnetic fields the smooth surface is not the only prerequisite. In fact, it has been known for a long time that the chemical surface composition of a niobium surface influences the superconducting properties. The (electro-)chemical preparation of a cavity with subsequent water rinsing inevitably leads to an oxidation of the surface. The exact composition of the oxide layer is not well-understood, but for many years oxides have been alleged to cause a degradation in cavity performance. The surface preparation can also lead to a diffusion of hydrogen into the niobium lattice, which has negative influences on the superconducting properties as well. Finally, any contamination with particles of the cavities surface could lead to field emission.

This thesis is divided in divided in six chapters. In the first chapter a brief introduction into properties of superconducting cavities is given. The results of the state-of-the-art preparation methods as used at the TESLA Test Facility (TTF) at DESY are presented. In the second chapter the process of electropolishing and a setup for the electropolishing are described.

In the third chapter the results achieved on electropolished cavities are compared with the accelerating gradients obtained on chemically etched cavities. First results on electropolished multi-cell cavities are shown. Chapter 4 describes the effect of a low temperature heat treatment at 100°C which is called 'in-situ bakeout'. The effect on the superconducting properties of niobium is described and measurements on the niobium surface chemical composition are discussed.

In chapter 5 some models describing the behaviour of niobium at high electromagnetic surface fields are presented and compared with the measurements performed within the scope of this thesis. Chapter 6 concludes with a summary and an outlook to further studies.

Chapter 1

Basics of superconducting radiofrequency cavities

1.1 Introduction

In this chapter the basic properties of radiofrequency cavities are reviewed.[1] The surface resistance and its dependence on temperature and surface magnetic and electric field will be introduced. Then the methods used within the TESLA collaboration to maximize the accelerating gradients and the results achieved to date are presented.

1.2 Accelerating cavities - Figures of merit

Accelerating cavities are used to increase the energy of a charged particle beam[2]. Obviously, the energy gain per unit length is therefore an important parameter of accelerating cavities. This is conveniently derived from the accelerating voltage a particle with charge e experiences while traversing the cavity:

$$V_{acc} = \left| \frac{1}{e} \times \text{energy gain during transit} \right| \tag{1.1}$$

For particles travelling with the velocity of light c on the symmetry axis in z-direction ($\rho = 0$) and a accelerating mode with eigenfrequency ω this gives:

$$V_{acc} = \left| \int_0^d E_z(z)\, e^{i\omega z/c}\, \mathrm{d}z \right| \tag{1.2}$$

[1] A good introduction into superconducting cavities is given in [Padamsee et al. 1998].

[2] There are a few applications where resonant cavities are used to decelerate particle beams.

The accelerating field is

$$E_{acc} = \frac{V_{acc}}{d} \tag{1.3}$$

To sustain the radiofrequency fields in the cavity, an alternating current is flowing in the cavity walls. This current dissipates power in the wall as it experiences a surface resistance[3]. One can look at the power P_{diss} which is dissipated in the cavity to define the global surface resistance R_{surf}:

$$P_{diss} = \frac{1}{2}\oint_A R_{surf} H_{surf}^2 \mathrm{d}A \tag{1.4}$$

$$= \frac{1}{2} R_{surf} \oint_A H_{surf}^2 \mathrm{d}A \tag{1.5}$$

Here H_{surf} denotes the magnetic field amplitude. Usually, one measures the quality factor[4] Q_0:

$$Q_0 = \frac{\omega W}{P_{diss}}, \tag{1.6}$$

where

$$W = \frac{1}{2}\mu_0 \int_V H^2 \mathrm{d}V \tag{1.7}$$

is the energy stored in the electromagnetic field in the cavity. R_{surf} is an integral surface resistance for the cavity. The surface resistance and the quality factor are related via the geometrical constant G which depends only on the geometry of a cavity and field distribution of the excited mode, but not on the resistivity of the material:

$$G = \frac{\omega\mu_0 \int_V H^2 \mathrm{d}V}{\oint_A H^2 \mathrm{d}A} \tag{1.8}$$

This gives

$$Q_0 = \frac{\omega\mu_0 \oint_V H^2 \mathrm{d}V}{R_{surf} \oint_A H^2 \mathrm{d}A} = \frac{G}{R_{surf}} \tag{1.9}$$

For the typical elliptical shape of superconducting cavities $G = 270\ \Omega$. For a nine-cell TESLA cavity the quality factor is typically $Q_0 = 1.2 \cdot 10^{10}$ at $T = 2$ K corresponding to a surface resistance of $R_{surf} = 10\ \mathrm{n}\Omega$.

One can see that the efficiency with which a particle beam can be accelerated in an radiofrequency cavity depends on the surface resistance. The smaller the resistance i.e. the lower the power dissipated in the walls, the

[3] This also the case for a superconductor where alternating fields give rise to the surface resistance for temperatures $T > 0$ K. More details can be found in section 1.3.4.1.

[4] The quality factor can also be defined as $Q_0 = f/\Delta f$ where f is the resonance frequency and Δf the full width at half height of the resonance curve in an unloaded cavity.

higher the radiofrequency power available for the particle beam. This is the fundamental advantage of superconducting cavities as their surface resistance is much lower and outweighs the power needed to cool the cavities to liquid helium temperatures. A nine-cell cavity dissipates about 100 W at 25 MV/m with a $Q_0 = 5 \cdot 10^9$. In the pulsed operation of TESLA with a duty cycle of 1% this is only 1 W of radiofrequency power, whereas 200 kW are available for the beam as shown in table 1.3.

1.3 Superconductivity

1.3.1 Introduction

Superconductivity was discovered in 1913 by Kammerlingh Omnes in Leiden. It was found that for mercury below a certain temperature (T = 4.2 K) no ohmic resistance could be measured. By now a large number of elements and compounds (mainly alloys and ceramics) have been found showing this behaviour. For superconducting cavities niobium shows the most interesting properties. The general features of superconductivity as well as the special properties of niobium are described.

1.3.2 Characteristic length scales of superconductivity

1.3.2.1 Meissner-Ochsenfeld effect

Two different types of superconductors were discovered. They have certain common features, but differ also in some important ways. When the material is cooled below the critical temperature T_c the ohmic resistance vanishes below the measurement limit. In addition, any external magnetic field up to a critical field $B < B_{crit}$ is expelled. This magnetic field expulsion is called the Meissner-Ochsenfeld effect. This behaviour significantly differs from the properties of an ideal conductor where the field would be trapped inside the material. Even if the field is switched off, an ideal conductor would keep the magnetic field and become a permanent magnet as the currents induced by the field will continue to flow. From a thermodynamical point of view, one can define the thermodynamical critical field B_c:

$$G_n - G_s = \frac{1}{2\mu_0} V B_c^2 \tag{1.10}$$

Here one takes difference of the free enthalpy G in the normal- and the superconducting state respectively. Experimentally, B_c can be determined from the area below the magnetization curve of the material.

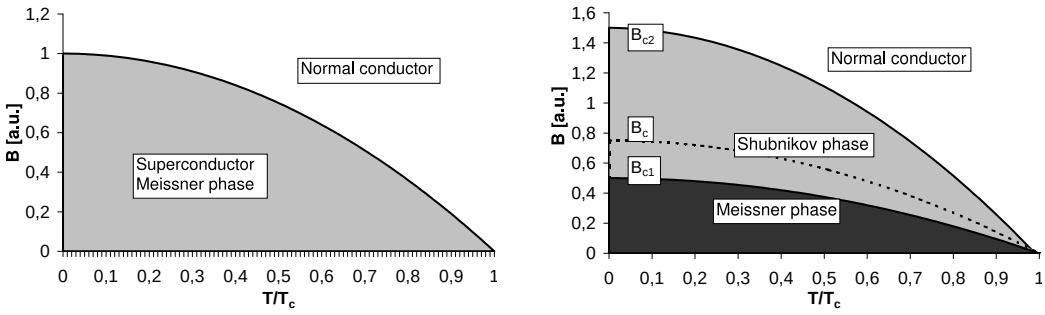

Figure 1.1: Phase diagrams for superconductors of type I (left) and type II (right).

If the field exceeds a critical value B_c in a superconductors of type I the superconductivity breaks down and the normal conducting state is restored. This critical field depends on the critical temperature:

$$B_c(T) = B_c(0)\left[1 - \left(\frac{T}{T_c}\right)^2\right] \tag{1.11}$$

For the second type of superconductor the magnetic field will start to penetrate the material above the lower critical field B_{c1}. Magnetic fluxons enter the material and their number increases with increasing field. If one raises the field further to a value of B_{c2} the material becomes normalconducting. The temperature dependence of the critical magnetic fields B_{c1} and B_{c2} is the same as for the B_c of a type I superconductor. This is shown in figure 1.1.

1.3.2.2 Coherence length in superconductors

For classical superconductors like lead or tin, a very successful microscopic theory was developed by Bardeen, Cooper and Schrieffer which is called BCS-theory [Bardeen et al. 1957]. They assumed that electrons begin to condense below T_c to pairs of electrons, the so called Cooper pairs. The two electrons in a pair have opposite momentum and spin. They experience an attractive force mediated via quantized lattice vibrations called phonons. This bound state of the two electrons is energetically favourable. As the overall spin of these two paired electrons is zero, many of these pairs can co-exist coherently, just like other bosons. The coherence length describes the distance over which the electrons are correlated. It is given by:

$$\xi_0 = \frac{\hbar v_F}{\Delta} \tag{1.12}$$

v_F denotes the velocity of the electrons near the Fermi energy and $2 \cdot \Delta$ is the energy necessary to break up a Cooper pair. Typical values for the coherence

length in niobium are around 39 nm. If one interprets the coherence length as the size of a Cooper pair, one immediately sees that it spans over many lattice constants. Within the BCS theory the energy gap can be calculated:

$$\Delta = 1.76 k_B T_c \tag{1.13}$$

The exact value of factor (1.76) in the relation of the energy gap and the critical temperature is material dependent and for niobium one finds higher values of $\Delta = 1.9 k_B T_c$, which can be seen for example in figure 1.3. The number of Cooper pairs $n_{cooper} = n_s/2$ is temperature dependent and only at T = 0 K all conduction electrons are condensed into Cooper pairs. The superconducting electrons co-exist with their normalconducting counterparts. The number of normalconducting electrons is given by the Boltzmann factor:

$$n_e(T \to 0) \approx n_s(0) \exp\left(-\frac{\Delta(T)}{k_b T}\right) \tag{1.14}$$

1.3.2.3 London penetration depth

Even in a type I superconductor the magnetic field is not completely expelled, but penetrates into the material over a small distance, as otherwise the shielding current density would have to be infinitely large. The so-called London penetration depth is given by the characteristic length of the exponential decay of the magnetic field into the superconductor.

$$B(x) = B(0) e^{-\frac{x}{\lambda_L}} \tag{1.15}$$

Its value is

$$\lambda_L = \sqrt{\frac{m}{\mu_0 n_s c^2}} \tag{1.16}$$

where e is the charge of an electron, m its mass and n_s the number of superconducting charge carriers per unit volume. A typical value for the penetration depth in niobium is 32 nm. The theory did not allow for impurities in the material nor for a temperature dependence of the penetration depth. Gorter and Casimir introduced the two-fluid model where a coexistence of a normal- and superconducting fluid of charge carriers is postulated.

$$n_c = n_n + n_s \tag{1.17}$$

They suggested a temperature dependence of the superconducting charge carriers.

$$n_s(T) = n_s(0) \cdot \left(1 - \left(\frac{T}{T_c}\right)^4\right) \tag{1.18}$$

Combining equations 1.16 and 1.18, the penetration depth shows the following temperature dependence:

$$\lambda_L(T) = \lambda(0)\left(1 - \left(\frac{T}{T_c}\right)^4\right)^{-\frac{1}{2}} \tag{1.19}$$

The Ginzburg-Landau parameter is defined as:

$$\kappa = \frac{\lambda_L}{\xi_0} \tag{1.20}$$

κ allows to distinguish between the two types of superconductors:

$$\kappa < \frac{1}{\sqrt{2}} \qquad \text{Superconductor type-I} \tag{1.21}$$

$$\kappa > \frac{1}{\sqrt{2}} \qquad \text{Superconductor type-II} \tag{1.22}$$

Niobium has $\kappa \approx 1$ and is a weak type-II superconductor.

The role of impurities was studied by Pippard [Pippard 1953] was based on the evidence that the penetration depth depends on the mean free path of the electrons ℓ in the material. The dependence of ξ on the mean free path is given by:

$$\frac{1}{\xi} = \frac{1}{\xi_0} + \frac{1}{\ell} \tag{1.23}$$

He introduced an effective penetration depth:

$$\lambda_{eff} = \lambda_L \cdot \frac{\xi_0}{\xi} \tag{1.24}$$

Here again ξ_0 is the characteristic coherence length of the superconductor. This relation reflects that the superconducting penetration depth increases with a reduction of the mean free path [Waldram 1964]. For pure ("clean") superconductor ($\ell \to \infty$) one has $\xi = \xi_0$. In the limit of very impure ("dirty") superconductors where $\ell \ll \xi_0$, the relation becomes

$$\xi = \ell. \tag{1.25}$$

The mean free path in the niobium is strongly influenced by interstitial impurities like oxygen, nitrogen and carbon. This point will become relevant in chapter 4 where the quality factor of a cavity and its dependence on the accelerating field are discussed.

Experimental values	
Critical temperature T_c	9.2 K
Coherence length ξ_0	39 nm
London penetration depth λ_L	30 nm
GL parameter κ	0.8

Table 1.1: Superconducting properties of polycrystalline high-purity niobium [Bahte 1998, Padamsee et al. 1998].

1.3.2.4 Microwave skin effect in normal metals

The shielding mechanism of a static magnetic field in a superconductor is analogous to the shielding of a microwave field in a normal metal. If a microwave of frequency ω is incident on a metal surface one can show that the field is decaying over a characteristic distance, the skin depth δ. For the case where the frequency is much lower than plasma frequency ($\omega << \omega_{plasma}$) the or the mean free path of the electrons ℓ is smaller than the penetration depth (or skin depth) δ one finds:

$$\delta = \sqrt{\frac{2}{\sigma \mu_0 \omega}} \tag{1.26}$$

σ is the conductivity of the metal. This is the regime of the normal skin effect. One can calculate the surface resistance

$$R_{surf} = \frac{1}{\sigma \delta} \tag{1.27}$$

According to this equation one would expect a strong reduction of the surface resistance at cryogenic temperature because σ grows for $T \to 0$. Unfortunately, for pure metals and at low temperatures ℓ may become larger than δ which leads to the anomalous skin effect. Then the electrons are not only scattered by phonons, but by impurities in the metal lattice. In the limit ($\ell \to \infty$) the surface resistance becomes [Padamsee et al. 1998]:

$$R_{surf} = \left[\sqrt{3}\pi \left(\frac{\mu_0}{4\pi}\right)^2\right]^{\frac{1}{3}} \omega^{\frac{2}{3}} \left(\frac{\ell}{\sigma}\right)^{\frac{1}{3}} \tag{1.28}$$

1.3.3 Radiofrequency critical magnetic field

The above mentioned description of the critical magnetic field applies for the dc case. For microwaves in the GHz-regime the situation is more complicated, as the current changes its sign every 10^{-9} seconds. Calculations have shown that the Meissner state can persist beyond B_{c1}. If no nucleation centers are available the possibility of a metastable state exists and therefore a delayed entry of the magnetic field - the so-called superheated state - might occur. Possible nucleation centers for magnetic flux are surface defects like protrusions or normalconducting inclusions. Therefore the surface condition and roughness are very important to achieve the superheating.

The superheated field has been calculated on the basis of the Ginzburg-Landau equations [Matricon and Saint-James 1967]. The superheating field is given for different κ in [Piel 1989]:

$$\begin{aligned} B_{sh} &= 0.75 B_c \quad \text{for} \quad \kappa \gg 1 \\ B_{sh} &= 1.2 B_c \quad \text{for} \quad \kappa \approx 1 \\ B_{sh} &= \tfrac{1}{\sqrt{\kappa}} B_c \quad \text{for} \quad \kappa \ll 1 \end{aligned}$$

A superheating field has been observed in type-I when a defect-free surface was used [Doll and Graf 1967]. Measurements on type-I and type-II superconductors at various frequencies indicate that the superheating field indeed exists at temperatures close to the critical temperature. The results are shown in figure 1.2. This was confirmed in more recent measurements where on 1.3 GHz niobium cavities it was shown that the superheating state can be achieved if the temperature is close to T_c [Hays and Padamsee 1997]. At temperatures at 4.2 K or 2 K and correspondingly higher fields (compare equation 1.11) the superheated state has not yet been established probably because other effects limit the maximum field gradient. These are for example local defects, which limit the maximum achievable field due to thermal breakdown as is described in section 1.5.2. At 2 K the maximum field is in the order of B_{c1} or slightly higher.

Property	Experimental data [mT] at 4.2 K	Calculated field [mT] at 0 K	Calculated field [mT] at 2 K	E_{acc} [MV/m] at 2 K
B_{c1}	130	164	156	37
B_c	158	200	190	45
B_{sh}	190	240	230	54
B_{c2}	248	312	297	62

Table 1.2: Critical magnetic fields of high-purity niobium. The corresponding acceleration gradient for the TESLA cavities is also given [Bahte et al. 1997], [Bahte 1998].

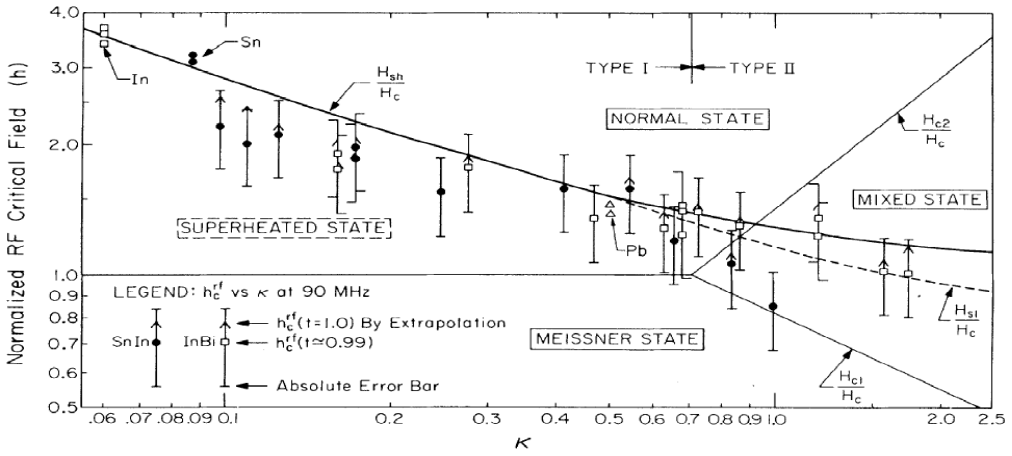

Figure 1.2: Measurements on the radiofrequency critical magnetic field in different superconducting alloys (SnIn, InBi) as a function of the Ginzburg-Landau parameter κ for temperatures near T_c [Yogi et al. 1977]. The curve $\frac{H_{sh}}{H_c}$ denotes the calculation by [Matricon and Saint-James 1967].

1.3.4 Microwave surface resistance

1.3.4.1 BCS resistance

For a direct current or low frequency alternating currents the superconducting electrons shield the normalconducting electrons from the electromagnetic field so that no power is dissipated. For alternating currents at microwave frequencies this is not true anymore. The inertia of the Cooper pairs prohibits them to follow the changing electromagnetic fields immediately, the shielding is not perfect anymore. The normalconducting electrons start to flow and dissipate power. This gives rise to a resistance which depends on the number of normalconducting electrons and the frequency of the alternating current. For temperatures $T < \frac{T_c}{2}$ and an energy of the microwave photons of $hf \ll \Delta$ the surface resistance can be approximated by:

$$R_{BCS}(T, f) = A\frac{f^2}{T}\exp\left(\frac{-\Delta}{k_B T}\right) \tag{1.29}$$

The factor A depends on material parameters like coherence length, electron mean free path, Fermi velocity and penetration depth. For niobium it is about $9 \cdot 10^{-5}\Omega\mathrm{K}/(\mathrm{GHz})^2$. Therefore the BCS resistance at 1.3 GHz is about 600 nΩ at 4.2 K and about 1 nΩ at 2 K.

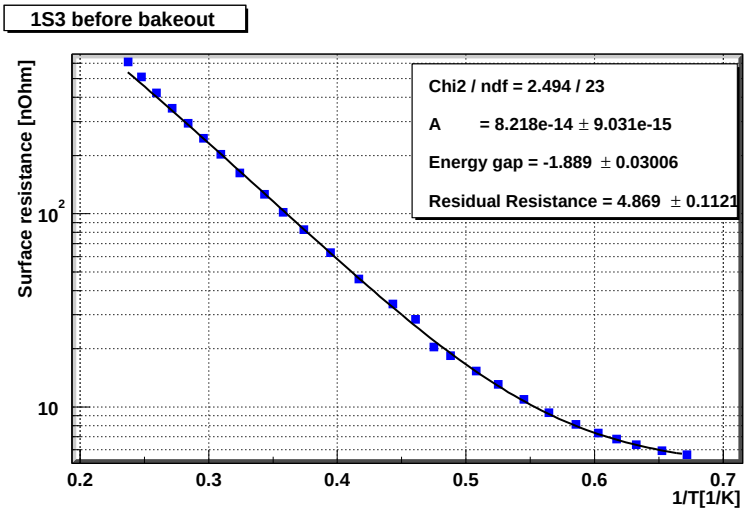

Figure 1.3: Measurement of the temperature dependence of the surface resistance of a single-cell niobium 1.3 GHz cavity. The fit to the curve results in an energy gap $\Delta = 1.889 \cdot k_b T_c$ and a residual resistance of 5 nΩ.

The result derived for R_{BCS} from the two-fluid model will give [Bonin 1996]:

$$R_{BCS}(T,f) = C \cdot \sigma_{nc} \cdot \lambda_{eff}^3 \frac{f^2}{T} \exp\left(\frac{-\Delta}{k_B T}\right) \tag{1.30}$$

C is a constant, which does not depend on the material properties. σ_{nc} is the conductivity in the normalconducting state. The dependence of R_{BCS} on the mean free path is therefore [Saito and Kneisel 1999]:

$$R_{BCS}(\ell) \propto \left(1 + \frac{\xi_0}{\ell}\right)^{\frac{3}{2}} \cdot \ell \tag{1.31}$$

There exists a minimum of R_{BCS} on the mean free path ℓ. A more detailed calculation of the BCS theory shows that the two-fluid model gives a good approximation for $\ell < 500nm$ [Halbritter 1970] (see figure 1.4).

1.3.4.2 Residual resistance

The total surface resistance contains in addition a temperature independent part, which is called residual resistance R_{res}. The residual resistance is usually dominated by lattice imperfections, chemical impurities, adsorbed gases and trapped magnetic field. Well prepared niobium surfaces show a residual resistance of a few nΩ (figure 1.3).

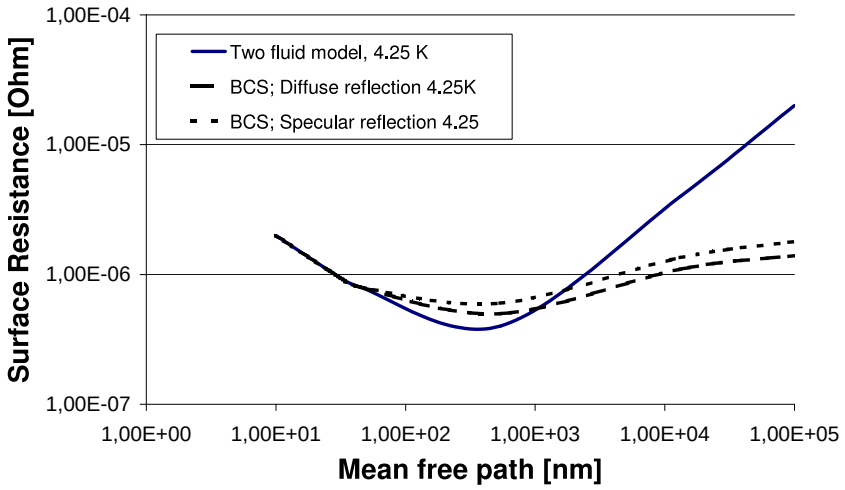

Figure 1.4: Calculated BCS surface resistance at 4.2K for 1.3 GHz plotted versus mean free path ℓ [Halbritter 1970]; this figure is taken from [Saito and Kneisel 1999].

Absorbed gases can lead to a high residual resistance [Piosczyk 1974]. The dielectric properties of N_2 and O_2 are the reason for this behaviour. Minor contributions come from dielectric losses of the natural oxide Nb_2O_5. They have been estimated to be in the order of 1 nΩ [Palmer 1988b] or below [Reschke 1995].

If a cavity is not shielded from the earth magnetic field its surface resistance is increased due to trapped magnetic fluxons. Those fluxons are trapped at impurities called pinning centers even though the superconductor tries to expel the magnetic field. The losses from fluxons can be calculated:

$$R_{fl} = \eta \frac{B_{ext}}{B_{c2}} R_{surf,nc} \tag{1.32}$$

B_{ext} is the external magnetic field and $R_{surf,nc}$ is resistivity of the material in the normalconducting state. $\eta \leq 1$ is a correction factor for the field expulsion. Measurements have shown that the trapping efficiency is very close to 1 even in high purity niobium [Bonin et al. 1992].

Any contamination of the surface with metallic parts (from screws, gaskets, etc.) or dielectric remnant from the surface treatment has to be avoided. It can enhance the residual RF losses to an intolerable level.

1.4 TESLA cavity production

The main drawback of superconducting (sc) accelerating structures has traditionally been the low gradient of the cavities combined with the high cost of cryogenic equipment. At the time of the first TESLA workshop [Padamsee 1990] superconducting RF cavities in particle accelerators were usually operated in the 5 MV/m regime. Such low gradients would have made a superconducting linear electron-positron collider of 500 GeV center-of-mass energy totally non-competitive with the normal-conducting colliders proposed in the USA and Japan. The ambitious design gradient of 25 MV/m was specified for TESLA. In the meantime this gradient has been safely established in multicell niobium cavities produced by industry, and in addition the cost per unit length of the linac has been considerably reduced by applying economical cavity production methods and by assembling many cavities in a long cryostat[5].

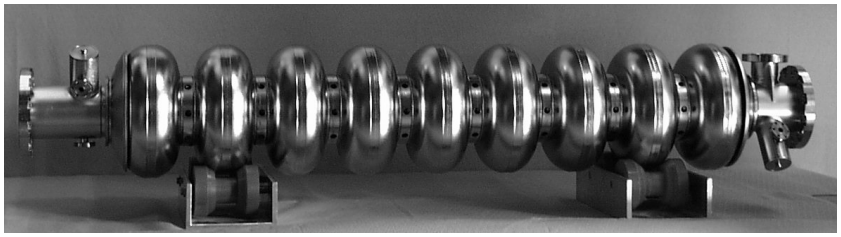

Figure 1.5: Picture of TESLA-type 9-cell cavity.

The TESLA cavities (see figure 1.5 and table 1.3) are similar in layout to the 5-cell 1.5 GHz cavities of the electron accelerator CEBAF which were developed at Cornell University and fabricated by an industrial company [Reece et al. 1995]. They exceeded the specified gradient of 5 MV/m considerably and hence offered the potential for further improvement. The CEBAF cavity manufacturing methods were adopted for TESLA with improved quality control of the superconducting material and of the fabrication methods, and important new steps were introduced in the cavity preparation collecting experiences from several different laboratories working on superconducting accelerating cavities (e.g. CEA Saclay, CERN, Cornell, KEK, Karlsruhe, Wuppertal and DESY):

[5] A recent review paper on the TESLA cavities can be found in [Aune et al. 2000]. A review paper on superconducting cavity science and technology can be found in [Padamsee 2001]. Also the developments on sputtered niobium films and other superconducting materials are reviewed.

type of accelerating structure	standing wave
accelerating mode	TM_{010} , π mode
fundamental frequency	1300 MHz
design gradient E_{acc}	25 MV/m
quality factor Q_0	$> 5 \cdot 10^9$
active length L	1.038 m
number of cells	9
cell-to-cell coupling	1.87 %
iris diameter	70 mm
geometry factor	270 Ω
R/Q	1024 Ω
$E_{\text{peak}}/E_{\text{acc}}$	2.0
$B_{\text{peak}}/E_{\text{acc}}$	4.26 mT/(MV/m)
tuning range	± 300 kHz
$\Delta f/\Delta L$	315 kHz/mm
Lorentz force detuning at 25 MV/m	≈ 600 Hz
Q_{ext} of input coupler	$3 \cdot 10^6$
cavity bandwidth at $Q_{\text{ext}} = 3 \cdot 10^6$	430 Hz
RF pulse duration	1330 μs
repetition rate	5 Hz
fill time	530 μs
beam acceleration time	800 μs
RF power peak/average	208 kW/1.4 kW
number of HOM couplers	2

Table 1.3: TTF cavity design parameters [Brinkmann et al. 2001].

fundamental mode	TM_{010} , π mode
fundamental frequency	1300 MHz
active length L	11.46 cm
iris diameter	78 mm
geometry factor	270 Ω
R/Q	105 Ω
$E_{\text{peak}}/E_{\text{acc}}$	1.98
$B_{\text{peak}}/E_{\text{acc}}$	4.2 mT/(MV/m)

Table 1.4: One-cell cavity parameters for the resonators used in this thesis.

- chemical removal of a thicker layer from the inner cavity surface
- a 1400°C annealing with titanium getter to improve the niobium heat conductivity and to homogenize the material
- rinsing with ultrapure water at high pressure (100 bar) to remove surface contaminants
- a closed chemistry system integrated in a clean-room facility
- destruction of field emitters by a technique called High Power Processing.
- better quality control of the niobium sheets with an eddy-current scanning method to detect foreign inclusions (e.g. tantalum grains)
- preparation of electron-beam welds with very tight specifications e.g. etching of the welding area, ultrapure water rinsing and clean room drying within less than 8 hours before welding to avoid contaminations in the weld

The application of these techniques, combined with an extremely careful handling of the cavities in a clean-room environment, has led to a significant increase in accelerating field.

The TESLA Test Facility (TTF) has been set up at DESY to provide the infra-structure for the chemical treatment, clean-room assembly and testing of industrially produced multicell cavities. An electron linac has been built as a test bed for the performance of the sc accelerating structures with an electron beam of high bunch charge. The linac is equipped with undulator magnets to generate FEL radiation in the VUV regime.

1.4.1 Cavity fabrication

1.4.1.1 Niobium properties

Niobium of high purity is needed. Tantalum with a typical concentration of 500 ppm is the most important metallic impurity. Among the interstitially dissolved impurities oxygen is dominant due to the high affinity of Nb for O_2 above 200°C. Interstitial atoms act as scattering centers for the unpaired electrons and reduce the RRR and the thermal conductivity, see section 1.5.2. The niobium ingot is highly purified by several remelting steps in a high vacuum electron beam furnace. This procedure reduces the interstitial oxygen, nitrogen and carbon contamination to a few ppm. The niobium specification for the TTF cavities is listed in Table 1.5.

Impurity content in ppm (wt)				Mechanical Properties	
Ta	≤ 500	H	≤ 2	Residual resistivity ratio RRR	≥ 300
W	≤ 70	N	≤ 10	grain size	≈ 50 μm
Ti	≤ 50	O	≤ 10	yield strength	> 50 MPa
Fe	≤ 30	C	≤ 10	tensile strength	> 100 MPa
Mo	≤ 50			elongation at break	30 %
Ni	≤ 30			Vickers hardness HV 10	≤ 50

Table 1.5: Technical specification for niobium used in TTF cavities.

After forging and sheet rolling, the 2.8 mm thick Nb sheets are degreased, a 5 μm surface layer is removed by etching and then the sheets are annealed for 1–2 hours at 700–800°C in a vacuum oven at a pressure of 10^{-5} – 10^{-6} mbar to achieve full recrystallization and a uniform grain size of about 50 μm.

1.4.1.2 Deep drawing and electron-beam welding

The 9-cell resonators are made from 2.8 mm thick sheet niobium. Half-cells are produced by deep-drawing. The dies are usually made from a high yield strength aluminium alloy. To achieve the small curvature required at the iris an additional step of forming, e.g. coining, may be needed. The half-cells are machined at the iris and the equator. At the iris the half cell is cut to the specified length (allowing for weld shrinkage) while at the equator an extra length of 1 mm is left to retain the possibility of a precise length trimming of the dumb-bell after frequency measurement (see below). The accuracy of the shape is controlled by sandwiching the half-cell between two metal plates and measuring the resonance frequency. The half-cells are thoroughly cleaned by ultrasonic degreasing, 20 μm chemical etching and ultra-pure water rinsing. Two half-cells are then joined at the iris with an electron-beam (EB) weld to form a "dumb-bell". The EB welding is usually done from the inside to ensure a smooth weld seam at the location of the highest electric field in the resonator. Since niobium is a strong getter material for oxygen it is important to carry out the EB welds in a sufficiently good vacuum. Tests have shown that $RRR = 300$ niobium is not degraded by welding at a pressure of less than $5 \cdot 10^{-5}$mbar (see also section 3.2.3).

The next step is the welding of the stiffening ring. Here the weld shrinkage may lead to a slight distortion of the cell shape which needs to be corrected. Afterwards, frequency measurements are made on the dumb-bells to determine the correct amount of trimming at the equators. After proper cleaning

by a 30 μm etching the dumb-bells are visually inspected. Defects and foreign material imprints from previous fabrication steps are removed by grinding. After the inspection and proper cleaning (a few μm etching followed by ultra-clean water rinsing and clean room drying), eight dumb-bells and two beam-pipe sections with attached end half-cells are stacked in a precise fixture to carry out the equator welds which are done from the outside. The weld parameters are chosen to achieve full penetration. A reliable method for obtaining a smooth weld seam of a few mm width at the inner surface is to raster a slightly defocused beam in an elliptic pattern and to apply 50 % of beam power during the first weld pass and 100 % of beam power in the second pass.

1.4.2 Cavity treatment

Experience has shown that a damage layer in the order of 100 μm has to be removed from the inner cavity surface to obtain good RF performance in the superconducting state. The standard method applied at DESY and many other laboratories is called Buffered Chemical Polishing (BCP), using an acid mixture of HF (48 %), HNO_3 (65 %) and H_3PO_4 (85 %) in the ratio 1:1:2 (at CEBAF the ratio was 1:1:1). The preparation steps adopted at DESY for the industrially produced TTF cavities are as follows. A layer of 80 μm is removed by BCP from the inner surface, 30 μm from the outer surface[6]. The cavities are rinsed with ultra-clean water and dried in a class 100 clean room. The next step is a two-hour annealing at 800°C in an Ultra High Vacuum (UHV) oven which serves to remove dissolved hydrogen from the niobium and relieves mechanical stress in the material. In the initial phase of the TTF program many cavities were tested after this step, applying a 20 μm BCP and ultra-clean water rinsing before mounting in the cryostat and cooldown.

Presently, the cavities are rinsed with clean water after the 800°C treatment and then immediately transferred to another UHV oven in which they are heated to 1350–1400°C. To capture the oxygen coming out of the niobium and to prevent oxidation by the residual gas in the oven (pressure $< 10^{-7}$mbar) a thin titanium layer is evaporated on the inner and outer cavity surface, Ti being a stronger getter than Nb. The high-temperature treatment with Ti getter is often called post-purification. The RRR increases by about a factor of 2 to values around 500. The titanium layer is removed afterwards by a 80 μm BCP of the inner surface. A BCP of about 30 μm is

[6]These numbers are determined by weighing the cavity before and after etching and represent therefore the average over the whole surface. Frequency measurements indicate that more material is etched away at the iris than at the equator.

applied at the outer surface since the thermal interface resistance ("Kapitza resistance ") of titanium-coated niobium immersed in superfluid helium is about a factor of 2 larger than that of pure niobium [Boucheffa et al. 1995]. After final heat treatment and BCP the cavities are mechanically tuned to adjust the resonance frequency to the design value and to obtain equal field amplitudes in all 9 cells. This is followed by a slight BCP, three steps of high-pressure water rinsing (100 bar) and drying in a class 10 clean room. As a last step, the RF test is performed in a superfluid helium bath cryostat.

A severe drawback of the post-purification is the considerable grain growth accompanied with a softening of the niobium. Postpurified-treated cavities are quite vulnerable to plastic deformation and have to be handled with great care.

1.4.3 Results on cavity performance at TTF

Figure 1.6 shows the excitation curve of the best 9-cell resonator measured so far; plotted is the quality factor Q_0 as a function of the accelerating electric field E_{acc}. An almost constant and high value of $2 \cdot 10^{10}$ is observed up to 25 MV/m.

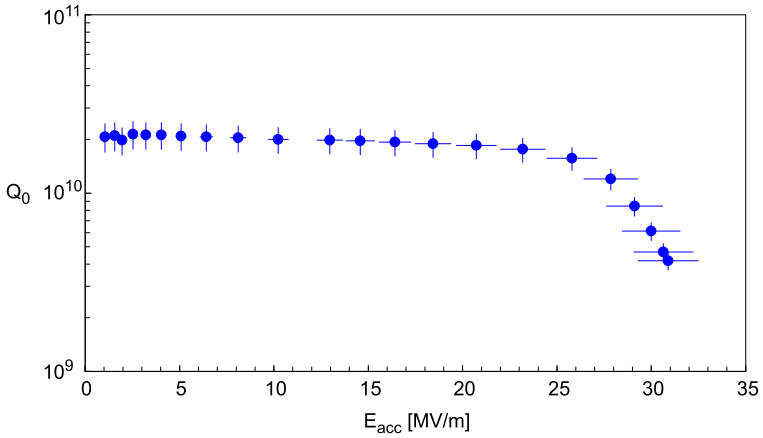

Figure 1.6: Excitation curve of the best chemically etched TESLA 9-cell cavity measured up to date. The cavity was cooled by superfluid helium of 2 K [Brinkmann et al. 2001].

The importance of various cavity treatment steps for arriving at such a good performance are illustrated in the next figure. A strong degradation is usually observed if a foreign particle is sticking on the cavity surface, leading either to field emission of electrons or to local overheating in the RF field. At Cornell University an *in situ* method for destroying field emitters was

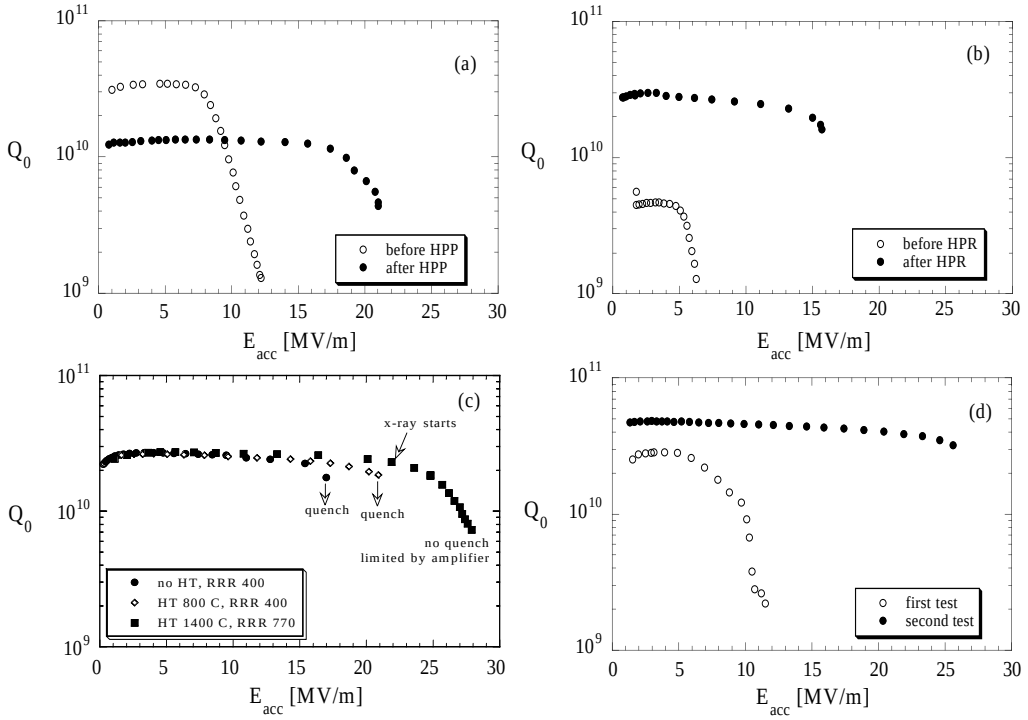

Figure 1.7: Improvement in cavity performance due to various treatments: (a) high power processing, (b) high pressure water rinsing, (c) successive application of 800°C and 1400°C heat treatment, (d) removal of surface defects or titanium in grain boundaries by additional BCP. All tests were done at 1.8 K [Aune et al. 2000].

invented [Graber et al. 1994], called high power processing (HPP), which in many cases can improve the high-field capability, see Fig. 1.7a. Removal of field-emitting particles by high-pressure water rinsing, a technique developed at CERN [Bernard et al. 1992], may eventually improve the excitation curve (Fig. 1.7b). The beneficial effect of a 1400°C heat treatment, first tried out at Cornell [Padamsee et al. 1990], Wuppertal [Müller 1988] and later in Saclay [Safa et al. 1995], is seen in Fig. 1.7c. Finally, an incomplete removal of the titanium surface layer in the BCP following the 1400°C heat treatment may strongly limit the attainable gradient. Here additional BCP is of advantage (Fig. 1.7d).

From the last TTF cavity production series, which is produced by one company, 9 cavities have been tested up to date (see Fig. 1.8). They exceed the TESLA-500 specification: the average gradient at $Q_0 \geq 1 \cdot 10^{10}$ is 26.1± 2.3 MV/m and the average quality factor at the design gradient of 23.5 MV/m is $Q_0 = (1.39 \pm 0.35) \cdot 10^{10}$.

The reproducibility of the cavity performance is excellent. The curves of all cavities show very similar features. The maximum achievable gradient is

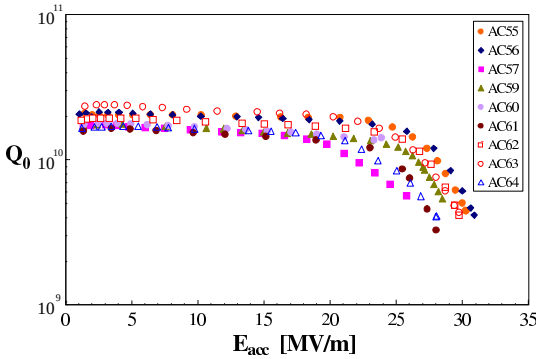

Figure 1.8: Excitation curves of cavities of the last TTF production. Tests were done at 2 K [Brinkmann et al. 2001].

clearly above 25 MV/m. The quality factor Q_0 is nearly constant up to an accelerating gradient of between 20 and 25 MV/m. In this region the real part of the surface resistance increases strongly. The final limit of most of these cavities is a thermal breakdown (quench). In some cavities it was not possible to get to this quench limit due to the available RF power in the continuous wave (cw) tests[7]. In Fig. 1.9 the performance of the cavities in the three production series is shown. The average gradient exhibits a clear trend towards higher values, and the width of the distribution is shrinking. It is obvious that the most recent cavities exceed the 23.5 MV/m operating gradient of TESLA-500 by a comfortable safety margin.

These values show that a clear improvement has been achieved with the above mentioned procedures. Still, most of the cavities are limited to gradients well below 35 MV/m corresponding to a maximum surface magnetic field of around 150 mT. Since the critical field of niobium at temperatures close to T_c is identical to B_{sh} [Hays and Padamsee 1997], it is a widespread believe that accelerating gradients of more than 50 MV/m ($B_{sh}(2K) > 200$ mT) in a perfect cavity could be achieved. The TESLA collaboration now aims to achieve gradients of 35 MV/m for the upgrade of the center-of-mass energy of the linac to 800 GeV. Therefore it is necessary to look closely at the limiting mechanisms of the cavities where known material[8] or fabrication defects can be excluded due to the tight specifications available.

[7]The amplifier used for cw measurements delivers 1000 W. This corresponds to 300-500 Watts at the cavity

[8]The resolution of the eddy current system used at the moment allows to detect tantalum inclusions with a diameter of about 200 μm.

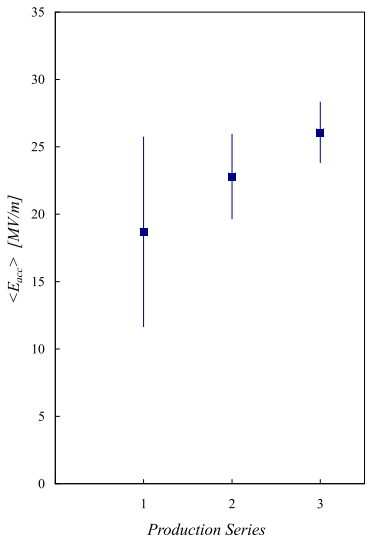

Figure 1.9: Average accelerating gradients at $Q_0 \geq 10^{10}$ of the cavities in the three TTF cavity productions measured in the vertical test cryostat. One can see the clear improvement due to tighter quality control of the sheet material and a tighter welding specification as well as improved handling in the clean-room environment.

1.5 Limiting mechanisms in TTF cavities

1.5.1 Diagnostic tools

The good reproducibility of the cavity performance allows to clearly identify loss mechanisms with advanced diagnostic techniques. Most of these tools are described in [Padamsee et al. 1998]. Therefore the focus in this part will be on the available tools in the test setups used for this thesis [9].

One very important diagnostic is the mapping of the outer cavity surface with temperature sensors (T-mapping). Systems consist either of rotating thermometer arms (available at Saclay for a single cell and at DESY for nine-cell cavities [Pekeler et al. 1995]) or fixed sensors on the surface at DESY [Pekeler 1996] and KEK for mono-cells) using a principle developed at Cornell University [Knobloch 1997]. The temperature maps allow to distinguish between localised hot spots due to foreign particle inclusions or multipacting, traces of field emitters or global heating effects. The resolution of the fixed T-mapping is a few mK. Usually the test setup also includes one (or more) X-ray sensors on top of the test cryostat. This is a good indicator for field

[9] Tests have been carried out at CEA-DAPHNIA (Saclay), CERN (Geneva), KEK (Tsukuba) and DESY (Hamburg).

emission. In Saclay this is supplemented with a sensitive electrometer which can detect electrons hitting the antenna used for monitoring the cavity field.

1.5.2 Thermal breakdown

Thermal breakdown can occur when a normalconducting defect starts to heat due to the induced ac currents. If the field is raised further the heat can lead to an increase of the temperature in the surrounding niobium material above its critical temperature T_c. As more material becomes normalconducting, more heat is generated and finally the cavity suffers a breakdown of superconductivity.

Several of the TTF nine-cell resonators show a thermal breakdown at gradients between 25-30 MV/m (Figure 1.10). Optical inspections done on these resonators did not reveal any special features like defects or particle inclusions, which usually lead to an enhanced heating. The absence of defects is a first hint that the topology of an etched surface itself might be an important limitation for the cavity performance. This will become more obvious in a later section where the results with another surface preparation technique namely electropolishing are presented.

1.5.2.1 Heat flow in bulk niodium

When a defect-free niobium surface is heated with the radiofrequency power, the heat flows through an area A with heat current $\dot{Q}/A$. The temperature in the niobium decreases linearly if the temperature dependence of

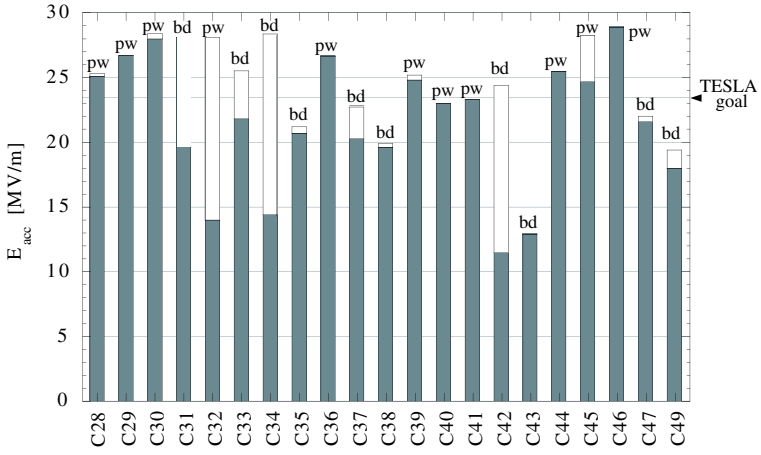

Figure 1.10: Maximum accelerating fields and limitations in the second production of TTF cavities. The limitation in the measurement of the cavities are given: Thermal breakdown (bd) and amplifier power limit (pwr).

the thermal conductivity λ can be neglected as shown in figure 1.11. As superfluid helium has a very high thermal conductivity the temperature of the helium bath is nearly constant everywhere. Nevertheless, there exists a very small interface layer between the niobium and the helium of about 10-100 atomic layers (Kapitza layer) in which the temperature decreases exponentially from the temperature of the outer niobium surface to the bath temperature [Sciver 1986].

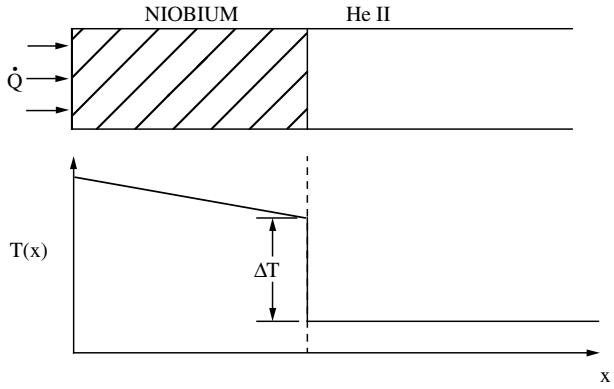

Figure 1.11: Distribution of the temperature in the niobium material and the superfluid helium. In the niobium the temperature decreases linearly, while in the helium bath the temperature is constant. In the interface layer the temperature drops quickly by an amount of ΔT to the temperature of the bath [Pekeler 1996].

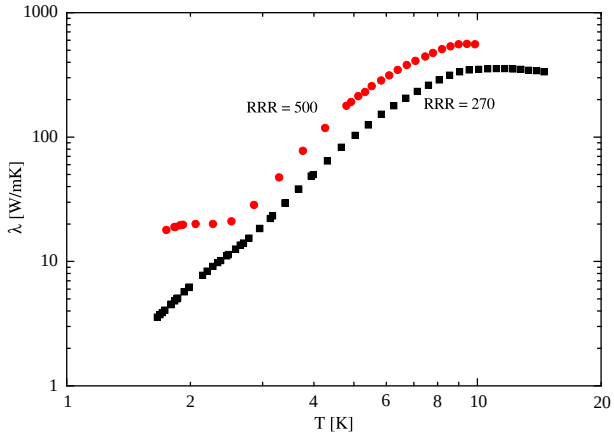

Figure 1.12: Measured heat conductivity of samples from the niobium sheets used in the TESLA cavities: before and after the 1400°C heat treatment (RRR = 280 and RRR = 500 respectively) [Brinkmann et al. 2001].

The temperature ΔT in the interface is proportional to $\dot{Q}/A$:

$$\frac{\dot{Q}}{A} = h_\mathrm{k} \cdot \Delta T \; ; \tag{1.33}$$

The factor h_k is called the Kapitza conductivity. And depends strongly on the bath temperature. The relation is [Mittag 1973, Fouaidy et al. 1992]:

$$h_\mathrm{k} = c_\mathrm{k} \cdot {T_\mathrm{B}}^n \; . \tag{1.34}$$

The values of c_k and n depend on the surface properties and the RRR of the niobium and are typically $0.5 < c_\mathrm{k} < 1.1$ and $2.5 < n < 3.8$.

The temperature on the outside therefore depends on the thermal conductivity λ, the thickness of the niobium and the Kapitza conductivity of the niobium-helium interface.

$$\frac{\dot{Q}}{A} = \frac{\lambda}{d}(T_\mathrm{i} - T_\mathrm{o}) = h_\mathrm{k}(T_\mathrm{o} - T_\mathrm{B}) \quad \Rightarrow \quad T_\mathrm{i} - T_\mathrm{B} = \frac{\dot{Q}}{A}\left(\frac{d}{\lambda} + \frac{1}{h_\mathrm{k}}\right) \tag{1.35}$$

T_i and T_o are the temperature of the inner and the outer surface, respectively. T_B is the helium bath temperature. With equation (1.34) and equation (1.35) one finds:

$$\Delta T_\mathrm{i} = \left(\frac{c_\mathrm{k} d}{\lambda} {T_\mathrm{B}}^n + 1\right) \Delta T_\mathrm{o} \; . \tag{1.36}$$

$\Delta T_\mathrm{i} = T_\mathrm{i} - T_\mathrm{B}$ and $\Delta T_\mathrm{o} = T_\mathrm{o} - T_\mathrm{B}$ denote the temperature differences on the inner and outer surface respectively. Measurements on samples have shown that the thermal conductivity of niobium with $RRR = 350$ in the temperature range of 1.5 K to 2 K is about $\lambda \approx 3$ W/(m·K) [Schilcher 1995]. For h_k one has at 1.8 K a value of 4000 W/(m^2 K) [Mittag 1973]. Together with a wall thickness of the niobium resonator of $d = 1.5$ mm the temperature increase on the inner surface ΔT_i is about three times the temperature increase on the outer surface ΔT_o.

$$\Delta T_\mathrm{i} \approx 3 \cdot \Delta T_\mathrm{o} \tag{1.37}$$

This is correct only for small temperature increases on the inner surface $\Delta T_\mathrm{i} = 1$ K, as the thermal conductivity depends strongly on the temperature. Thermal simulations are shown in figure 1.13 for a slightly different parameter set and show that the temperature increase is about 2 times higher on the inner surface than on the outer surface.

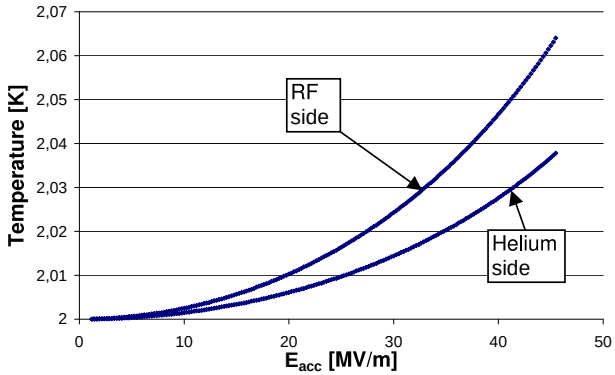

Figure 1.13: Temperatures on the RF side and the helium side of the niobium sheet. This simulation is done for B_{crit} = 240mT, a residual resistance of 6 nOhm, a niobium sheet thickness of 2.6 mm and a RRR=436 [Reschke 2001]. The $T_c(45MV/m)$ is 4.15 K.

1.5.2.2 Thermal conductivity

The thermal conductivity plays an important role for the maximum breakdown field if the cavity has a normalconducting defect on the surface. This can also be a niobium particle with bad thermal contact to the surface or a niobium tip where the field enhancement leads to a breakdown of superconductivity. The microwave surface resistance increases strongly above $T_c/2$ and reaches the value of normalconducting niobium at T_c. This is approximately 3 mΩ at 10 K.

One parameter to characterize the thermal conductivity of the niobium is the RRR, the residual (normalconducting) resistitivity ratio, which is defined as:

$$RRR = \frac{\rho_{nc}(300K)}{\rho_{nc}(4.2K)} \tag{1.38}$$

The specific electrical dc resistivity ρ consists according to Matthiessen's rule of a temperature dependent part $\rho(T)$ due to scattering with the lattice vibrations (phonons) and a residual resistance which is mainly due to impurity atoms [Schulze 1981]:

$$\rho_{nc}(T) = \rho_{res} + \rho_{phonon}(T) \tag{1.39}$$

For the temperature depending part one has $\rho(300K) = 1.46 \cdot 10^{-7}\Omega m$, $\rho(4.2K) = 8.7 \cdot 10^{-11}\Omega m$ [Fuss 1976]. The residual resistivity part is given by:

$$\rho_{res} = \sum_i \left(\frac{\Delta\rho}{\Delta C}\right)_i C_i \tag{1.40}$$

The coefficients for a few selected impurity elements are given in table 1.6.

Element	O	N	C	Ta	Zr
$\frac{\Delta\rho}{\Delta C}$ [10^{-11} Ωm/wt.ppm.]	2.64	3.49	3.33	0.12	0.6

Table 1.6: $\Delta\rho/\Delta C$ for different impurities in niobium [Hörmann 1986].

To relate the RRR with mean free path, one could assume Drude's law:

$$\rho = \frac{m v_F}{n e^2 \ell} \tag{1.41}$$

As for cryogenic temperatures Drude's law is not applicable and the derivation of a analytical formula is difficult, one reverts to the empirical formula [Bonin 1996]:

$$\ell \approx 2.65 \cdot RRR \qquad \text{where } \ell \text{ is given in nm} \tag{1.42}$$

There exists an empirical formula which holds for the thermal conductivity $\lambda_{thermal}$ [Padamsee et al. 1998]:

$$RRR \approx 4 \cdot \lambda_{thermal}(4.2K)[W/mK] \tag{1.43}$$

Some measurements on samples are shown in figure 1.12. Thermal model calculations (figure1.14) show that the thermal conductivity plays an important role to achieve very high RF magnetic fields. For the etched TESLA cavities, there is a considerable gain in performance with high RRR of 500 after postpurification since the defect size at 25 MV/m is then several ten μm. For fields of more than 150 mT (36 MV/m) the maximum defect size reduces down to about 10 μm.

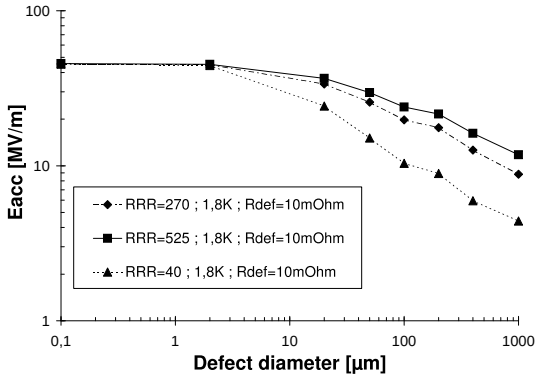

Figure 1.14: Simulation of the cavity performance in the presence of a normalconducting defect. Plotted is the maximum accelerating gradient below thermal breakdown as a function of defect diameter. These thermal simulations are done for 1.3 GHz and T_{bath} = 1.8 K assuming a critical magnetic field B_{crit} = 200 mT. The results indicate that at highest fields above 35 MV/m the defect size has to be extremely small [Reschke 1997].

1.5.3 Field emission

Field emission has been a serious limitation ever since accelerating cavities were built. Unfortunately, the superconducting cavities present no exception [Graber 1993], [Reece et al. 1995], [Reschke 1995], [Knobloch 1997], [Silari et al. 1999]. The high surface electric fields lead to electron emission from scratches or particles located on the surface via electron tunneling. Fowler and Nordheim developed a theory for the direct current case in which they found for the electron current emitted from a surface area A:

$$I_{FN} = A \cdot \frac{C}{\phi t^2(y)} E^2 \exp\left(-\frac{B\phi^{\frac{3}{2}} v(y)}{E}\right) \tag{1.44}$$

$B = 8\pi\sqrt{2m_e}/3he$ and $C = e^3/8\pi h$ are constants, ϕ is the workfunction of the metal. t(y) and v(y) are functions of $y = e^3E/4\pi\epsilon_0\phi^2$ which vary on slowly with electric field and can be set to 1 in first order approximation.

These electrons are subsequently accelerated inside the cavity and hit the walls. This process dissipates power and therefore can cause an exponential decrease of the quality factor with the accelerating field.

Although maximum care during assembly is taken at TTF it is by no means trivial to prevent field emission free nine-cell cavities. Several one-cell cavities have been assembled in the TTF infrastructure resulting in excellent performance without detectable field emission up to gradients of more than 40

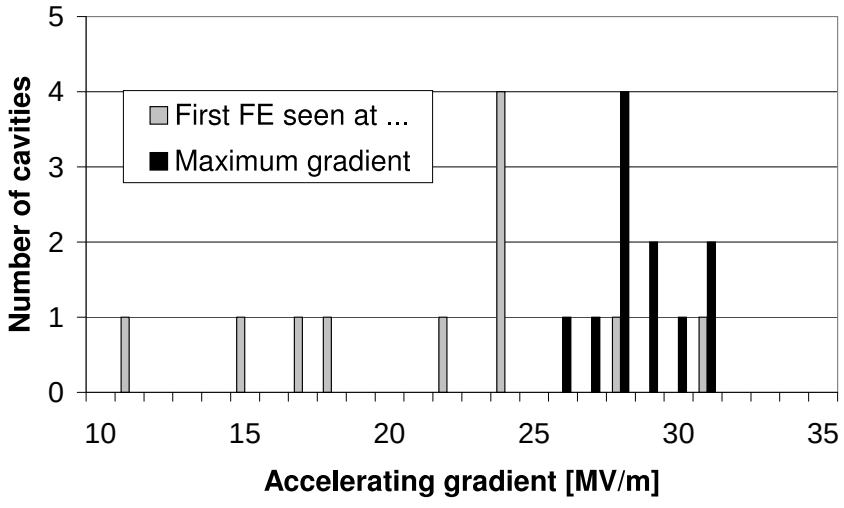

Figure 1.15: Accelerating gradient of the third production of TESLA nine-cell cavities shown in figure 1.8 when during the first power rise the first field emission signal is measured. Also shown is the maximum gradient of the test. A few cavities show no X-ray signal at all, whereas others show field emission at fields of 10 - 15 MV/m.

MV/m. The problem is more pronounced in multi-cell cavities. Their surface is larger, so that inevitably the chances to miss a field emitter during high pressure water rinsing are higher. In addition, electrons can be accelerated in a multi-cell through several cells, reach higher energies and therefore lead to a larger energy loss in the cavities [Stolzenburg 1996].

An interesting observation is that that the drop in quality factor is so similar in all the resonators shown in figure 1.8, although in figure 1.15 one clearly sees that field emission starts at significantly lower values of the accelerating field. We will see in the next part that the degradation is probably also due to another effect and that field emission contributes only partly to this behaviour.

1.5.4 Degradation of the quality factor without electron field emission

The curves shown in figure 1.8 are of similar shape, although the threshold for X-ray emission is quite different. Moreover in a few tests nine-cell cavities have shown virtually no x-rays at all (see figure 1.16). Hence field emission cannot be the only explanation for the quality factor degradation at high field. In 1-cell cavities at Saclay and other places a quality degradation at fields around 20 MV/m was observed without any sign of electron emission[10]. A detailed description will follow in chapter 4. For the moment it will be sufficient to describe the effect by an strongly increasing surface resistance above accelerating fields of around 20 - 25 MV/m. Apparently this "Q-drop without X-rays" shows up also in nine-cell cavities, as with the efforts of the TESLA collaboration the field emission thresholds have been pushed to a very high level.

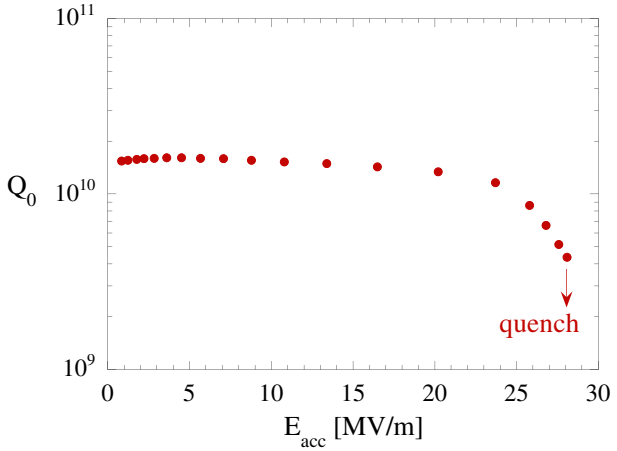

Figure 1.16: Excitation curve of a TESLA nine-cell cavity without field emission. The strong increase in surface resistance can be seen above 25 MV/m. Test was done at 2 K.

[10] See [Visentin et al. 1998], [Visentin et al. 1999], [Kneisel 1999], [Lilje et al. 1999].

1.5.5 Multipacting

Another phenomenon related to free electrons inside the cavity vacuum that can cause a limitation for resonators is called "Multipacting" [11]. This stands for multiple impacting. If some electrons are impinging on the cavity wall, they can cause the emission of secondary electrons. Dependent on the secondary electron emission coefficient (SEEC) which typically shows an energy dependence (figure 1.18), the number of new electrons can be larger than 1. These particles are accelerated in the electromagnetic field and hit eventually the wall again. If this process takes place in resonance to the RF phase, an avalanche of electrons will occur and cause the cavity to breakdown. When the electrons travel forth and back between two points on the cavity surface, this is called two-point multipacting (see figure 1.17).

A typical place for two-point multipacting to occur is the equator region of elliptical cavities. Temperature maps have shown this in 352 MHz cavities [Weingarten et al. 1984]. Fortunately, niobium has an SEEC very close to 1 as can be seen in figure 1.18. The SEEC depends delicately on the adsorbed gas layers. Usually, multipacting barriers can be passed within a few minutes. This means that the electrons in the avalanche force gases to be desorbed. In this way the surface can be cleaned and the SEEC will drop below 1. This process is usually called "Conditioning" or "Processing". In a measurement at Cornell University it has been has reported that multipacting at frequencies of 1.5 GHz takes place at field levels of around 17 MV/m and confirmed the hot spots via temperature mapping [Knobloch 1997, Knobloch et al. 1997].

Although not a serious limitation for the chemically etched nine-cell cavities so far, it should be mentioned that multipacting is seen during nearly every test of a 1.3 GHz cavity at TTF. The field level is between 17 - 20 MV/m. Typically, conditioning takes a few minutes or less in a continuous wave (cw) test. Figure 1.19 shows T-maps taken at different stages during conditioning on electropolished one-cell cavities. The heating is seen to move along the equator during conditioning until the SEEC is reduced below 1 in the whole area affected by the multipacting.

[11] See e.g. [Farnsworth 1934], [Hatch and Williams 1954], [Budliger and Laisne 1968].

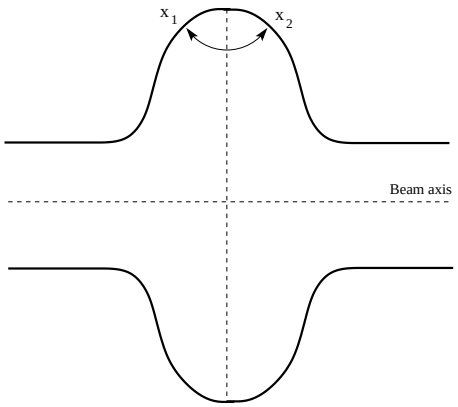

Figure 1.17: The two-point multipacting can occur in the equator region. Please note that the electron trajectories are exaggerated. The distance between the two impact points is typically in the order of a few millimeters to a centimeter [Knobloch 1997]. This is also visible in the temperature maps in figure 1.19.

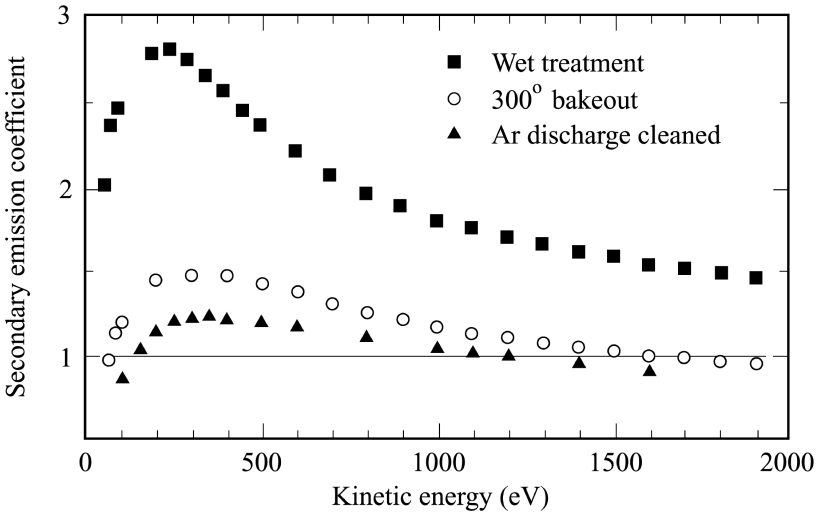

Figure 1.18: Secondary emission coefficient (SEEC) of niobium after different surface treatments [Piel 1989]. A bakeout at 300 °C leads to a strong reduction. This is due to the dissolution of the natural Nb_2O_5 layer which has a higher SEEC than niobium.

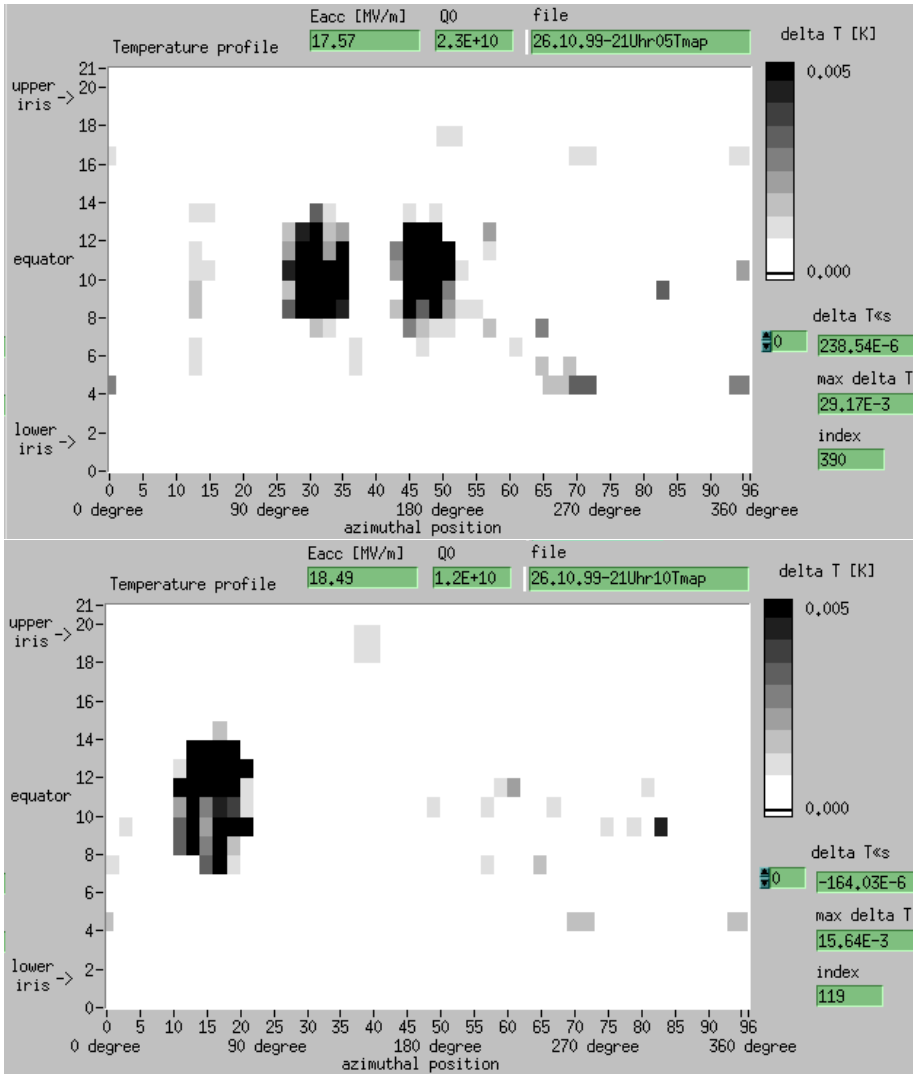

Figure 1.19: Temperature mappings on a 1.3 GHz one-cell cavity at different stages during conditioning of multipacting. After a few seconds of conditioning, the hot spot which can be seen at 17.5 MV/m is conditioned (top). A new area with heating appears at a slightly higher gradient of 18.5 MV/m (bottom). The full conditioning takes a few minutes. Note that the heating is typically much below 1 K, whereas in a thermal breakdown caused by material defects the temperature rises by several Kelvin.

Chapter 2

Electropolishing of niobium cavities

2.1 Introduction

In this chapter the electrolytic polishing of niobium will be discussed, as it allows to improve the accelerating gradients at which the breakdown occurs substantially. Results from KEK [Saito et al. 1997b, Saito et al. 1997a] have shown significantly higher breakdown fields of over 160 mT corresponding to about 40 MV/m in several electropolished 1.3 GHz one-cell cavities. These results have been achieved with niobium material of moderate quality RRR = 200. Up to date only one chemically etched L-Band cavity has achieved these surface fields corresponding to 40 MV/m [Kneisel et al. 1995]. High magnetic fields were previously observed in electropolished X-band cavities in the 1970s [Diepers et al. 1973][1]. A KEK-Saclay collaboration has convincingly demonstrated that EP raises the accelerating field by more than 7 MV/m with respect to BCP, while electropolished cavities suffer a clear degradation when they are subjected to a subsequent BCP [Kako et al. 1999]. Hence there is strong evidence that electropolishing is the superior surface treatment method. In the following chapter the method of electropolishing will be described in detail.

[1] See also references in [Kneisel 1980].

2.2 Surface treatments of niobium cavities

2.2.1 Chemistry basics

Niobium has a natural Nb_2O_5-layer with a thickness of about 5 nm. Below this natural layer other oxides and suboxides can be found [Grundner 1977, Grundner and Halbritter 1980, Dacca et al. 1998]. Nb_2O_5 is rather inert and can be dissolved only with hydrofluoric acid (HF). HF is an essential ingredient, in order to remove defects from the production process by dissolving either the defective material itself or the surrounding niobium. The defects can for example are abrasive particles from the grinding process, imprints from the forming, niobium protrusions from scratches or dirt particles on the surface. Cleaning the niobium surface with (electro-)chemical methods is the most practical way to achieve reproducible conditions on the large inner surfaces of TESLA cavities of about 1 m^2. These wet (electro-)chemical processes can be applied safely to niobium resonators, if the security and environmental standards regarding HF-containing acid mixtures are obeyed. Nitrous gases, oxygen and hydrogen can be produced during etching or electropolishing. A review including many references into the preparation of niobium cavities is given in [Kneisel 1980].

2.2.1.1 Chemical etching

Chemical etching is done by using acid mixtures that attack the Nb_2O_5 with HF and dissolve it. As HF dissolves pure niobium only very slowly, usually a strong oxidising acid is added to the mixture, which re-oxidises the niobium [Gmelin 1970, Hillenbrand et al. 1982]. The oxide will be dissolved by the HF again. The most frequently used oxidising agent for niobium is nitric acid (HNO_3). The material removal rate varies strongly depending on the contents of HF as well as the temperature of the acid mixture. A mixture of HF (40%) and HNO_3 (65%) removes 30 μm per minute [Hillenbrand et al. 1982]. As these reactions are strongly exothermic and large quantities of gases (hydrogen, nitrous gases, HF) are produced this mixture is not applicable to large surfaces.

For a better process control a buffer substance like phosphoric acid H_3PO_4 with a concentration of 85% can be added [Guerin 1989] and the mixture is cooled to temperatures below 15°C which also reduces the migration of hydrogen into the niobium material as described below [Hillenbrand et al. 1982, Röth 1993]. The standard procedure with a removal rate of about 1 μm per minute is also called "Buffered chemical polishing" (BCP) with an acid mixture containing 1 part HF, 1 part HNO_3 and 2 parts H_3PO_4 in volume.

Another possibility is to use concentrated sulphuric acid (H_2SO_4) as a buffer [Hillenbrand et al. 1982, Antoine et al. 1999].

It has to be mentioned that polishing is not quite the right term, as the acid attacks preferentially at the grain boundaries and therefore the surfaces are not as smooth as they can be achieved with electropolishing (see figure 2.7).

At TTF, a closed circuit chemistry system is used where the acid is pumped from a storage tank through a cooling system, a filter and the cavity back to the storage. The gases produced are not released into the environment without prior neutralization and cleaning. The cavities are rinsed with low pressure ultrapure water immediately after the chemical treatment.

By now there exists compelling evidence (see section 4.1) that the etching process with BCP limits the accelerating fields of cavities to about 25 - 30 MV/m even if the thermal conductivity of the niobium is excellent due to the postpurification used for TTF nine-cell cavities. Typical accelerating gradients achieved with BCP are shown in figure 1.9. These results are consistent with measurements on etched one-cell cavities in other labs [Safa 1997, Saito et al. 1997b, Kneisel 1997]. Only in rare cases etched cavities exceeded 30 MV/m [Kneisel et al. 1995].

In addition, the etching process is accompanied by undesired effects like insertion of hydrogen into the niobium bulk and grain boundary etching. The first effect can be reduced by cooling the acid below 15°C [Röth 1993]. Grain boundary etching can in principle strongly suppressed by using an acid mixture with a high etching rate. This, however, is not possible in nine-cell TESLA cavities with their large surface area, since the reaction would become too fast and a large amount of heat is generated which again speeds up the reaction. This is very difficult to control and should be avoided.

2.2.1.2 Electrolytic polishing

An alternative method to etching is electrolytic polishing or "electropolishing" (EP) in which the material is removed in an acid mixture under flow of an electric current. Sharp edges and burrs are smoothed out and a very glossy surface can be obtained. The major advantage of this method is a much improved control of the chemical reaction, as a further control parameter namely the electric voltage is introduced. The electrical field is high at protrusions, so that the niobium will be dissolved first. On the contrary in the grain boundaries the field is low and no material will be removed. There are competing theories about the mechanisms of EP. The basic ingredient in all theories is a viscous layer of electrolyte forming near the anode [Ponto and Hein 1986] which is the basis for the smoothening effect as is shown in figure 2.1.

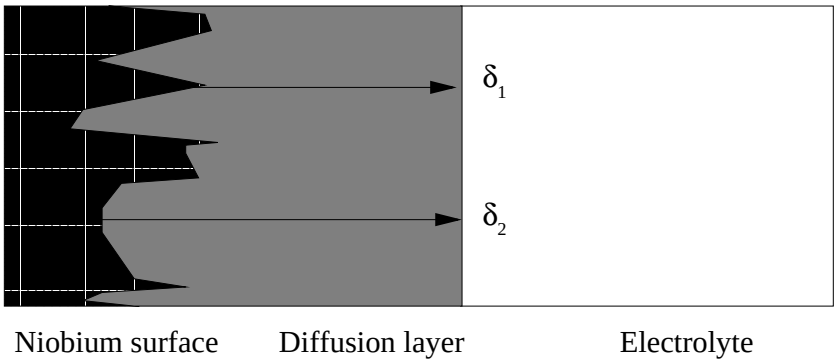

Figure 2.1: Schematic of the viscous layer near the anode in the electropolishing process. The thickness of the layer determines the current flowing. Therefore, more current flows along δ_1 than along δ_2. The peak will be smoothed out first.

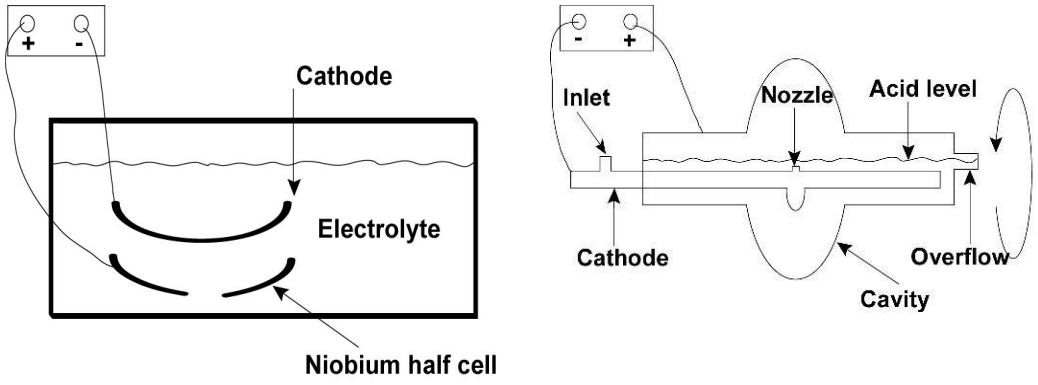

Figure 2.2: Left: Schematic of a halfcell EP system. Right: Schematic of a cavity EP system. Detailed descriptions of the two systems are given in the text.

The simplest idea is to assume that a current passing through the electrolyte experiences a higher viscosity and resistivity than the rest of the liquid. For a rough surface the thickness of the film varies. Above protrusions it is thinner and hence the resistivity lower. Therefore the current density becomes higher at these places and they dissolve faster. The time needed to form this layer is typically in the order of milliseconds. For strongly agitated electrolytes the above explanation does not seem to work anymore.

Electropolishing of niobium cavities has been known since 30 years. The most widely used electrolyte is a mixture of concentrated HF and concentrated H_2SO_4 in volume ratio of 1:9 [Diepers et al. 1971b]. A pulsed electric current was used in a horizontal EP setup for superconducting niobium cavities at CERN in collaboration with Karlsruhe [Citron et al. 1979]. A continuous method for horizontal EP has been developed at KEK [Saito et al. 1989].

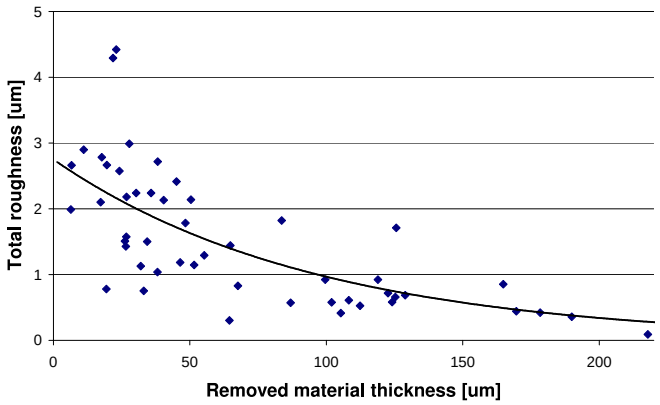

Figure 2.3: Measured surface roughness of several electropolished niobium samples depending on the amount of material removed [Ferreira 1998]. The surface becomes smoother with removing more material. These results are in good agreement with data from KEK [Saito et al. 1997b].

The chemical processes are summarized as follows [Kneisel 1980], [Ponto and Hein 1986]:

$$2\mathrm{Nb} + 5\mathrm{SO_4^{--}} + 5\mathrm{H_2O} \rightarrow \mathrm{Nb_2O_5} + 10\mathrm{H^+} + 5\mathrm{SO_4^{--}} + 10\mathrm{e^-} \quad (2.1)$$

$$\mathrm{Nb_2O_5} + 6\mathrm{HF} \rightarrow \mathrm{H_2NbOF_5} + \mathrm{NbO_2} \cdot 0.5\mathrm{H_2O} + 1.5\mathrm{H_2O} \quad (2.2)$$

$$\mathrm{NbO_2} \cdot 0.5\mathrm{H_2O} + 4\mathrm{HF} \rightarrow \mathrm{H_2NbF_5} + 1.5\mathrm{H_2O} \quad (2.3)$$

Most systems for EP of accelerator cavities are horizontal as shown in figure 2.2. The horizontal system has a variety of advantages. Most notably all produced gases (mainly hydrogen) can be kept away from the niobium surface [Citron et al. 1979]. This avoids concentration inhomogeneities in the viscous layer. Gas bubbles sticking on the surface would produce etching pits. In a vertical setup these bubbles would slowly move upwards along the upper half cell's surface and cause radial wells [Bloess 1998]. A disadvantage of the horizontal arrangement is that the cavity has to be rotated. It is not trivial to achieve a leaktight rotary sleeve for this acid mixture. In addition the speed of the removal is reduced by a factor of two as the surface is immersed only half of the time in the acid to allow the hydrogen gas to escape through the upper part of the beam tube.

2.2.1.3 Oxipolishing

Yet another important electrochemical process for the surface preparation of niobium is a procedure called "Oxipolishing" [Hillenbrand et al. 1982, Kneisel 1980]. The niobium surface is anodized using an electrolyte[2]. Various electrolyte can be used, but the most common for niobium are diluted $NH_4(OH)$, diluted HNO_3 and diluted H_2SO_4. The thickness of the oxide layer produced can be adjusted with the applied voltage. For 50 V one gets a layer of 100 nm. In a second step this layer is dissolved with HF. One can regard this as a step-by-step EP. The advantage of OP is that very tiny thicknesses can be removed. But this implies that for a removal of only 1 μm already several steps are needed. It is important to note that contaminations like fluorine or sulphurus from (electro-)chemical preparations can be removed very efficiently by oxipolishing [Kneisel 1980, Ferreira et al. 1999b].

2.2.1.4 Comparison of etched and electropolished surfaces

In figure 2.7 BCP and EP treated niobium samples are compared. One can see that the BCP does not smooth out the grain boundaries as well as EP. The average roughness of chemically etched niobium surfaces is in the order of $R_a = 1\mu$m [Antoine et al. 1999, Kläui and Lilje 2001]. The step height on etched surfaces at grain boundaries can be even in the order of a few μm (see figure 2.5). In the area of the electron-beam-weld which is also the region of the highest magnetic surface field the steps can be as high as 30 μm and are nearly perpendicular to the magnetic field lines [Geng et al. 1999]. It is well-known that surface roughness can lead to an geometric field enhancement and therefore to a local breakdown of superconductivity at lower field [Knobloch et al. 1999] (see section 5.3).

This interpretation is underlined by the fact, that in several chemically etched cavities showing a breakdown no foreign inclusions was found during inspection. Typically, breakdown occurs in the high magnetic field region as shown in figure 2.4. It has been observed that is possible to shift the quench position along the equator region with a new chemical etching, but the maximum achievable field is not improved [Kako et al. 1997], [Kako et al. 1999].

[2] Anodization was also used to form a protective layer of dielectric oxide on the niobium surface [Diepers et al. 1971a].

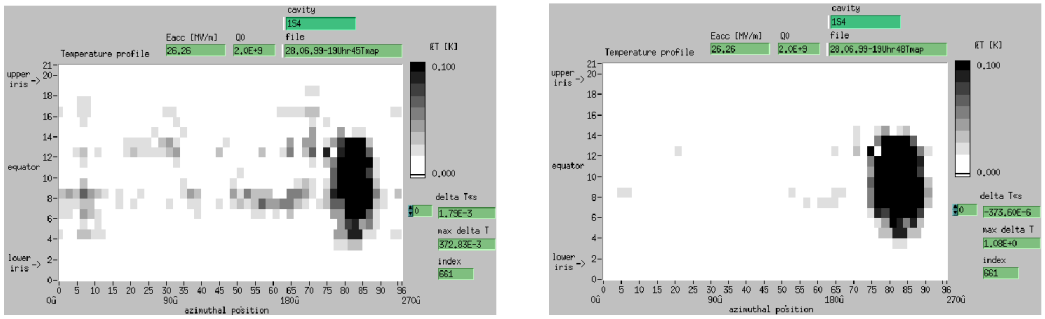

Figure 2.4: Quench location in an etched cavity. The left picture shows the breakdown with the incident power level adjusted to the minimum level needed for the breakdown. One can see both, the average heating in the high magnetic field region is in the order of 100 mK and the average heating in the thermal breakdown area (300 mK) . In the right picture more incident RF power was used so that the quench location heats up much more (1 K).

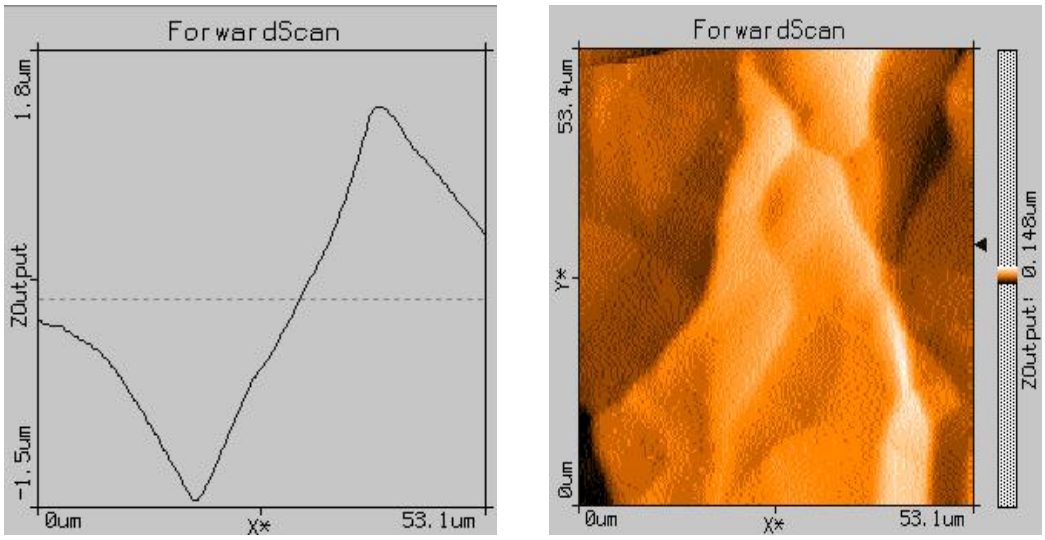

Figure 2.5: Atomic force microscope (AFM) measurements on chemically etched samples [Kläui and Lilje 2001]. A surface step of about 3 μm at a grain boundary is shown.

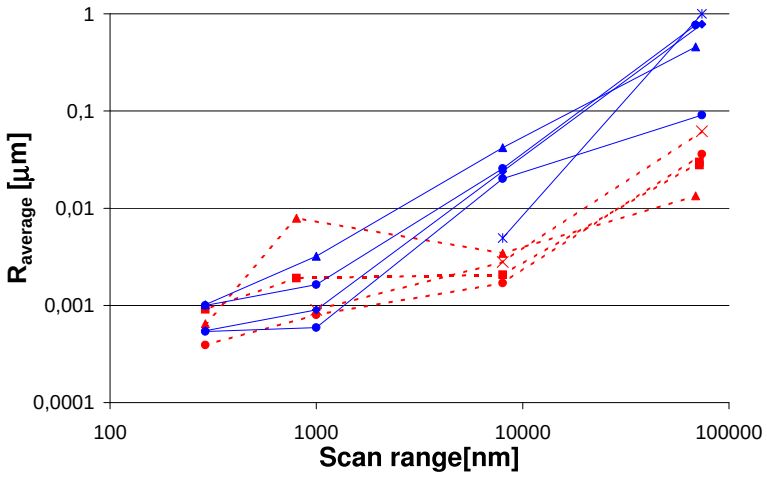

Figure 2.6: Average roughness as a function of the scan length of the atomic force microscope [Kläui and Lilje 2001]. EP samples are shown with dotted lines, while BCP samples are shown with full lines. At large scan length EP yields about one order of magnitude lower average roughness than BCP. At lower scan length the difference between EP and etching becomes smaller. The reason is that at small scan length, one stays on top of a single grain, whereas for large scan length the grain boundaries give the main contribution to the roughness.

The roughness on the EP surface is typically one order of magnitude lower than that of an etched sample on length scales larger than 10 μm as can be seen in figure 2.6. On the nanometer scale the roughness is comparable. This can be explained by the fact that for a small scan length the measurements takes place on top of a single grain. The main difference between EP and etching is the smoothening of the grain boundaries. These are measured only when the scan length is sufficiently large. [Antoine et al. 1999] claim that there exists a scan length ($\approx 1\mu$m) where electropolishing gives a rougher surface. This could not be verified in the present measurements as seen in figure 2.6.

An important question for electropolishing is of course how much material has to be removed to achieve a smooth surface. On electropolished samples the total roughness drops below 1 μm after 150 μm of material have been removed as can be seen in figure 2.3. As a layer of 100 - 150 μm has to be removed anyway from the cavity due to the damage done during the manufacturing process, as described in section 1.4 , it is reasonable to do an EP of at least 100 μm on a cavity after manufacturing to achieve both the smoothening of the surface and the removal of the damage layer removal.

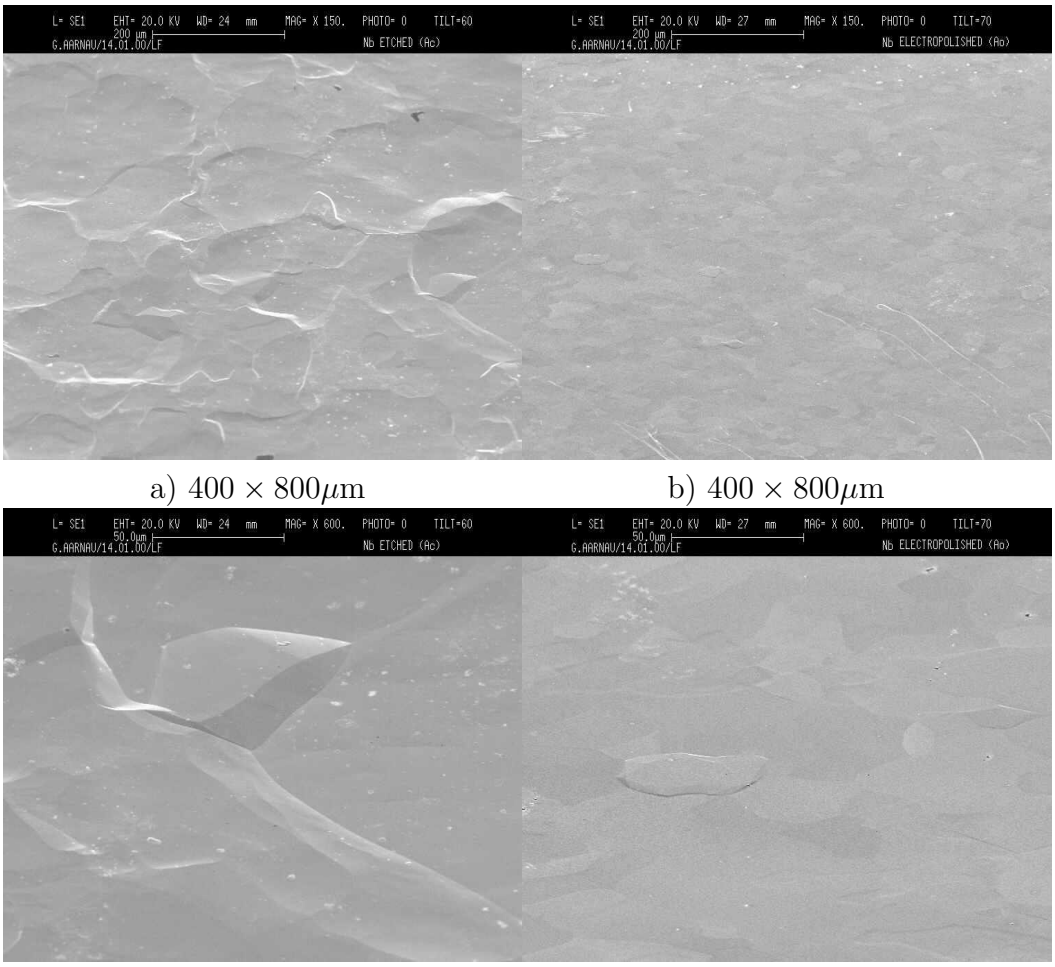

a) $400 \times 800\mu$m b) $400 \times 800\mu$m

c) $100 \times 200\mu$m d) $100 \times 200\mu$m

Figure 2.7: Niobium surfaces after etching (left) and electropolishing (right). SEM micrographs are courtesy of CERN [Ferreira et al. 1999a].

2.2.2 Detailed description of the EP systems

2.2.2.1 Half cell electropolishing

The results from KEK led the TESLA collaboration to investigate the electropolishing for niobium. In cooperation with CERN a setup for the EP of half cells was developed within this thesis. In this setup an electrolyte developed at CERN [Birabeau and Guerin 1974, Birabeau and Guerin 1982] was used (refer to table 2.1). It is especially interesting, as the rate of removal is typically 1 - 2 μm per minute and therefore higher than that developed by the Siemens company [Diepers et al. 1971b] which is typically below 1 μm per minute. A pre-polishing of about 100 μm was applied to the half cells. Here the idea was to do most of the polishing process on simple subunits. Then 4 cavities were electron-beam welded at a company with a standard procedure using a vacuum of around 10^{-5} mbar. 11 cavities were welded at CERN with a much better vacuum between $5 \cdot 10^{-7}$ and $2 \cdot 10^{-6}$ mbar.

Two tests on one-cell cavities were carried out applying only high pressure rinsing after welding. The results were disappointing as can be seen in figure 2.8. The first cavity showed a degradation at 2 MV/m without a sign of field emission. The field emission started at 5 MV/m. As the CERN half-cell electropolishing system uses a copper electrode, the degradation was assumed to be due to a layer of copper on the surface. The second cavity was therefore rinsed with nitric acid and a small chemical etching of 2 μm was applied. The degradation at very low field disappeared, but the onset of field emission was still on a very low level. After a further etching of 20 - 50 μm both cavities improved their performance substantially to values of about 25 MV/m, which are standard for chemically etched cavities with a RRR = 200 - 300. Therefore a chemical treatment or possibly EP in the order of 20 - 50 μm after electron-beam-welding appears unavoidable to remove weld spatter and deposited niobium vapour.

2.2.2.2 Electropolishing of complete cavities

The setup for the electropolishing of single-cell cavities built in collaboration with CERN will be described now. To make use of the experience at KEK the most important parameters were chosen very similar to the KEK system [Saito et al. 1989] and are shown in table 2.1. An overview of the system is shown in figure 2.9.

Due to the strong acids used in the EP, only a few materials are possible to use. Especially for HF only fluoroplastics are applicable. All parts in contact with the acid should be either made from PFA[3], PVDF[4] or PTFE[5].

[3] Polyperfluoroalkoxyethylene
[4] Polyvinylidene Fluoride
[5] Polytetrafluoroethylene, also called Teflon®

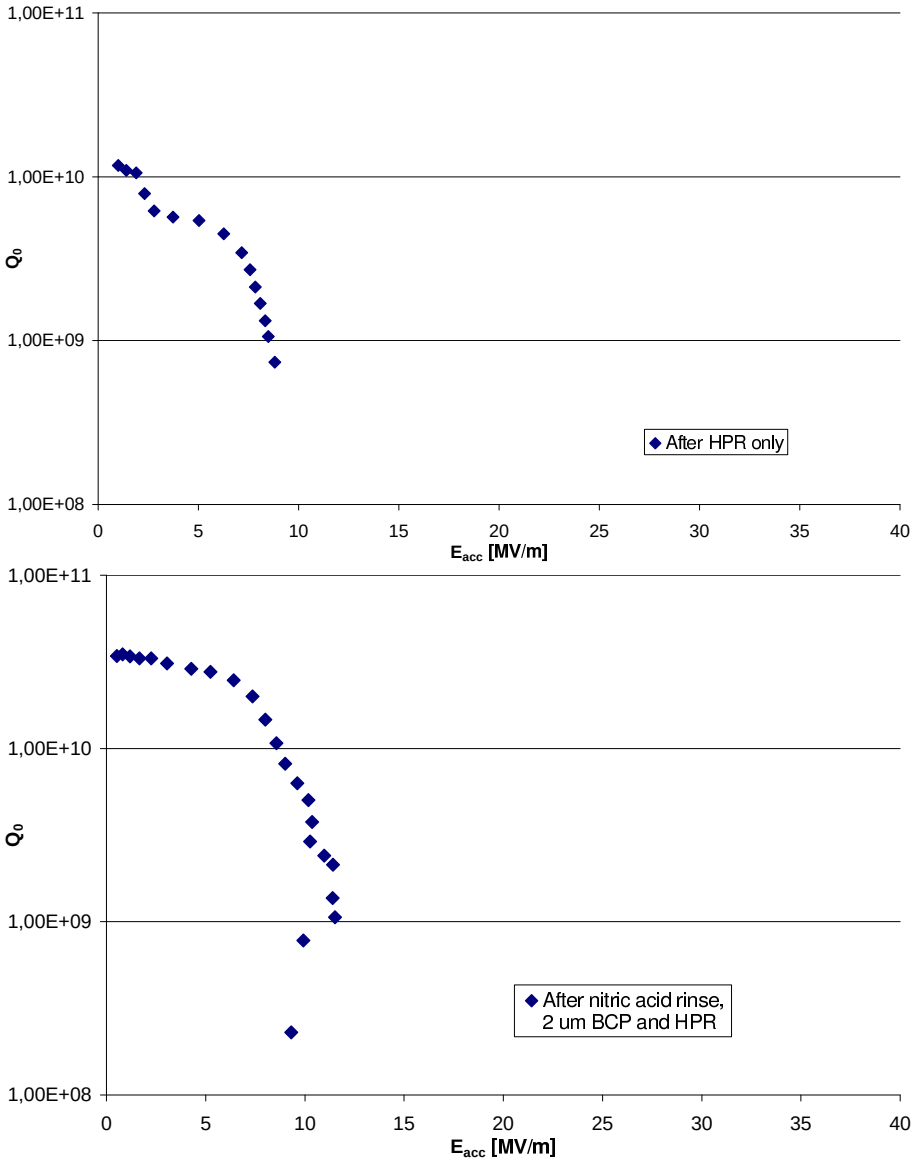

Figure 2.8: Tests on niobium cavities welded from electropolished half cells. One cavity was tested with high pressure ultra-pure water rinsing only. A clear degradation of the quality factor is seen a very low field. Field emission starts at 5 MV/m. The other cavity was rinsed with nitric acid and a very short etch of only 2 μm was applied. The degradation at low field disappeared. Field emission started at 8 MV/m. Both cavities improved their performance substantially after further etching.

The whole system has to be placed in a vented area where the exhaust gases are pumped through a neutralisation system to avoid any environmental hazards. The acid mixture should be used in a closed-circuit, as this is a much safer procedure. The electrolyte is stored in containers cladded with Teflon which can be cooled via cold water flowing through Teflon-covered piping. The volume above the electrolyte can be covered with dry nitrogen to avoid a degradation due to water vapour absorption by the strongly hygroscopic H_2SO_4. The acid mix is pumped with a membrane pump through a cooler and a filter with 1 μm pore size before it reaches the inlet of the cathode. Then the electrolyte flows through the cathode to the center of the cell (see figure 2.2(b)). The acid flows back to the storage tank via an overflow.

After the cavity is installed horizontally in the system with the cathode, the pump will be started to fill the lower half of the cavity with electrolyte. The acid mixture attacks the niobium very slowly when no voltage is applied. Typically less than 1 nm per hour is removed without applied voltage. After the equilibrium filling level is reached, the rotation is switched on and a leak check is done. When now the current is switched on, the current-voltage characteristic is measured quickly. The voltage applied is increased in steps of 1 V and the current is measured. After this preparation the voltage is set to the value where the current oscillations are at a maximum. Typical values are shown in table 2.1 with a current oscillation of about 10 - 15% around the average value. The temperature has to be around 30 - 35°C during the EP. Too high a temperature ($>$ 40°C) would result in pits on the surface, which have to be avoided.

When the desired amount of material has been removed, the current is switched off. The rotation is stopped and the cavity is put into vertical position to empty the acid from the resonator. Then the cavity is dismounted and rinsed with pure water. Here also the electrode is dismounted. Another low pressure water rinsing follows and the wet cavity is taken into a glovebox with nitrogen atmosphere. Here the cavity is rinsed with an ultrapure high pressure water jet to to remove remaining chemical residues. A rinsing with filtered butanol is applied to improve the drying process. The cavity is then stored overnight in vacuum at around 10^{-3} mbar [Ehmele 2000]. Then the cavity is either rinsed with high pressure water at CERN or filled with nitrogen gas and sent to CEA or DESY for high pressure water rinsing and tests.

For the cathode either pure aluminium or copper can be used. In the CERN setup copper is used, while KEK uses aluminium. It should be mentioned that a copper electrode has a disadvantage: While the current is flowing, the copper surface becomes passivated and is not attacked by the acid

EP for half cells	24 %	HF 40%
Acid mixture	21 %	H_2SO_4 96%
	38 %	H_3PO_4 83 %
	17 %	Butanol
Voltage	4 - 6	V
Current density	100 - 140	A/cm^2
Removal rate	1 - 2	μm/min
EP for cavities	10 %	HF 40%
Acid mixture	90 %	H_2SO_4 96 %
Voltage	15 -20	V
Current density	50 -60	A/cm^2
Removal rate	0.5	μm/min
Temperature of electrolyte	30 - 35	°C
Rotation	1	rpm
Acid flow	5	l/s

Table 2.1: EP parameters for the EP of half-cells and the EP of one-cell cavities at CERN.

mixture. But when the current is switched off copper ions can be dissolved and can precipitate on the niobium. It was observed in a test that this leads to an increased residual resistance and to strong field emission level below 10 MV/m (see figure 2.8). Therefore a further rinsing step was introduced at CERN after the first low pressure water rinsing after EP. The cavities are now rinsed in sequence with concentrated HNO_3 (60 %), water, HF and water again. These steps are repeated twice. The HNO_3 removes the copper and oxidise the niobium. Hydrofluoric acid removes the oxide layer and several contaminants as indicated by surface studies [Ferreira et al. 1999b]. One might call this an oxipolishing where the natural oxide layer is removed only two times. The overall removal by this step in the preparation is about 10 nm. After this the cavity will go into a glove box with nitrogen atmosphere and will be high pressure water rinsed.

An important point should be mentioned here as it will become more relevant in chapter 4. At DESY, CEA and CERN no heating above 50°C is applied to the cavities after they have been fitted with antennas and vacuum valves for the cryogenic test. In contrast at KEK and also CEBAF a heating above 80°C is part of the standard procedure to remove the water film adsorbed to the niobium more easily to improve vacuum conditions. Due to the wet chemical processes and the several rinsing treatments, water sticks on the surface in abundance. When the degradation of the quality factor at high accelerating fields will be discussed, this heating treatment plays an essential role to cure this degradation.

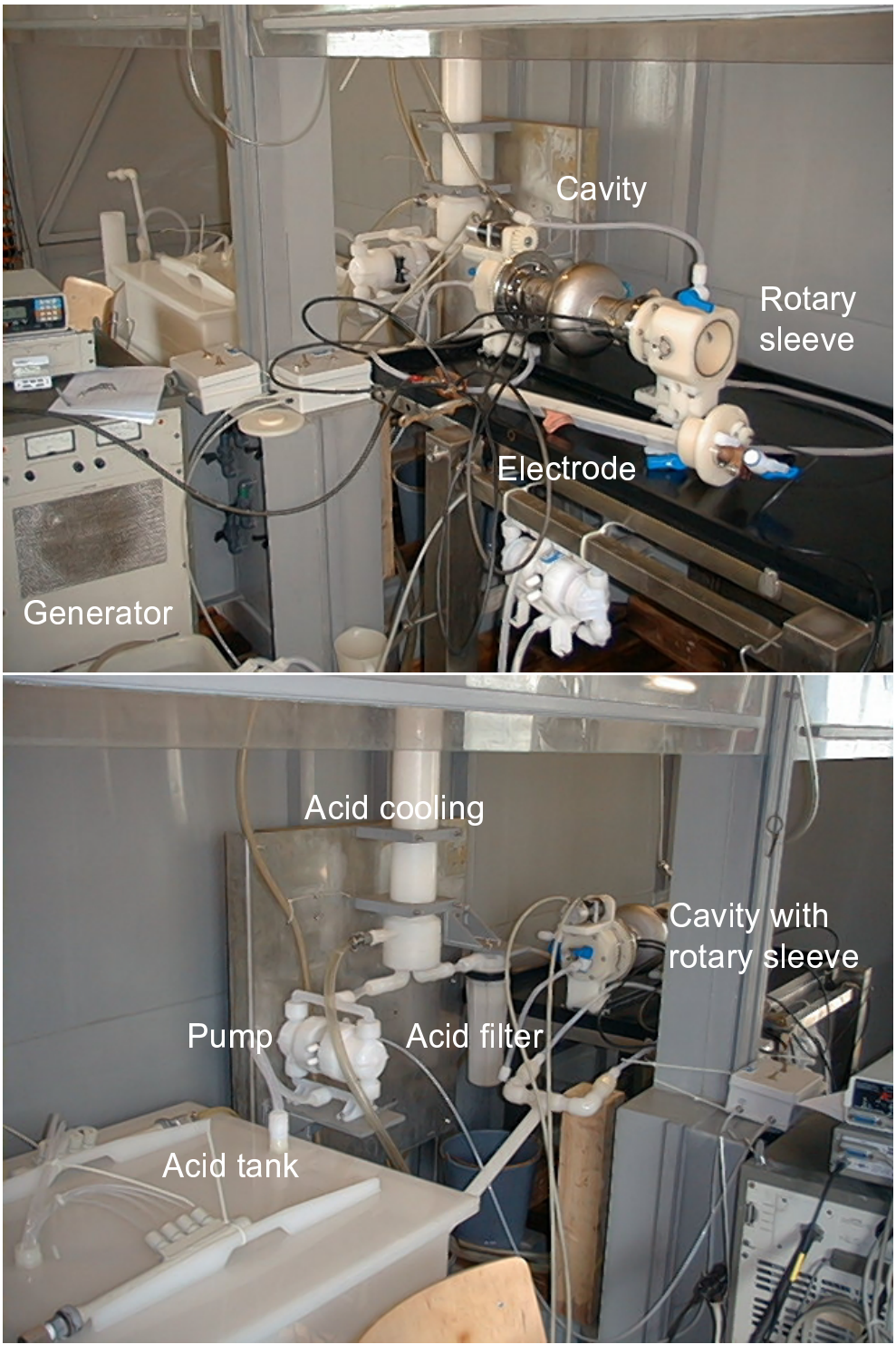

Figure 2.9: Pictures of the closed one-cell electropolishing setup at CERN. The setup is housed in a vented area.

Chapter 3

Results on electropolished cavities

3.1 Description of the measurement setup

The cavity is equipped with input and pickup antennas and vacuum sealed in a class 10 cleanroom and then transferred to the test cryostat[1]. A layout of the cryostat is shown in figure 3.1. The input antenna is connected via a bellow to the cavity, so that the distance between antenna tip and cavity can be changed. The fundamental TM_{010} mode of the cavity is below the cut off frequency of the beam tube. Thus the electromagnetic field decays exponentially in the pipe (see figure 3.2). As a consequence the coupling strength of the input coupler can be varied by several orders of magnitude by moving the center piece of the input coupler by a few centimeters. In the TTF vertical test cryostats[2] the external coupling of the input antenna can be varied from about $Q_{ext} = 5 \cdot 10^8$ up to $Q_{ext} = 5 \cdot 10^{10}$ so that a matched coupling ($Q_{ext} = Q_0$)[3] can be achieved in the temperature range from 4.2 K to 1.6 K. The second antenna is used as a pickup probe with a much higher $Q_{ext} \geq 10^{11}$ for monitoring the cavity field which is proportional to the square root of the power coupled out by the antenna.

The pickup signal is also used for the feedback loop (see figure 3.3). As the superconducting cavities have a very high quality factor the width of the resonance curve is extremely small ($\approx \frac{1}{10}$ Hz). Small changes in the

[1] A very detailed description of the measurement setup can be found in [Padamsee et al. 1998, Pekeler 1996, Knobloch 1997].

[2] In this cryostat the antenna is fixed, while the cavity is moved via a linear motor.

[3] This means that all the input power is dissipated in the cavity i.e. $P_{\text{inc}} = P_{\text{diss}}$ and no power is reflected. The case of non-critical coupling is treated in detail in [Padamsee et al. 1998, Pekeler 1996].

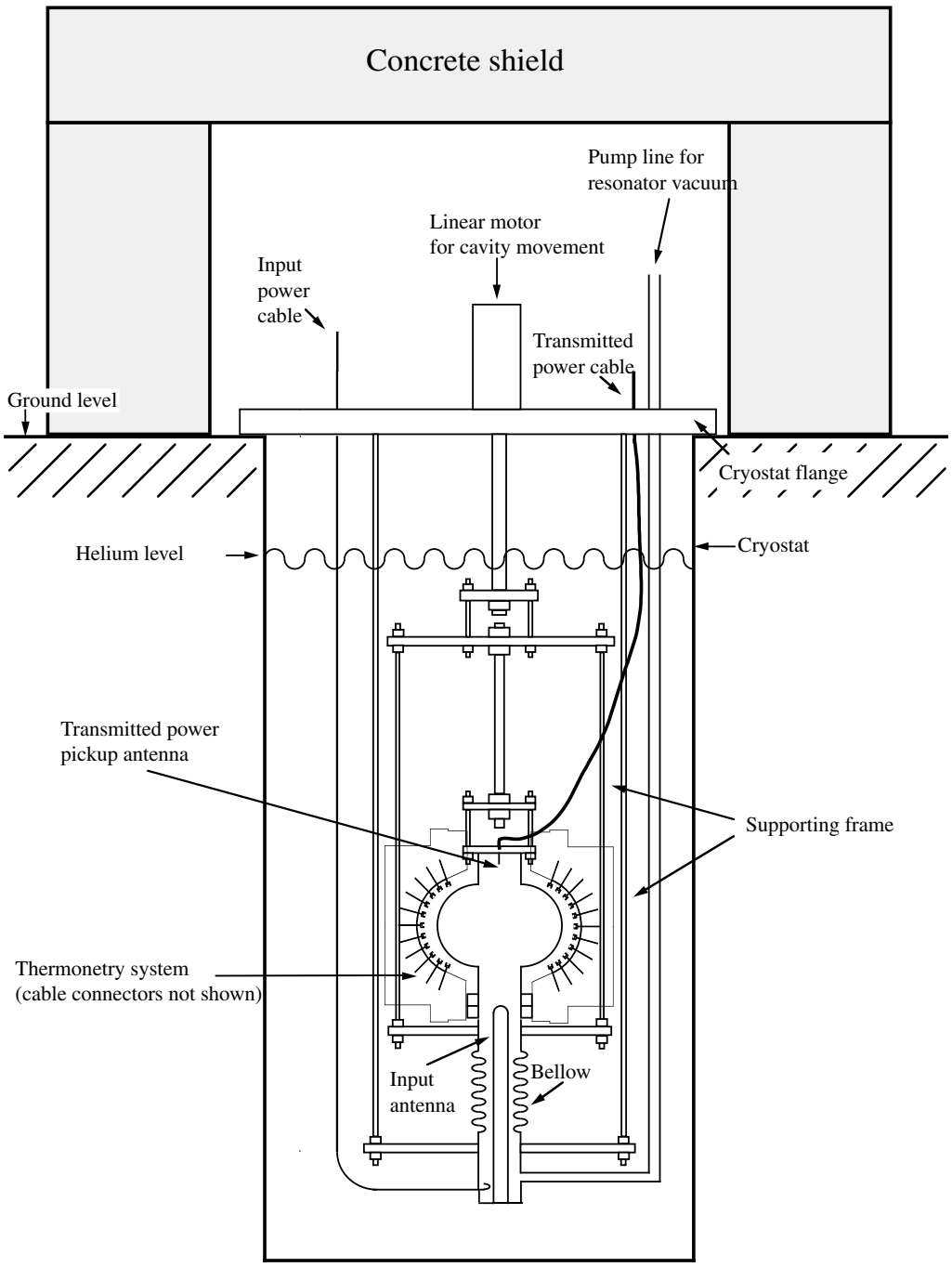

Figure 3.1: Schematic of the vertical cryostat used for continuous wave measurements. The cavity is fully immersed in superliquid helium. The thermometry system consists of 768 carbon resistors mounted on 24 boards surrounding the cavity [Pekeler 1996].

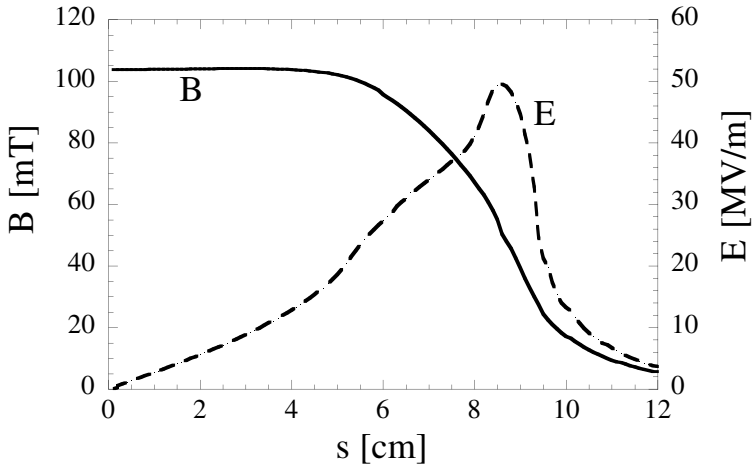

Figure 3.2: Local magnetic and electric field along the cavity surface. $s = 0$ corresponds to the equator of the cavity. Field values have been calculated for 25 MV/m [Pekeler 1996].

helium pressure of the cryostat cause changes of the resonance frequency of the cavity. Therefore the frequency generator has to be controlled with a phase-locked loop (PLL), where the phase difference between the input signal, taken from a directional coupler, and the pickup signal are compared.

The thermometry system [Pekeler 1996] consists of 768 carbon resistors. To ensure thermal contact with the niobium even in superfluid helium, the resistors are glued to the surface with Apiezon N grease, which has a high heat conductivity at helium temperature.

When the cavity is mounted in the cryostat, it will be first cooled with liquid helium at 4.2 K (atmospheric pressure). Cooling down to 2 K is achieved via pumping down the helium down to 30 mbar. The cryogenic power available is about 100 Watts at 2 K.

3.1.1 Quality factor

The quality factor of the cavity is measured when the incident power is switched off. Then the field excited in the cavity decays exponentially. One can use the differential equation

$$P_{\text{total}} = -\frac{dU}{dt} , \qquad \text{with} \qquad P_{\text{total}} = P_{\text{diss}} + P_{\text{ext}} + P_{\text{t}} . \tag{3.1}$$

where P_{diss} is the power dissipated in the cavity, P_{ext} the power coupled out via the input antenna and P_{t} the power coupled out from the pickup probe. Usually, the pickup probe is very weakly coupled, so that P_{t} can be neglected.

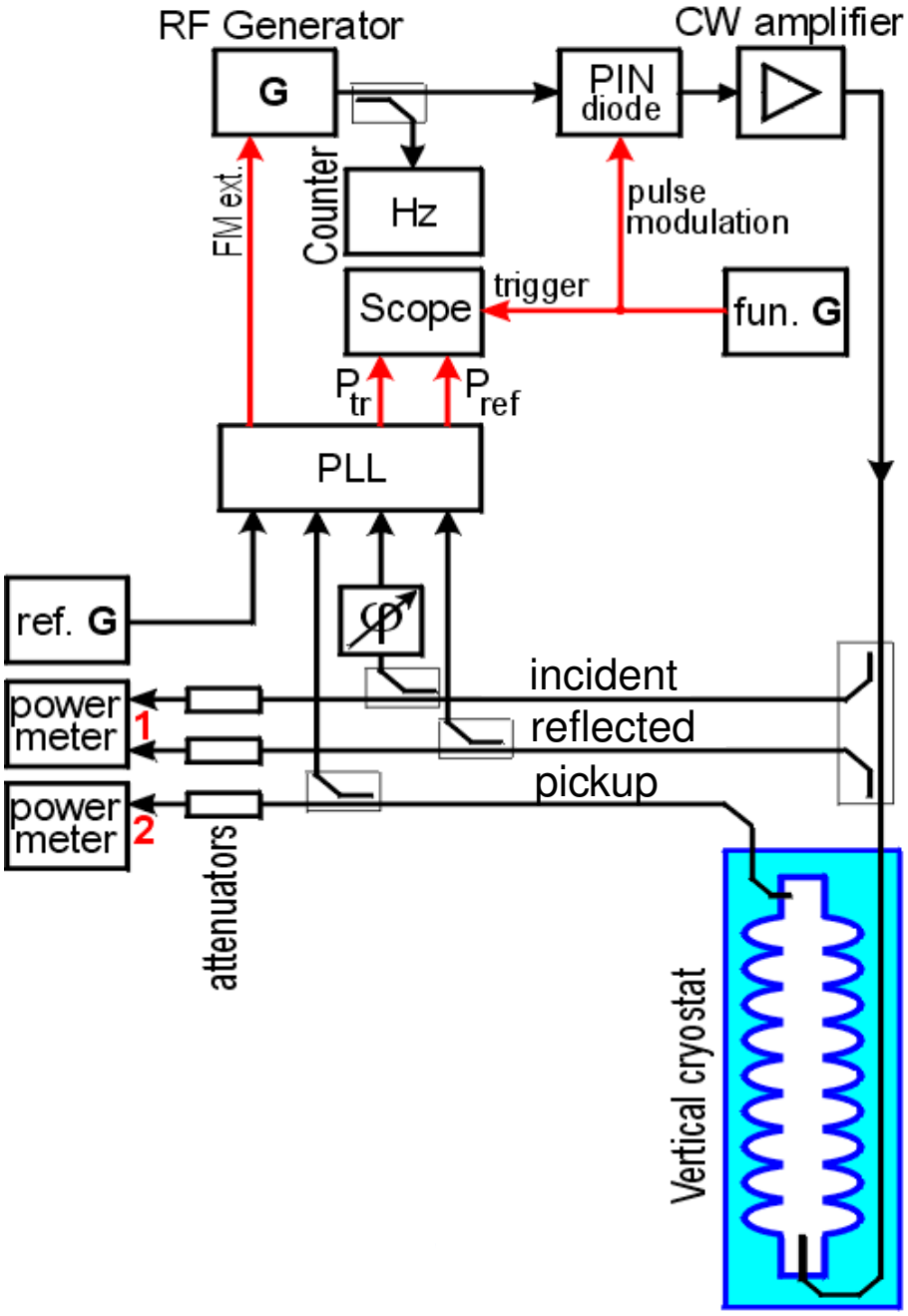

Figure 3.3: Schematic of the cavity testing system at TTF. Shown are the components which are needed to the incident, reflected and pickup power and the feedback circuit [Pekeler 1996, Gössel et al.].

The external quality factor Q_{ext} is defined by:

$$Q_{\text{ext}} = \frac{\omega U}{P_{\text{ext}}} \,, \tag{3.2}$$

The loaded quality factor Q_{L} is defined by:

$$Q_{\text{L}} = \frac{\omega U}{P_{\text{total}}} \,, \tag{3.3}$$

Hence one can relate

$$\frac{1}{Q_{\text{L}}} = \frac{1}{Q_0} + \frac{1}{Q_{\text{ext}}} \tag{3.4}$$

Integrating the differential equation gives:

$$\begin{aligned} U(t) &= U_0 \cdot \exp\left(-\frac{t}{\tau_{\text{L}}}\right) \,, \\ \text{where} \qquad \tau_{\text{L}} &= \frac{Q_{\text{L}}}{\omega} \,. \end{aligned}$$

Therefore from measuring the decay time τ the loaded quality factor Q_{L} can be determined. In the case of critical coupling one has:

$$Q_{\text{L}} = \frac{Q_0}{2} \tag{3.5}$$

3.1.2 Accelerating gradient

The accelerating gradient can be calculated via:

$$E_{\text{acc}} = k_{\text{e}}\sqrt{U} = k_{\text{e}}\sqrt{\frac{P_{\text{diss}} Q_0}{\omega}} \,. \tag{3.6}$$

The proportionality factor k_{e} of accelerating gradient and stored energy is only dependent on the geometrical layout of the resonator which can be calculated using numerical codes. In the case of the single-cell cavities tested in this thesis $k_{\text{e}} = 8.35(\text{MV/m})/\sqrt{\text{J}}$. All the measurements reported here are continuous wave measurements.

3.2 Cavity measurements

3.2.1 Comparison of etching and electropolishing

The test results on etched single-cell cavities are very consistent with the performance achieved in the TESLA nine-cell cavities. The average gradient achieved in the one-cell cavities without any heat treatment is 24 MV/m. Limitation is thermal breakdown in nearly all cases. If one takes the single-cell performance of those etched nine-cell cavities which were tested between the 800°C and 1400°C heat treatments an average gradient of 23.5 MV/m and again the main limitation is thermal breakdown. Only the 1400°C heat treatment which is routinely applied to the etched cavities will allow to achieve the gradient of more than 25 MV/m routinely as has been shown in figure 1.7.

A summary of the performance after etching and electropolishing is given in figure 3.4. The average gradient of the batch of electropolished cavities is 35.7 MV/m. Therefore it is very clear that electropolishing leads to higher gradients. The smoother surface offers less defects and is easier to clean from chemical residues as will be discussed in chapter 5.

3.2.2 High temperature heat treatments of electropolished cavities

3.2.2.1 Q-disease and 800°C annealing

During the process of electropolishing hydrogen is produced which can enter the niobium lattice very easily. It is well-known that the amount of interstitial hydrogen in very pure niobium must be kept below certain limits [Röth 1993]. If too much hydrogen is dissolved in the niobium a subtle effect called "Q-disease" can occur. The dissolved hydrogen forms niobium hydrides at temperatures around 100 K. These Nb-H compounds have very high microwave losses and raise the residual resistance by more than an order of magnitude.

The concentration of hydrogen should be kept below the concentration levels of interstitials which can trap the hydrogen, so that no hydride formation can take place [Röth 1993]. For a RRR≈30 material a hydrogen concentration of over 800 atppm is tolerable. The typical values of etched niobium are in the order 100 - 400 atppm hydrogen in the bulk material and 4 at% in a surface layer of about 50 nm [Röth 1993]. Cooling the acid to temperatures below 15°C keeps the concentration below 200 atppm. High temperature treatments at 800°C reduce this level to a concentration of 3 atppm

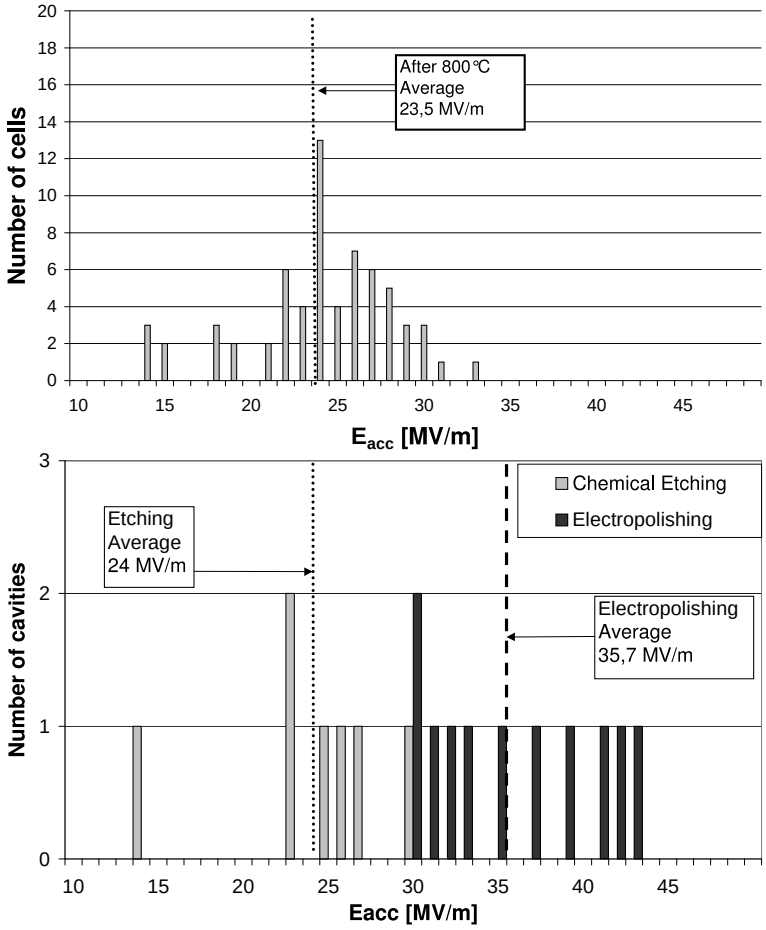

Figure 3.4: Top: Distribution of the single-cell performance of nine-cell TESLA cavities after 800°C heat treatment only. The average is 23.5 MV/m. Bottom: Distribution of the maximum accelerating gradients of etched and electropolished single-cell cavities. The average gradient for etched cavities is 24 MV/m. For the electropolished batch the average gradient is 35.7 MV/m. The $Q(E_{acc})$ curves on the etched cavities are shown in figure 4.3 and for the electropolished cavities in figure 4.5.

in the bulk [Röth 1993]. The concentration in the surface layer is ≤ 1 at%. Therefore, for cavities made from $RRR \geq 200$ material the heat treatment at 800°C is unavoidable.

The hydride formation depends on the time during which the cavity is kept in the dangerous region around 100 K. With a fast cooldown from 300 K to 4.2 K within 1 hour, the hydrides will not be formed. Only if one uses a slow cooldown in the order of several hours or keeps the cavity on purpose in this temperature region the problem can occur. A few cases have been observed where the hydrogen loading led to Q-disease even with a fast cooldown, especially after the cavities where mechanically ground with a wet lubricant (e.g. tumbling). For this effect the concentration of the untrapped hydrogen has to be above 4.5 at%. The cure against the hydrogen loading is a combination of a furnace treatment at 800°C [Röth 1993] and cooling the acid for etching to below 15°C as is used as a part of the standard cavity preparation at TTF (section 1.4).

The cavities studied in thesis were made from electropolished half-cells. In the half-cell EP system the niobium was not protected from the hydrogen gas by a membrane. Therefore the Q-disease was expected to occur during slow cooldown which in fact happened. An example is shown in figure 3.5. The cavity was tested after fast cooldown and shows a normal residual resistivity of about 8 nΩ. After the test the cavity was heated to 100 K, kept at this temperature level for 2 days and cooled to 1.6 K for a new test. The residual resistance increased to more than 400 nΩ and the field dependence of the quality factor shows the typical behaviour as described in [Röth 1993].

In the next step the cavity was heated in a vacuum furnace to 800°C to remove the hydrogen from the bulk material. A short electropolishing of about 20 μm was done to clean the surface from dirt which might have been introduced during the furnace treatment. Again the cavity was tested after fast cooldown and showed a normal residual resistance (8 nΩ). After keeping the cavity at 100 K for 2 days, no change in the behaviour was observed. This indicates that "Q-disease" was cured by the furnace treatment. Even more, no additional hydrogen was introduced during the short EP, indicating that the precautions taken in the setup (introduction of a PTFE-cloth around the cathode) to avoid hydrogen contamination were successful.

After the furnace treatment at 800°C, the average high field behaviour was only slightly improved during the treatment (see Q(E) curves in figure 3.6). In figure 3.7 the results of several cavities before and after the heat treatment at 800°C are shown. The average gradient is 35 MV/m before and 36.3 MV/m after this treatment. One cavity of very low performance (20 MV/m) has been omitted from the statistics, because optical inspection revealed a defect on the weld seam of this cavity.

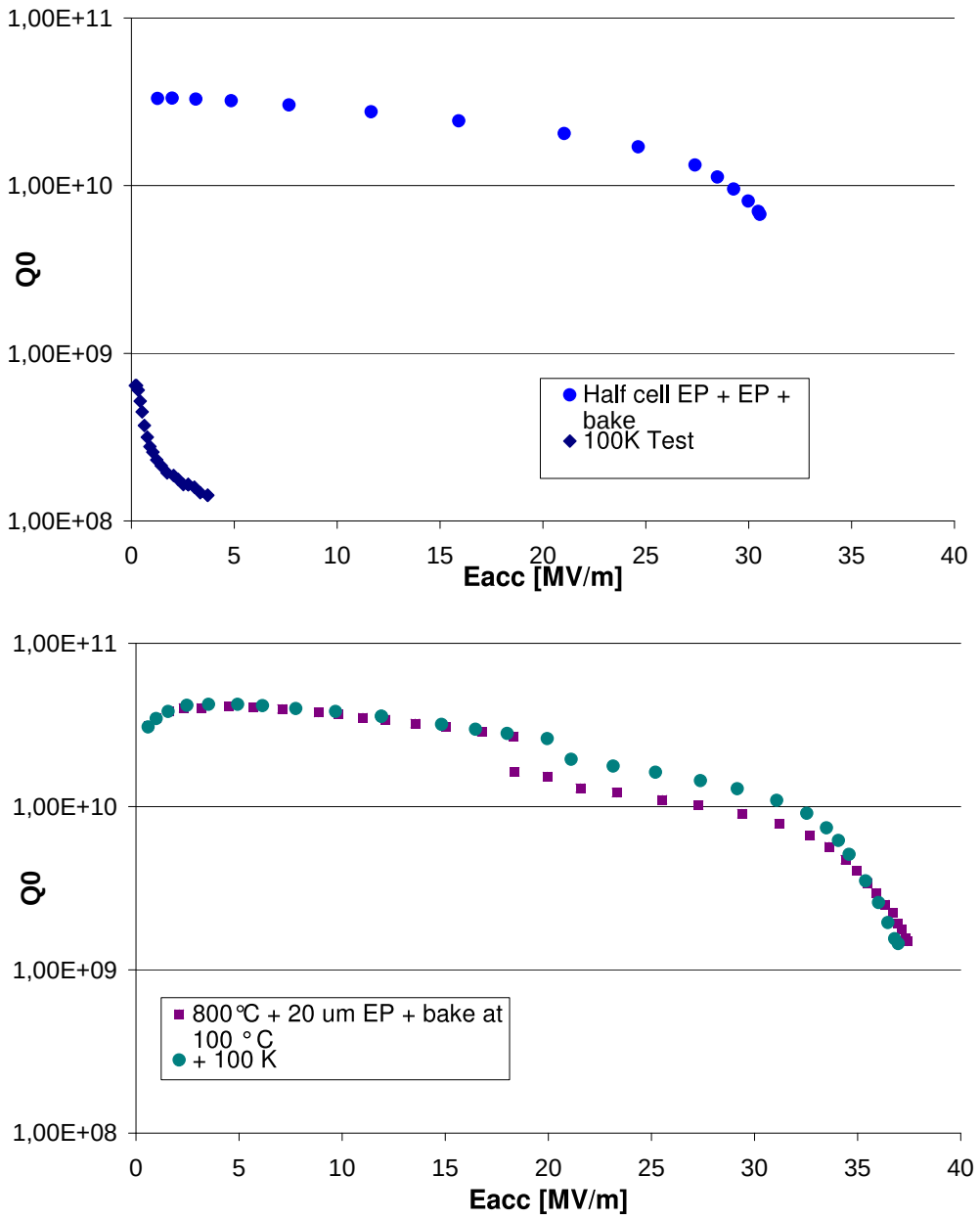

Figure 3.5: Top: An electropolished cavity shows a severe degradation in quality factor after it was kept at 100 K for 2 days. Bottom: The same cavity after 800°C furnace treatment and a short EP of 20 μm. Even when the cavity is kept a 100 K no sign of the "Q-disease" is found. Test temperature was 1.6 K. Tests were done at CEA Saclay.

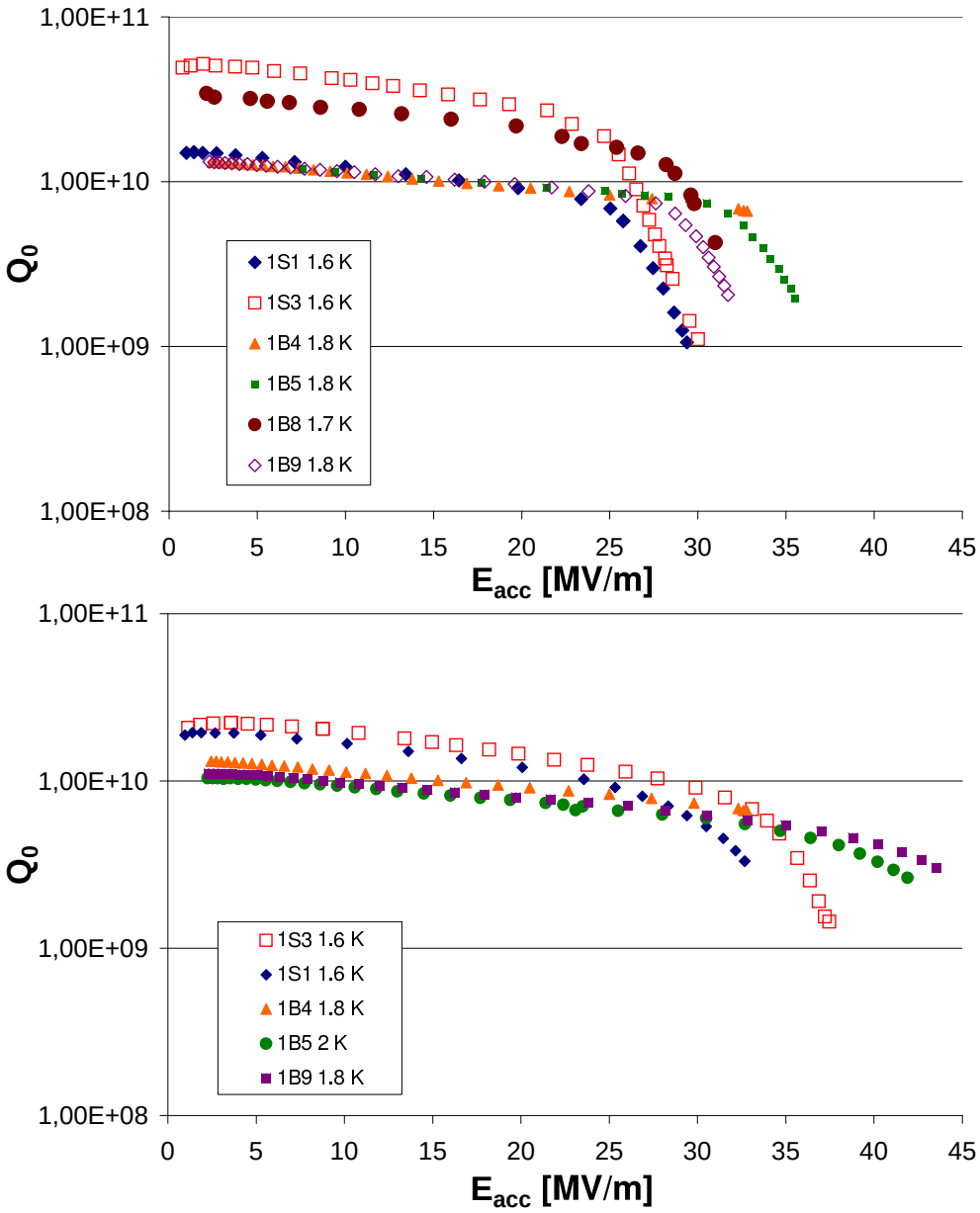

Figure 3.6: Excitation curves of one-cell cavities after 800°C heat treatment without (top) and with 'in-situ' bakeout (bottom). The tests have been performed in different cryostats with different magnetic shielding and different liquid helium temperatures (1.6 - 2 K) .

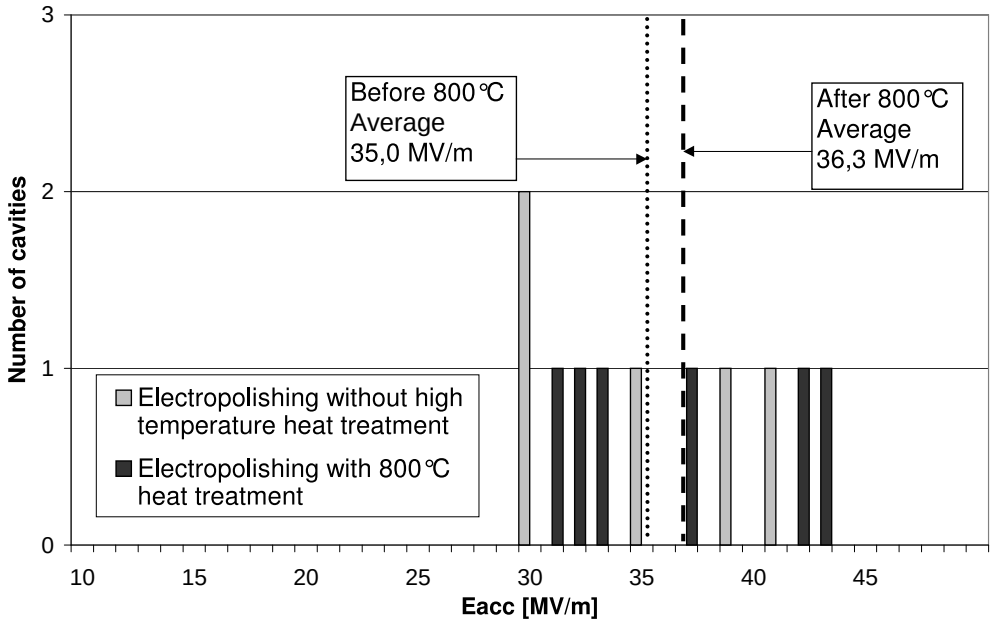

Figure 3.7: The graph shows the distribution of accelerating gradients before (see fig 4.5) and after (see fig. 3.6) the furnace treatment at 800°C. One cavity with a weld defect has been omitted from this graph.

3.2.2.2 Postpurification with titanium getter at 1400°C

Although the electropolishing of niobium cavities offers already very high gradients with niobium of RRR = 300, one cavity was tested after purification with titanium getter layer. The RRR increased to about 500. The evaporated titanium layer was removed with an EP of 100 μm. The tests before and after 'in-situ' baking are shown in figure 3.8. The cavity has a Q-drop without X-rays at the typical field level of 25 - 30 MV/m and reaches a maximum field of 35 MV/m which is the same value as before the 1400°C treatment. It was observed that the degradation of the quality factor after 800°C heat treatment starts at even lower field than in the case where the cavity has not been subjected to any high temperature heat treatment. The reason for this behaviour is unclear.

After "in-situ" baking the cavity is limited at 37 MV/m with a thermal breakdown. The maximum quench field is not improved during after the thermal conductivity is increased. The quality factor at maximum field appears to be after the 1400°C furnace treatment, but this observation is not conclusive since the 'in-situ' bakeout at low temperatures has also an influence on the Q_0.

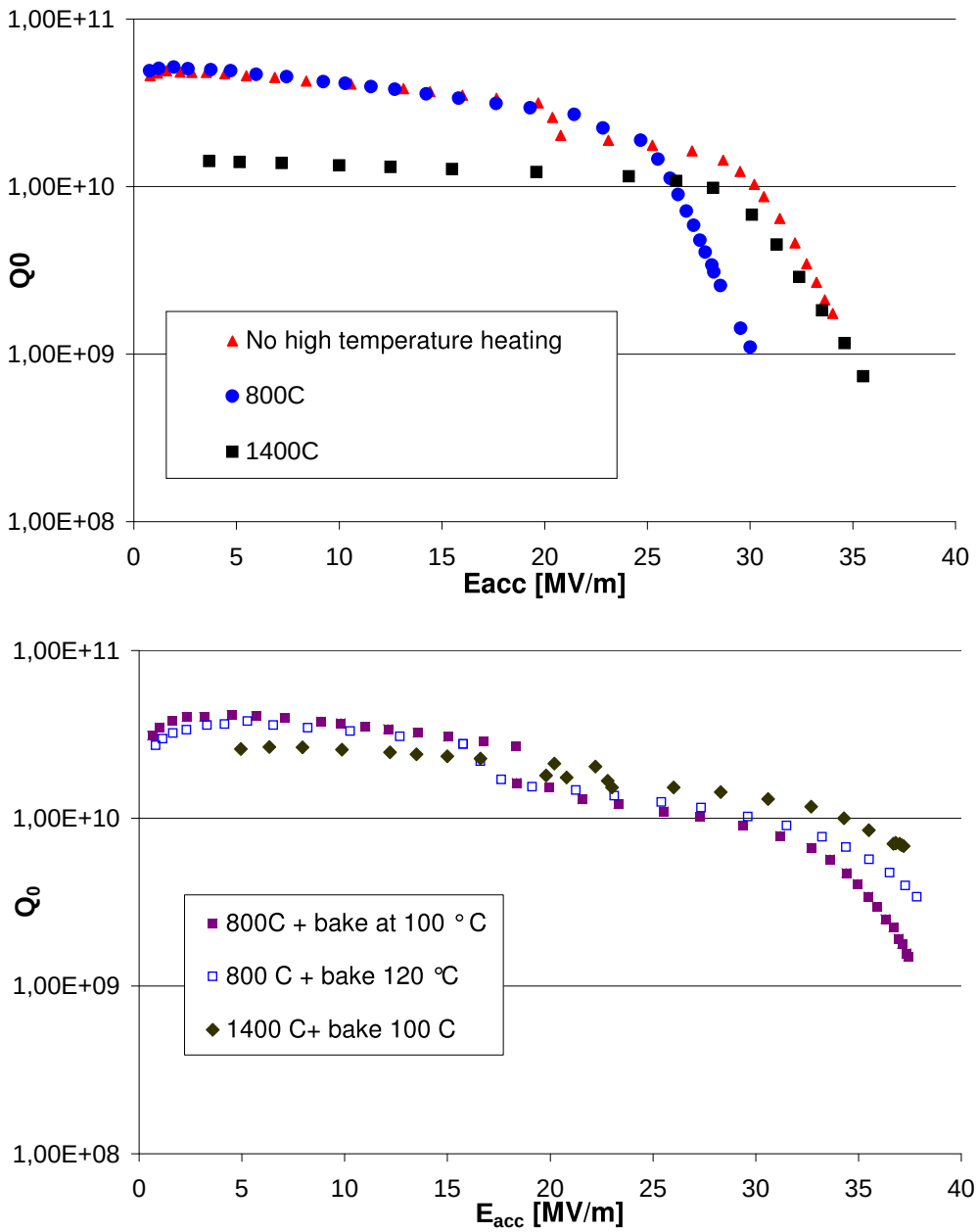

Figure 3.8: Test results of an electropolished resonator subjected to different high temperature heat treatments. The cavity was tested after no heat treatment, after 800°C hydrogen degassing and stress annealing and after postpurification at 1400°C with titanium getter. Top: No 'in-situ' bakeout. It is not clear why the degradation of the quality factor appears at a lower field after the 800°C furnace treatment than without any high temperature heat treatment. Bottom: After 'in-situ' bakeout. The bakeout is efficient in each case. No improvement in the maximum gradient is seen after postpurification. Test temperature was 1.6 K for all tests.

3.2.3 Influence of the electron-beam welding on the cavity performance

The standard fabrication of the TESLA cavities is based on deep-drawing of half-cells and electron-beam welding. The quality of the EB weld seam at the equator is crucial to the maximum performance achievable in the cavities and has been a problem in one batch of the first production of TESLA cavities. Therefore the one-cell production was performed in two different EB welding machines. The idea here was to have one batch of 4 cavities with well established EB welding parameters performed by an industrial company with experience in the niobium welding (ACCEL Instruments, Bergisch-Gladbach). In contrast, the second batch of 11 cavities was welded at CERN where the EB welding machine is equipped with a stainless steel vacuum chamber made according to ultra high vacuum standards. Whereas the vacuum in the standard production is of the order of a few times 10^{-5} mbar, the pressure in the CERN system could be lowered down to $3 \cdot 10^{-7}$ mbar by using a cryopump and a longer time for pumping down.

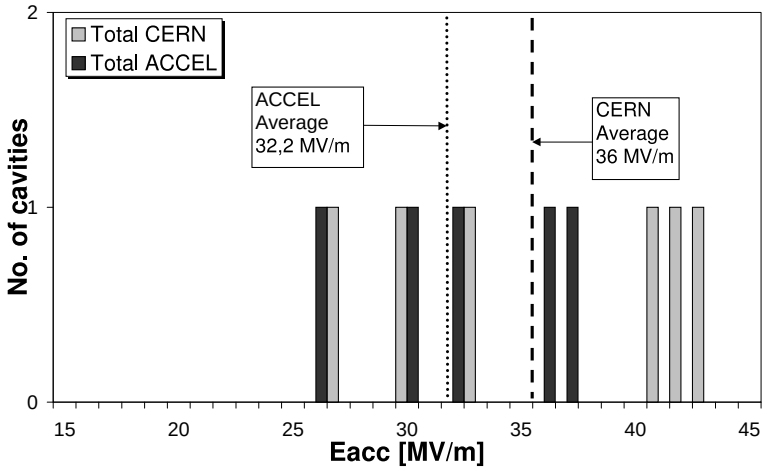

Figure 3.9: Comparison of accelerating gradients of cavities welded under "normal" vacuum conditions ($\approx 10^{-5}$ mbar) by the company ACCEL and under improved vacuum conditions ($< 10^{-6}$ mbar) in the electron beam welding machine at CERN. The data for etched and electropolished cavities are shown. The best test on each cavity is taken.

As the residual gas in the machine is partly gettered by the molten niobium in the weld seam, the RRR in this region can be reduced. For EB welds material of RRR ≈ 400 the reduction can be in the order of 20 % (RRR ≈ 300) for a vacuum of 10^{-5} mbar whereas for TIG[4] welds the reduction can be very

[4]Tungsten-Inert-Gas

large (RRR ≈ 400 is reduced to RRR ≈ 120) [Proch et al. 1998]. It was expected, that the better vacuum conditions lead to an improved cavity performance. Indeed, the average gradient of the CERN batch is 3.8 MV/m higher as compared to the cavities prepared under "normal" vacuum conditions (see figure 3.9).

The disadvantage of the CERN machine is the electron gun, which does not allow for the orthorhombic weld pattern which produces the smoothest underbead of the weld seam [Brinkmann et al. 2001, Padamsee et al. 1998]. One cavity of the CERN batch has a macroscopic defect on a weld seam, which was found during visual inspection. This cavity was omitted from the figure 3.9.

These results indicate that a electron-beam welding facility should combine both, a state-of-the-art electron gun and a vacuum system fabricated according to ultra-high vacuum standards. At the moment DESY sets up a electron-beam welding facility for niobium welding which combines these two features.

3.2.4 Multi-cell electropolishing

The application of electropolishing to multi-cells was also investigated within this thesis. As KEK has used the electropolishing already for five-cell 500 MHz cavities for TRISTAN [Saito et al. 1989] in the 1980s, a lot of valuable expertise was available. Four 9-cell TESLA resonators have been electropolished in Japan in collaboration with KEK at a company (Nomura Plating) so far. One of these cavities was not tested, as a leak appeared during electropolishing due to a not fully penetrated weld seam at a higher order mode coupler. This cavity was sent to the manufacturer for repair.

The results of the other cavities are summarized in figures 3.10 to 3.12. The first cavity to be electropolished was a prototype cavity with 1400°C getter treatment. In the etched state, the cavity eventually reached 29 MV/m but only after strong multipacting. After EP the multipacting barrier turned out to be so strong that the cavity performance was severely hampered by multipacting and limited at 21 MV/m as shown in figure 3.10. Still, the visual inspection has shown that all cells are polished so that there is no problem with the electrical current distribution in the long structure of a nine-cell cavity in the EP setup.

The second cavity was taken from the first production series in which all cavities were subjected to the 1400°C treatment. The performance improved significantly from 22 MV/m after etching to 32 MV/m after EP. This is the highest accelerating gradient measured in a cw RF test in a nine-cell TESLA cavity.

The third cavity was sent for electropolishing after an annealing furnace treatment at 800°C. The cavity showed already an excellent performance before EP. It is the best cavity which was measured without the 1400°C treatment. The thermal breakdown field was not changed after EP. In a second test the cavity was tested for "Q-disease". After keeping the cavity at 100 K for 2 days no sign of enhanced microwave losses due to hydrides was found. Therefore the protection of the niobium material from hydrogen via a PTFE cloth around the electrode seems to be efficient also for a longer EP process. The electropolishing of 100 μm takes about 3 hours.

All cavities had problems with the field homogeneity in the accelerating mode, so that additional tuning was necessary after delivery to DESY. As an electropolishing facility for 9-cell cavities is not yet available at DESY no chemical treatment was applied, but only high pressure ultra-pure water rinsing. In order to get more reproducible results, a new batch of 10 nine-cell cavities is going to be electropolished in Japan. It is intended to mount 8 electropolished cavities in the linac for a long time performance test with electron beam.

The results are already very encouraging especially since no principal technical problems have been discovered in the multi-cell EP. The production of hydrogen gas during the electropolishing process as well as the current distribution in the nine-cell structure are under control.

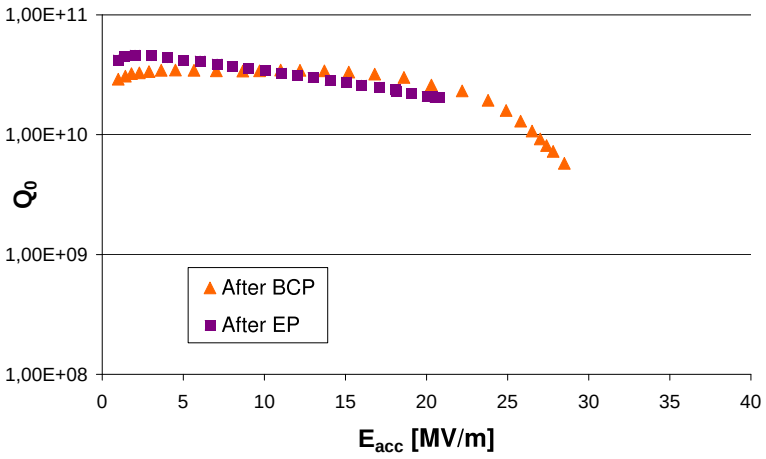

Figure 3.10: Excitation curve of the prototype 9-cell cavity after BCP and electropolishing (EP). The test at DESY after etching reached 29 MV/m only after a long conditioning of a multipacting barrier around 20 MV/m. The test after electropolishing at KEK has shown that the cavity was severely hampered due to the multipacting and was limited to 21 MV/m. Test temperature was 1.8 K.

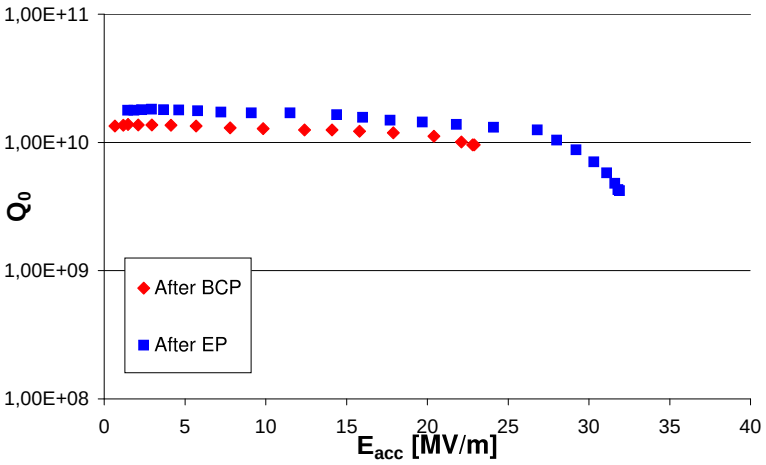

Figure 3.11: Excitation curve of the second TESLA 9-cell cavity send to KEK after chemical etching (BCP) and after electropolishing (EP). The cavity performance improved significantly after electropolishing. Before these test this cavity had been heat treated at 1400°C. Test temperature was 2 K.

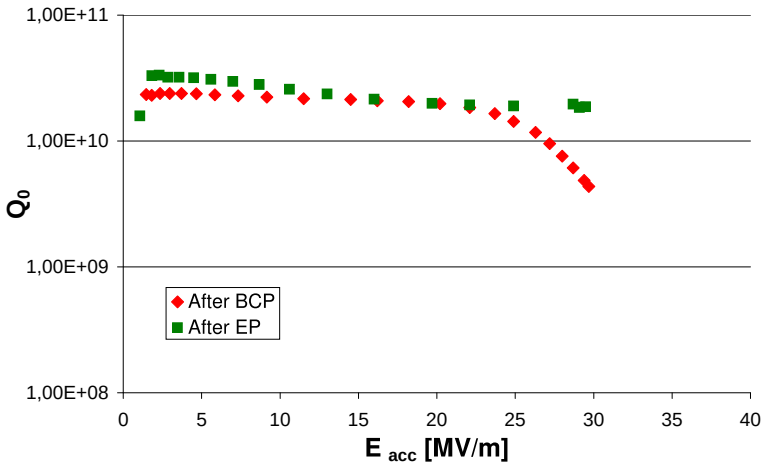

Figure 3.12: Excitation curve of the third TESLA 9-cell cavity after chemical etching (BCP) and after electropolishing (EP). This cavity was treated in a vacuum furnace at 800°C for stress annealing and hydrogen degassing. After 100 μm electropolishing the maximum accelerating gradient did not change, but the quality factor at high fields improved significantly. In another test the cavity was found not to have "Q-disease". Test temperature was 2 K.

Chapter 4

Quality degradation at high fields without field emission

4.1 First measurements on electropolished cavities

The excitation curves of the electropolished cavities exhibit a strong degradation in quality factor at high field as can be seen in figure 4.1. No signs of X-rays were detected and also the electron pick-up antennas did not show signals. Therefore field emission of electrons seemed to be excluded as a field-dependent loss mechanism. With temperature mapping a global heating was found in the area of high magnetic fields around the equator (Figure 4.1). Apparently, a new loss mechanism appears in the resonators. This effect is sometimes called "Q-drop without X-rays".

4.2 Low temperature 'in-situ' baking

All Q(E) curves at KEK on defect-free resonators showed only a moderate drop of the quality factor resistance at high accelerating fields as shown in figure 4.2 [Saito et al. 1997a, Saito et al. 1997b, Kako et al. 1999]. The first results on electropolished single cell cavities in the CEA-CERN-DESY collaboration were disappointing as the measurements at KEK never indicated such a behaviour.

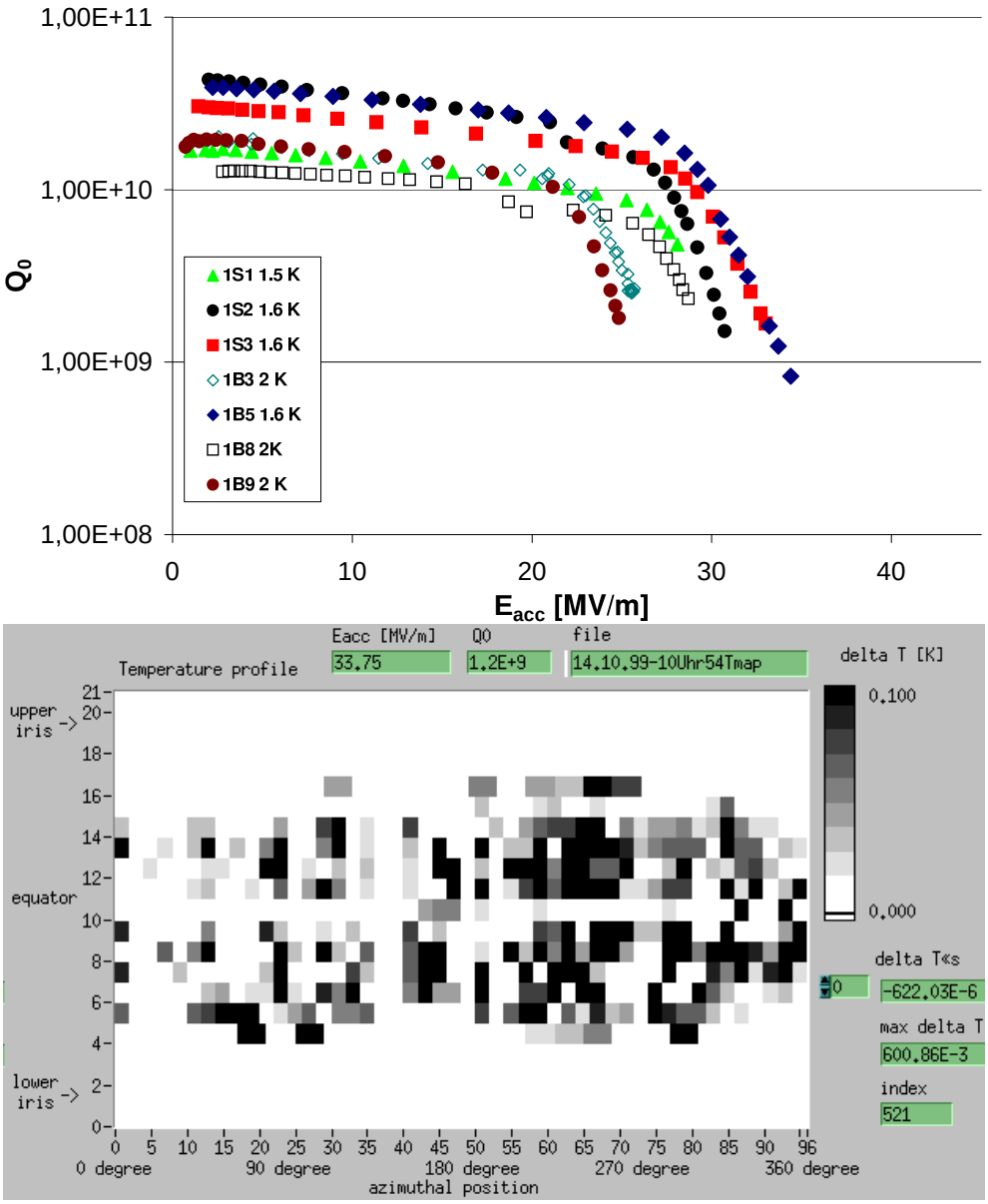

Figure 4.1: Top: Results of electropolished single cell resonators. Note the strong degradation of of the quality factor above surface magnetic fields corresponding to 100 mT (E_{acc} = 25 MV/m). No 'in-situ' baking is applied to the resonators. Bottom: Temperature mapping of an electropolished single cell resonator. The heating of the surface (dark areas) takes place near the equator in the high magnetic field area.

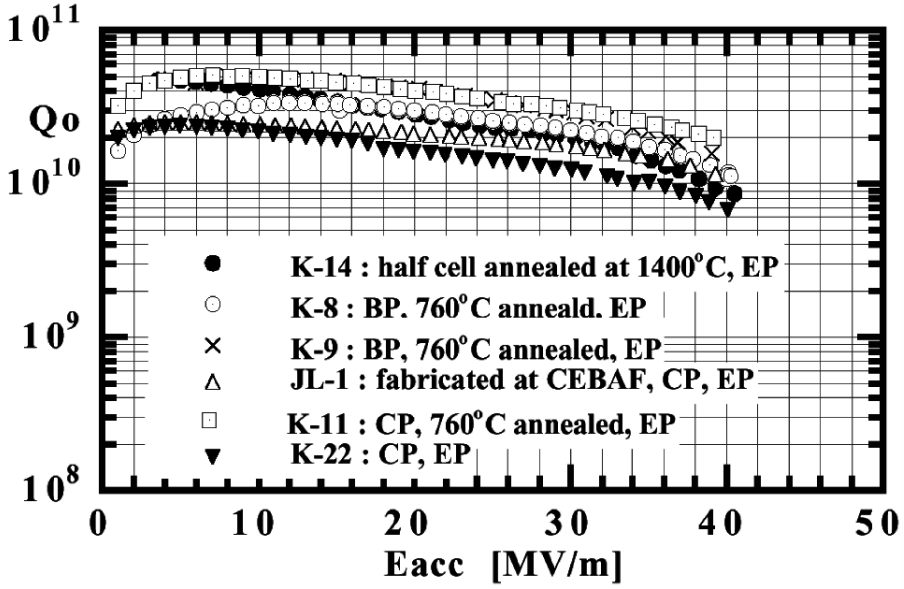

Figure 4.2: Results from electropolished single cell resonators at KEK [Kako et al. 1999]. No evidence of a strong degradation of the quality factor is seen in these measurements. As part of the standard preparation for the measurement a low temperature baking between 85 - 120°C was applied. Test temperature was 1.5 - 1.7 K.

At Saclay a similar strong degradation was observed for chemically etched cavities [Kako et al. 1997, Safa 1997, Visentin et al. 1998]. Several examples of cavities treated with BCP are shown in figure 4.3. The temperature mapping in figure 4.3 shows a global heating of the surface in one of these cavities below the breakdown field, as was the case for the un-baked electropolished cavities in figure 4.1.

As noted by [Visentin et al. 1998] it is possible to improve the behaviour of cavities at high gradients by a simple 'in-situ' bakeout. This heating is applied after the last high pressure water rinsing with the cavity being under vacuum at temperatures around 170 °C for 70 hours. The cavity is kept in the cryostat under helium atmosphere. The baking was intended to improve vacuum conditions.

An example of a very good etched cavity is shown in figure 4.4. The baking improves the quality factor at the maximum field of 30 MV/m by a factor of almost 3. As is usual [Visentin et al. 1998] for chemically etched cavities the maximum field level did not change at all. Field emission was observed in neither of the two tests.

Building on the experience the electropolished cavities have been baked at temperatures of around 100°C with remarkable success. For example in figure 4.5 several single cell cavities show a very high accelerating gradient

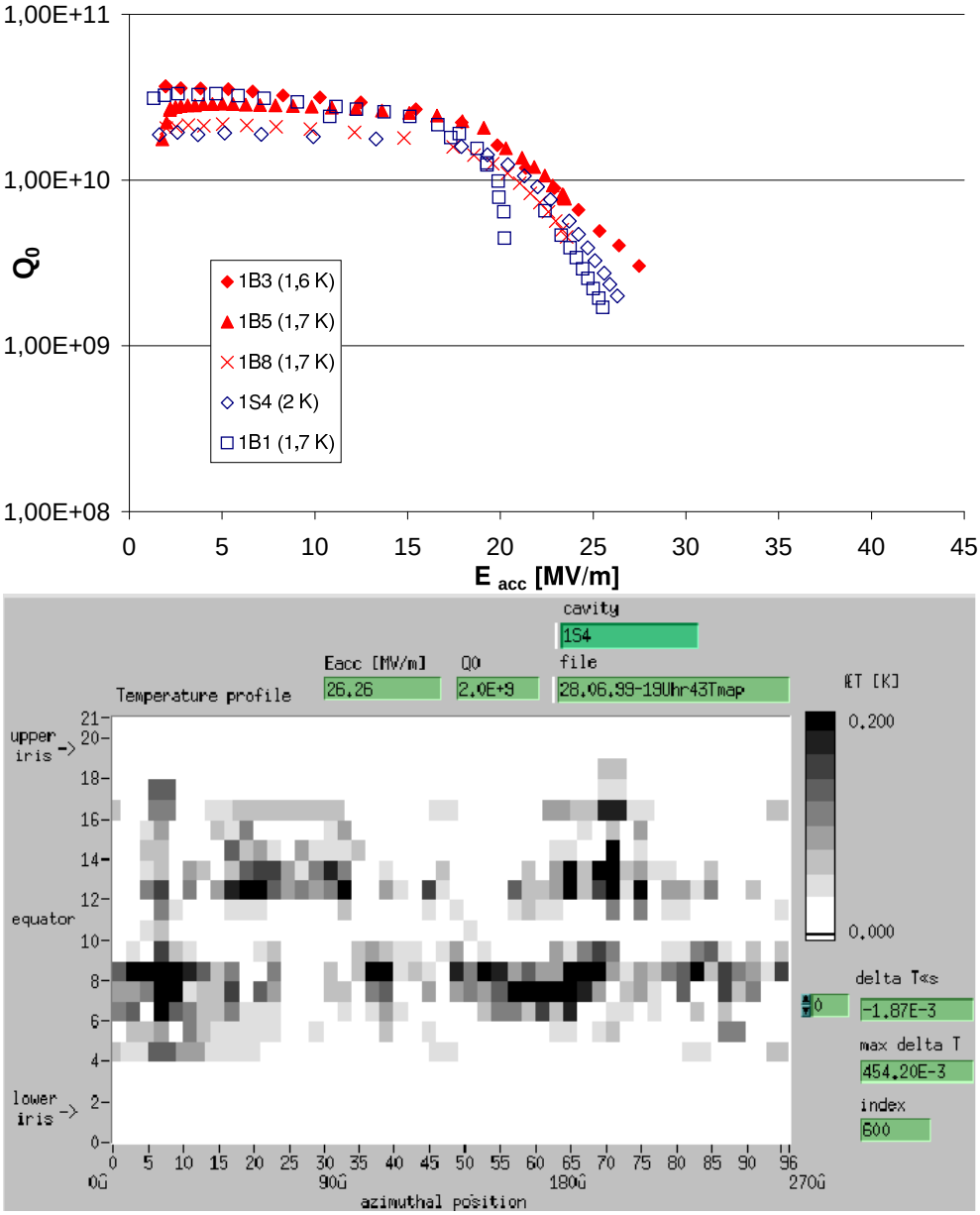

Figure 4.3: Top: Excitation curves of etched single cell resonators. Note the strong degradation of of the quality factor above surface magnetic fields corresponding to 100 mT (E_{acc} = 25 MV/m). No 'in-situ' baking was applied to the resonators. All cavities are limited by a thermal breakdown. Bottom: The temperature mapping of one of the above mentioned cavities shows a global heating in the area of high magnetic fields below the breakdown field. No pronounced hot spot can be located at this field level. This behaviour is very similar to the one observed in the EP cavities in figure 4.1.

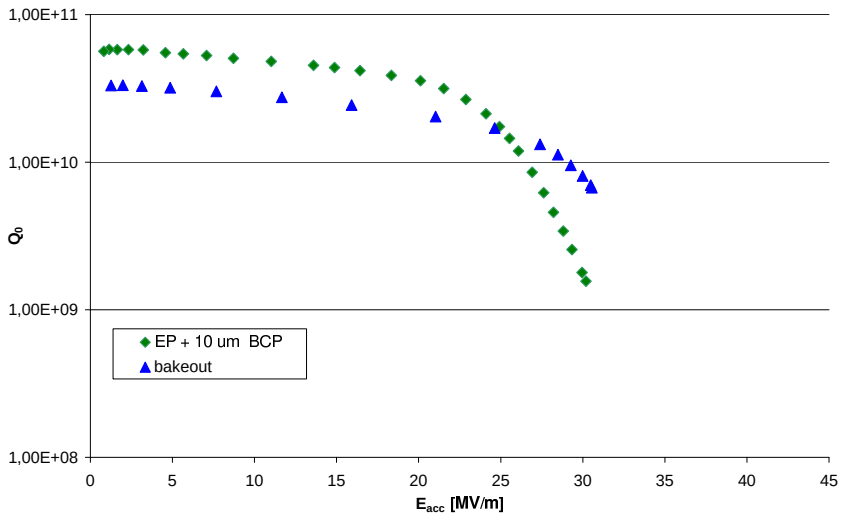

Figure 4.4: After the 'in-situ' bakeout the cavity Q_0 improves at highest gradients. The breakdown field level remained unchanged in this cavity. This was observed in several chemically etched niobium cavities also in other labs [Visentin et al. 1998, Kneisel 1999]. Note that this cavity was not subjected to a high temperature furnace treatment. Test temperature was 1.6 K.

of up to 40 MV/m with quality factors above $5 \cdot 10^9$. This behaviour is very similar to the observations done at KEK. Apparently, the bakeout at around 100° C which has been part of the standard procedure improved the high field performance of the cavities. At KEK, only a few measurements have shown a strong degradation in quality factor, where the baking was presumably insufficient [Kako 1998]. In the next section a more detailed look on the effects of 'in-situ' baking at 100 - 150° C will be given.

4.3 Characteristics of 'in-situ' baked cavities

Since the discovery of the positive effect of baking niobium cavities at low temperatures[1] around 100 - 150 °C several experiments have been done on the effect, revealing numerous features of the process [Visentin et al. 1998, Visentin et al. 1999, Lilje et al. 1999, Kneisel 1999]. The last paper is the most comprehensive description of the effect. A summary on the baking is found in the proceedings of the 9th Workshop of RF Superconductivity [Proch 1999].

[1]This should be compared to the high temperature heat treatments at 800°C (for hydrogen degassing and stress annealing) and 1400°C with titanium getter (to increase of the thermal conductivity) which have been described in section 1.

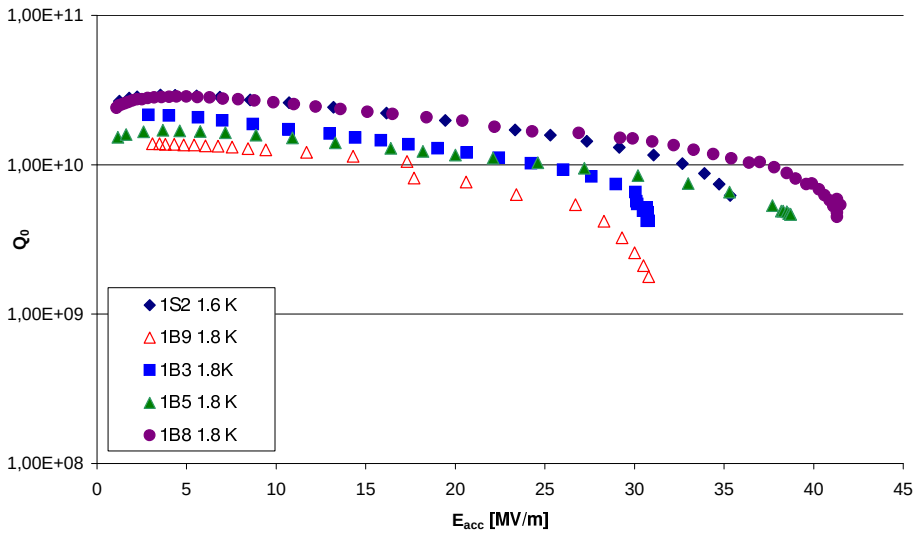

Figure 4.5: Excitation curves of electropolished one-cell cavities with 'in-situ' bakeout. The tests have been performed in different cryostats with different magnetic shielding and different temperatures.

Improvement of the quality factor at high fields

Of course the most desirable effect of the 'in-situ' bakeout is to cure the strong field-dependent degradation of the quality factor, but there are several other observations which give some hints on the process in the niobium surface. In figure 4.6 an example for an electropolished cavity is given. The cavity degraded before baking at 30 MV/m to a $Q_0 = 1 \cdot 10^9$, but did not show a thermal breakdown. The limitation in the test was the available RF power. After bakeout the cavity could be excited to fields well above 35 MV/m. When a cavity shows a thermal breakdown like in the chemically cavity shown in figure 4.4 the field level is not increased but at least the quality factor can be improved substantially. This difference between electropolished and chemically etched cavities will be discussed in another section (Sec. 3.2).

Improvement of the BCS surface resistance

In figure 4.7 the temperature dependence of the surface resistance before and after the bake can be seen in the range from 4.2 K down to 1.5 K. In this case the temperature dependent surface resistance R_{BCS} is reduced by a factor of 1.5 for the whole temperature range of 4.2 K to 1.5 K. In some cases an even higher reduction of the surface resistance by a factor of 2

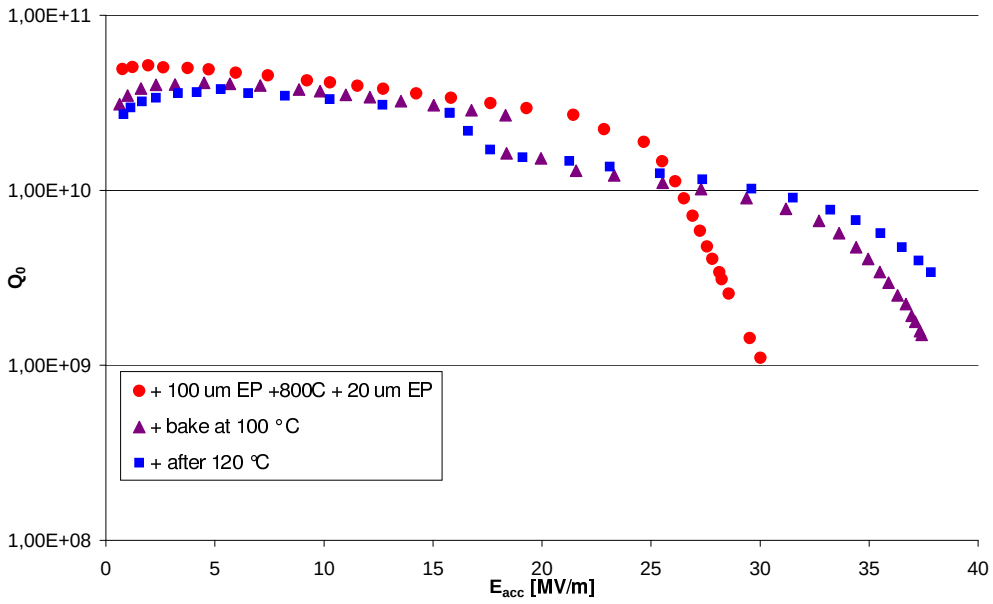

Figure 4.6: Improvement of the high accelerating surface field behaviour. A baking temperature of 120 - 140°C seems to be the optimum. The small degradation at an accelerating field of 18 MV/m is due to multipacting. Test temperature was 1.6 K.

was observed. This high reduction in R_{BCS} was also seen in other laboratories [Kneisel 1999]. In earlier studies at Cornell University on the influence of oxide layers in 8.6 GHz niobium cavities a very similar behaviour was observed when heating oxidized cavities 'in-situ' to temperatures of 250°C [Palmer 1988a, Palmer et al. 1990].

Changes on the residual resistance

As can be seen in figures 4.7 and 4.8 the residual surface resistance is increased by the bakeout. The small degradation in figure 4.7 case is tolerable and rather typical [Proch 1999]. In figure 4.8 the result shows that the baking can lead to a significantly increased surface resistance. The results from [Palmer 1988a] at higher temperatures around 300°C confirm this behaviour. The cavity shown in figure 4.8 was not baked in a cryostat or in an apparatus with inert gas atmosphere with good temperature control, but simply heated with heater bands. Most likely, the temperature exceeded the specified 120°C (see below) and the niobium was heated was heated at least up to more than 200°C where the heaters were in direct contact with the wall. To avoid this a setup for baking has to include a good temperature control and the heating should be done in an inert gas atmosphere. A dedicated baking system is available now at DESY.

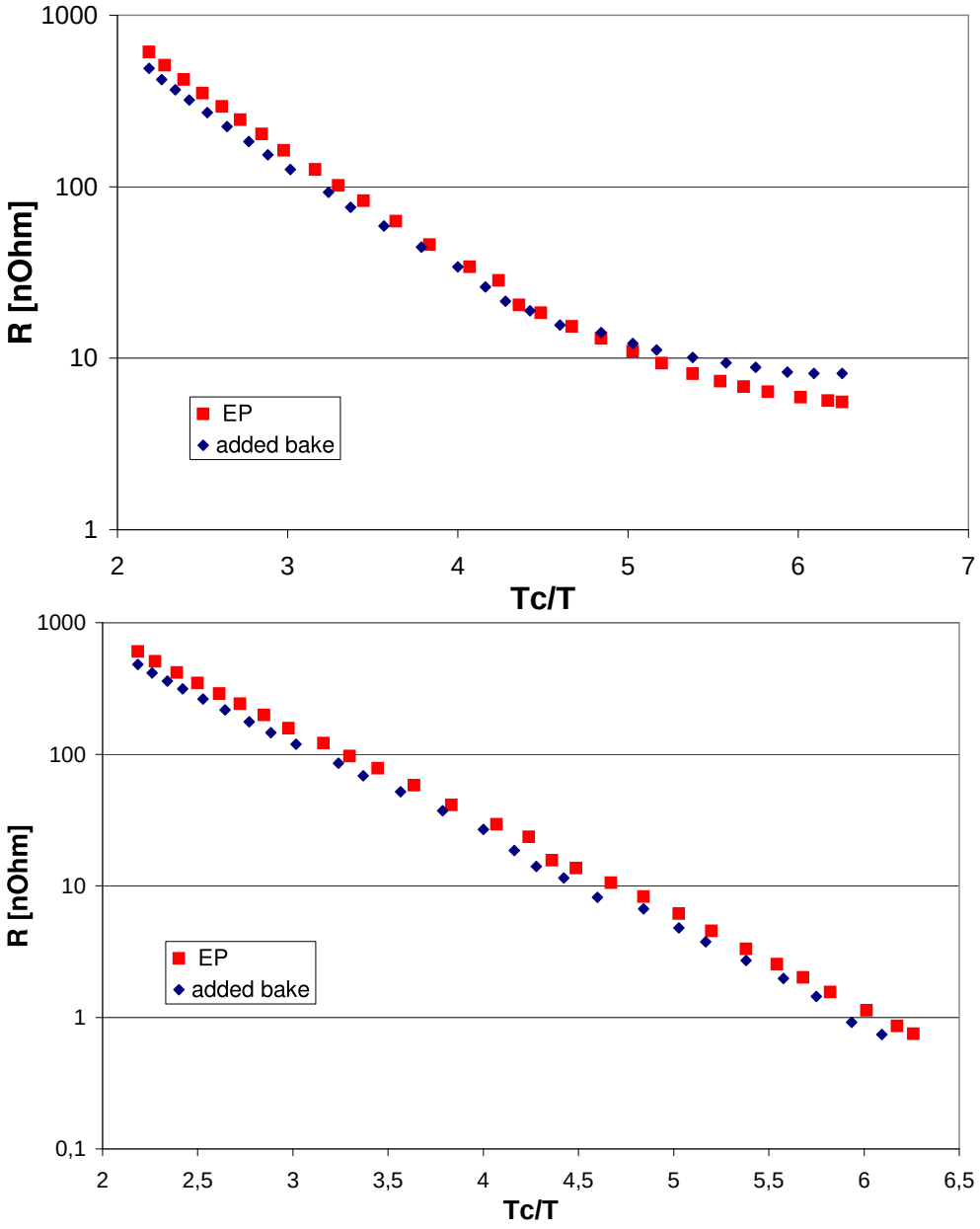

Figure 4.7: Bakeout in a cryostat with helium atmosphere. Top: The curves shows the temperature dependence of the surface resistance before and after 'In-situ' bakeout. Bottom: The BCS surface resistance. A residual resistance of 4.7 nΩ for the unbaked case is subtracted. For the baked case a residual resistance of 7.4 nΩ is subtracted.

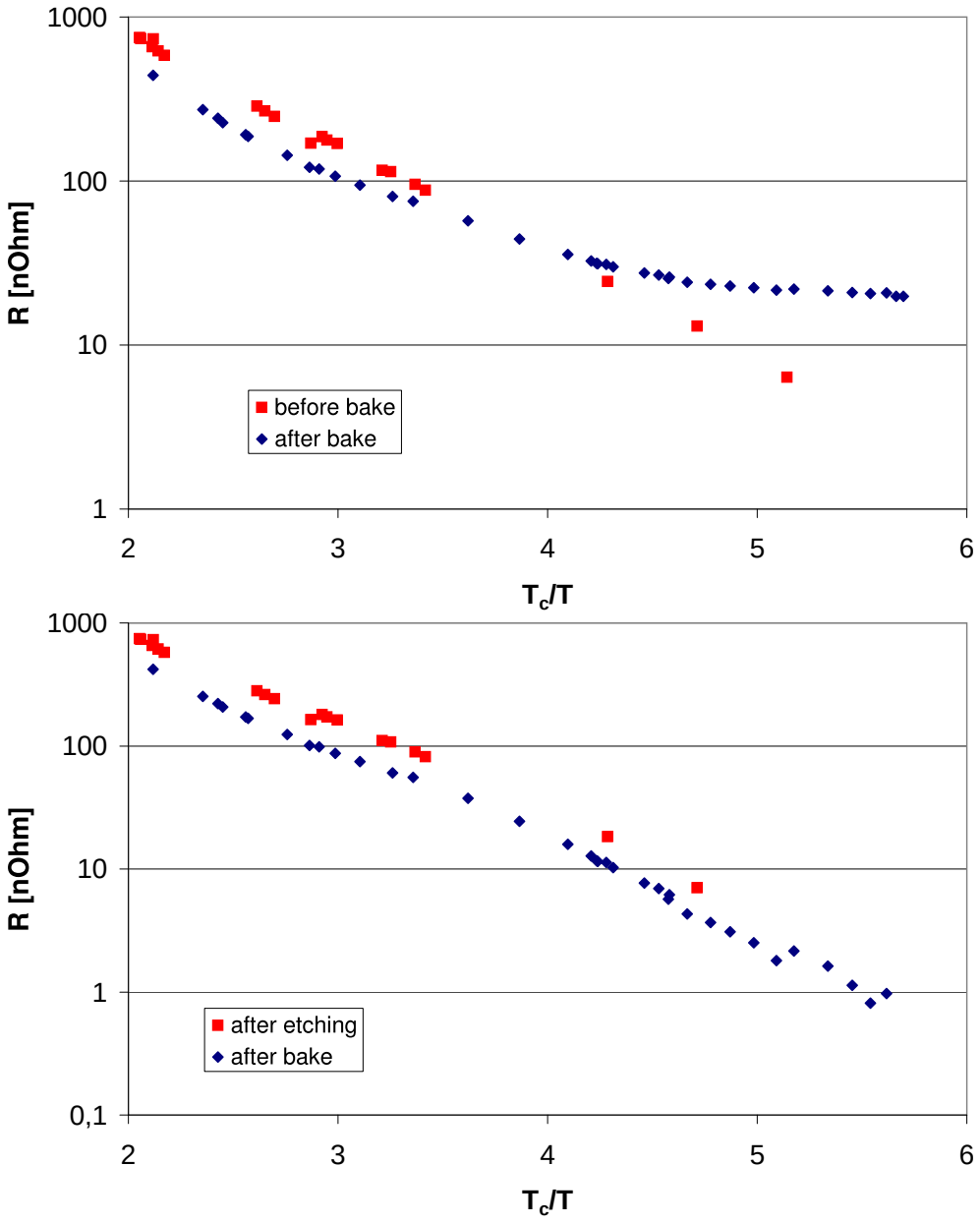

Figure 4.8: Unsuccessful bakeout in air using strip heaters. Top: The residual resistance is very high after bakeout ($\approx$ 20 nΩ). Bottom: After subtracting the residual resistance it is evident that the temperature-dependent resistance is also lower as in figure 4.7.

Study of the Q degradation at different helium temperatures

Tests at several temperatures in the range between 1.5 K and 2.2 K have been performed on an electropolished cavity before and after 'in-situ' bakeout (see figures 4.9 and 4.10). At low field the quality factor is reduced as expected from BCS theory before and after bakeout (see figure 4.9).

At high field, the degradation of the quality factor before bakeout has always the same behaviour, if the helium temperature $T \leq 2$ K. The degradation starts at 30 MV/m. The maximum breakdown field is also not changed when the temperature is below or equal to 2 K. This is also true for the case in which the cavity is 'in-situ' baked (see figure 4.10 bottom). These results are consistent with thermal model calculations, which are shown in figure 4.11 by [Reschke 1997]. For a bath temperature of either 1.8 K or 2 K there is no difference in the maximum breakdown field. Only when the temperature is close to the Lambda-point (2.17 K) the breakdown field is reduced. This can be understood since the heating will cause a superfluid to normalfluid transition with the consequence that the heat cannot be conducted away fast enough and will cause the niobium to heat up further, so that the breakdown of the cavity will happen at a lower field. This applies for unbaked and baked cavities.

If one increases the temperature above the lambda-point, a degradation of the quality factor due to the insufficient cooling can already be seen at very low field. The breakdown field of the cavity is reduced further to values below 30 MV/m.

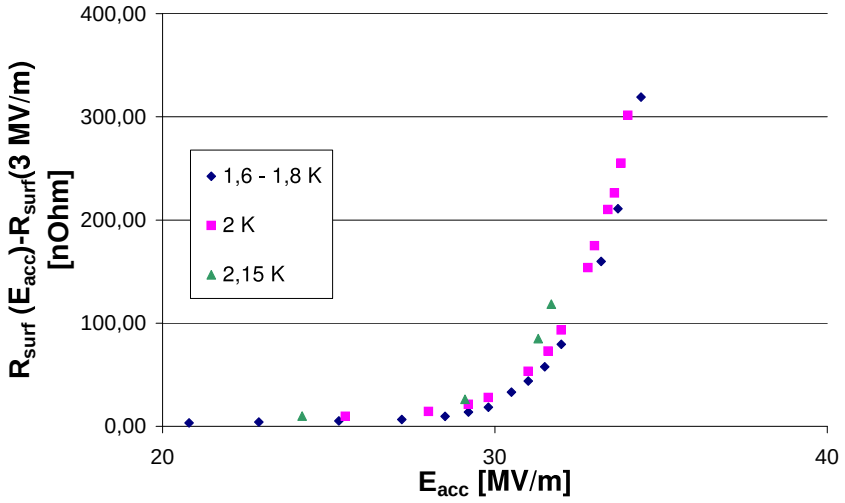

Figure 4.9: Increase of the surface resistance with accelerating gradient before the bake depending on the bath temperature. The surface resistance at low field has been subtracted. The increase shows very similar behaviour for different temperatures.

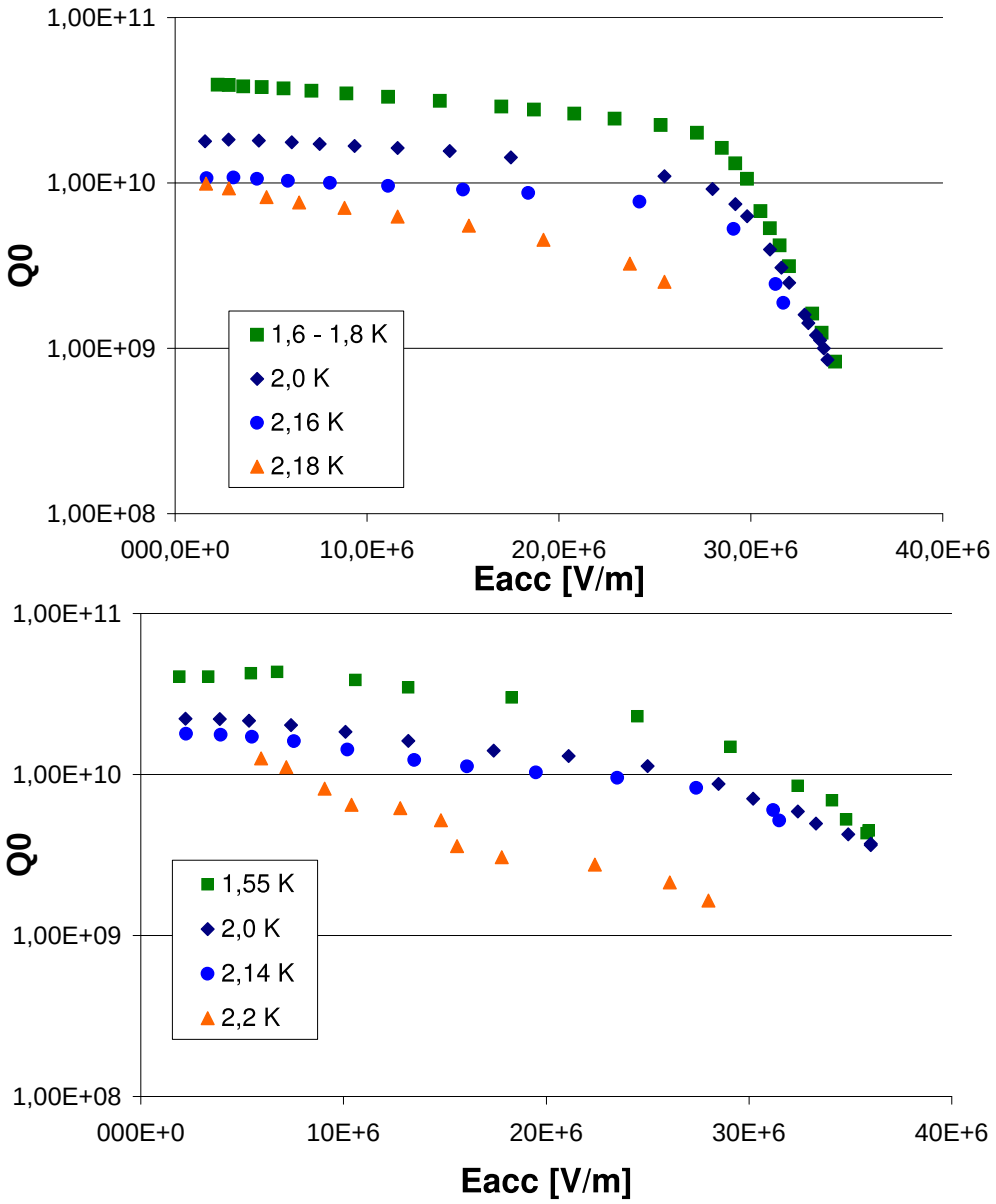

Figure 4.10: Excitation curves of the same electropolished cavity before (Top) and after bakeout (bottom) for different liquid helium temperatures. At low field the quality factors are corresponding to the expected increase of the surface resistance with temperature. The degradation of the quality factor at high field for the unbaked cavity is not dependent on the temperature at temperatures below 2 K. The maximum breakdown field is reduced when the helium temperature is too close to the Lambda-point (2.17 K) in both cases (unbaked and baked). At temperatures above the Lambda-point a degradation in quality factor starts already at low field and the maximum accelerating gradient is limited below 30 MV/m.

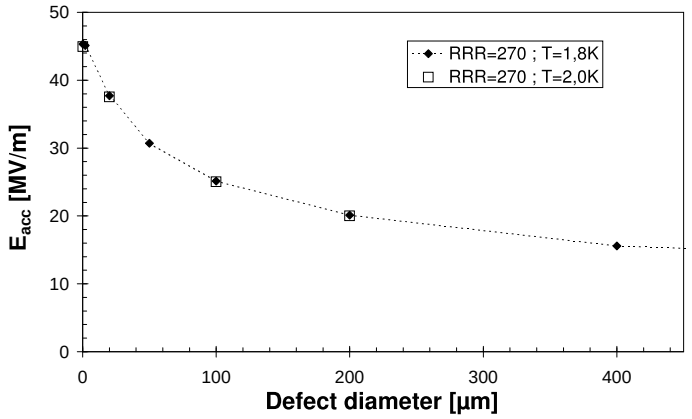

Figure 4.11: Thermal simulations on the dependence of the breakdown field on the bath temperature. There is no difference in the maximum achievable field before breakdown between 1.8 K and 2 K. These simulations assume a critical field $B_{crit} = 200$mT.

Dependency of the R_{BCS} on the duration of the bakeout

P. Kneisel has measured the change of the temperature-dependent part of the surface resistance as a function of baking time, keeping the temperature fixed at 145°C [Kneisel 1999]. The results are shown in figure 4.12. A short bakeout will not be sufficient to get the full effect. At least 40 hours are needed to saturate the reduction of the surface resistance.

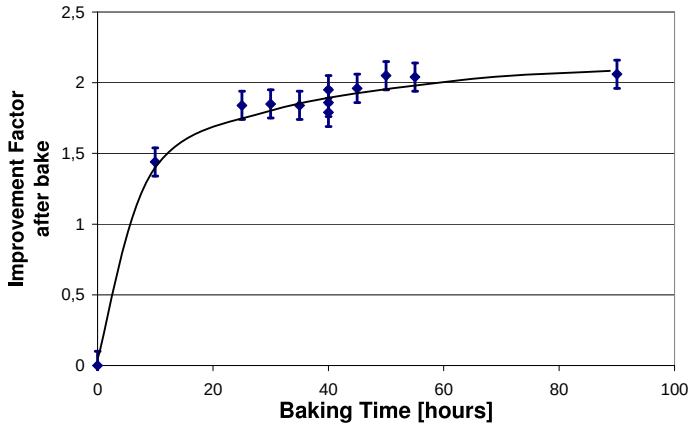

Figure 4.12: Reduction of the R_{BCS} after different baking times. The effect saturates after approximately 40 hours [Kneisel 1999].

Vacuum properties

The vacuum in the niobium cavities is typically in the order of a few times 10^{-8} mbar. During the bakeout, the pressure inside the cavity is kept below 10^{-6} mbar. After the bakeout the vacuum is typically improved by nearly one order of magnitude ($\approx 10^{-9}$ mbar) as compared to the situation before the bakeout. The mass spectrum of the residual gas shows that during bakeout the partial pressure of water is dominant (Figure 4.13). This is not surprising as the cavity surface is treated with electro-chemical surface treatments which involve several water rinsing steps with low and high pressure. Only after 1 - 2 days of baking, the hydrogen partial pressure becomes the dominant part. Other gases have a negligible contribution to the overall pressure in the system.

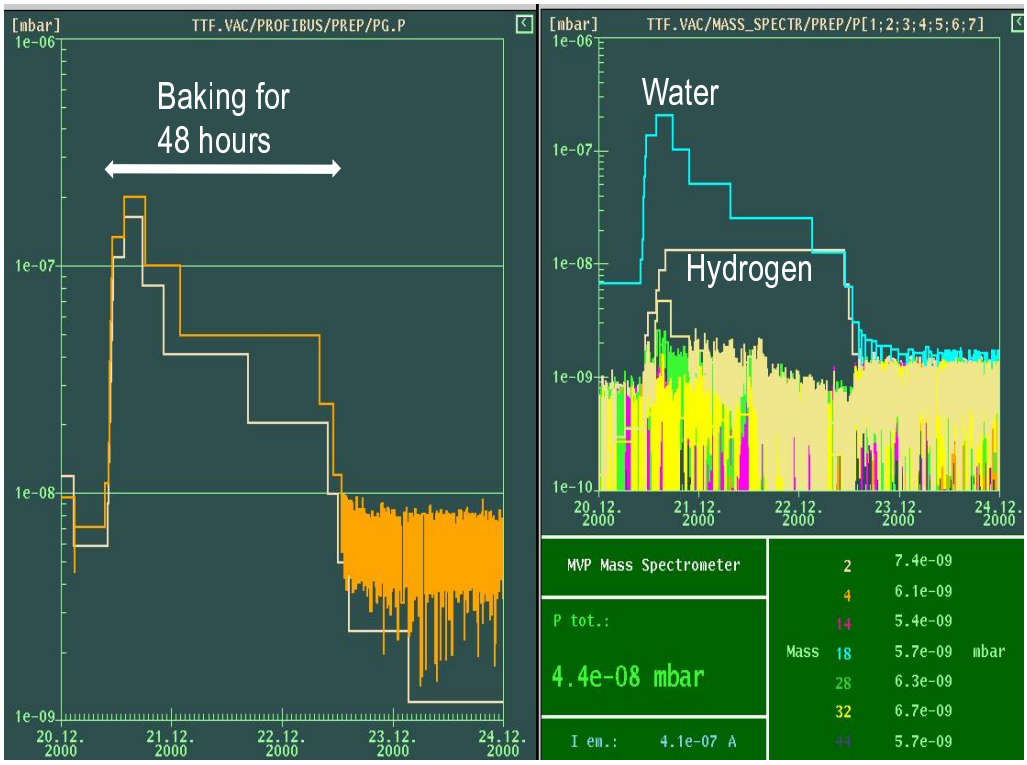

Figure 4.13: Left: Total pressure in the cavity during bakeout. Right: Partial pressures measured with the mass spectrometer on the oil-free pumpstand during 'in-situ' bakeout of a niobium cavity. The dominant partial pressure in the system is water for several hours. Only to the end of the bakeout hydrogen becomes equally important.

Stability of the bake

The long-term stability of superconducting cavities in particle accelerators is of course an important issue. With the discovery of the baking effect, there was some concern that a long exposure of the surface to air might destroy the effect of the baking. The suspicion was that the benefit of baking either comes from the desorption of water from the surface or the reduction of oxides on the surface. A first measurement at KEK indicated that a degradation of the maximum accelerating gradient might be possible [Saito 1999].

At Saclay an electropolished cavity was baked out. The gradients are plotted 4.14. After the test the cavity was exposed to clean air for different time intervals. Before each measurement high pressure water rinsing was applied to avoid a particle contamination. Within the measurement errors no significant change in the cavity behaviour was observed even after exposure to air for 2 months (figure 4.14).

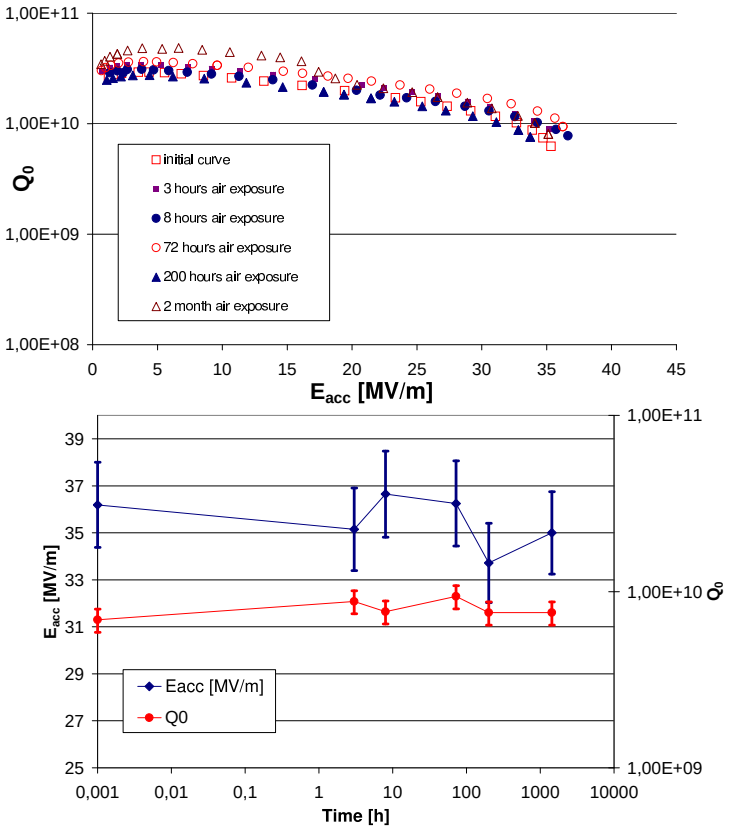

Figure 4.14: Top: Excitation curves of a cavity exposed to clean air. Bottom: Quality factor and accelerating gradient as a function of exposure time to clean air. Within the measurement errors no difference in the behaviour of the cavity was observed. Test temperature was 1.6 K.

Dependence on the bakeout temperature

The baking temperature used in most of the tests performed in this thesis was 100°C. As can be seen in figure 4.6 a higher temperature of 120°C can improve the quality factor further. In other experiments the baking temperature was 145°C [Kneisel 1999] or even 170°C [Visentin et al. 1998]. However, it was found out more recently that a bake at 170°C can reduce the quench field of by 5 MV/m [Visentin et al. 1999]. Bakeout experiments at very high temperatures (200 - 600°C) confirm that the quench field degrades [Visentin et al. 2001]. Therefore 140°C seems to be a reasonable upper limit to prevent that the benefit of the bakeout is counterbalanced by an increase in residual resistance as discussed in section 22. This conclusion is supported by the measurements made on 8.6 GHz niobium cavities [Palmer 1988a].

Depth of the surface layer affected by the 'in-situ' bakeout

P. Kneisel has made an experiment where he removed a thin layer from the niobium surface by oxipolishing and measured the surface resistance of the cavity [Kneisel 1999, Kneisel 2000]. He found that the reduction in R_{BCS} is lost after a removal of about 300 nm. The high field behaviour of the cavity could not be studied, as the cavity was limited by thermal breakdown and field emission in some measurements. The surface sheath with reduced BCS surface resistance is hence eight times thicker than the London penetration depth ($\lambda_L = 32nm$). The baking effect is due to changes within this surface layer. In the next section the the properties of this surface layer will be reviewed.

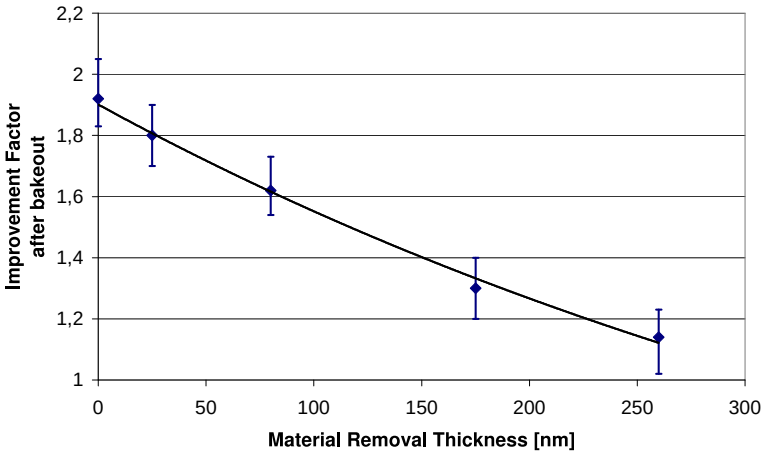

Figure 4.15: Change of the improvement factor of a baked cavity after removing material from the surface in small steps with oxipolishing [Kneisel 1999]. The benefit of the baking is lost after approximately 300 nm have been removed from the surface.

4.3.1 Surface studies on niobium

The results on the bakeout effect described in the previous section have shown that the superconducting properties of niobium in a thin surface layer are changed. A simplified picture of the surface assumes that the niobium bulk is covered by several different oxides and adsorbates. These consist of

- a layer of adsorbates which consists of water, hydrocarbons and other gases
- a dielectric oxide layer of Nb_2O_5
- a layer of metallic NbO, which is weak superconductor ($T_c = 1.4$K)
- a layer of niobium metal with interstitially dissolved oxygen atoms ("oxygen lattice gas")
- the niobium bulk material with impurity atoms

In reality the niobium sheet material is polycrystalline and has features like grain boundaries. In the grain boundaries the diffusion of impurities is enhanced. An example is the diffusion of titanium during the high temperature treatment into the grain boundaries [Antoine et al. 1995]. Lattice effects on the individual crystallites can serve as channels for oxygen atoms and therefore the oxidation might not be homogeneous. Oxidation can lead to stress between the surface oxide layer and the bulk metal [Halbritter 1987].

This surface composition depends delicately on the surface treatments like etching, electropolishing, high temperature heating and 'in-situ' bakeout. The wet (electro-) chemical processes will inevitably contaminate the surface layer.

Several studies have been made to relate the surface layer composition to the superconducting properties of niobium. The depth probed by the magnetic field and the surface shielding currents is of the order of the magnetic penetration depth ($\approx 30 - 40$ nm). The result by Kneisel has shown that about 300 nm are changed by the heating. This is nearly on order of magnitude larger than the London penetration depth.

4.3.1.1 Oxygen and Niobium

In the 1970s low niobium cavity performance was frequently attributed to oxide layers. With the progress to higher gradients other effects like field emission [Reschke 1995], foreign material inclusions or hydrogen contamination [Röth 1993] were considered the main limitations. The Q-drop has

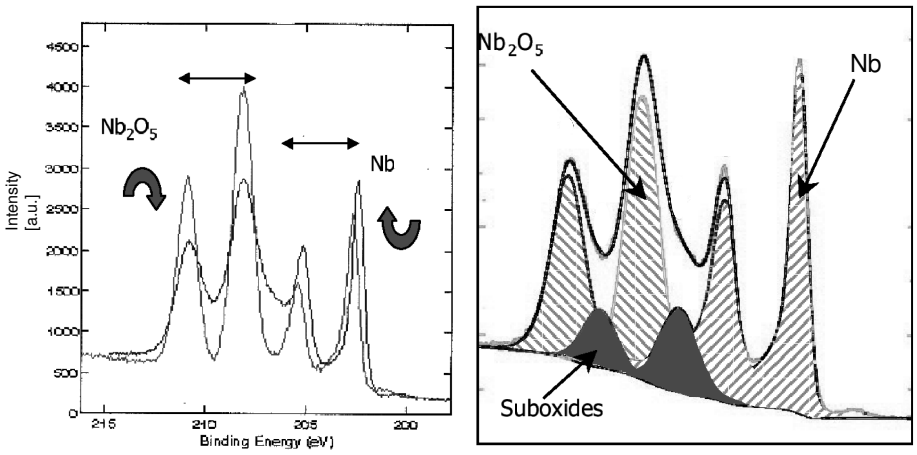

Figure 4.16: Left: XPS spectrum of niobium before and after baking. The niobium pentoxide signal is reduced, whereas the metallic niobium signal is increased. Right: Deconvolution of the XPS spectrum after baking. For a better fit the appearance of suboxides is assumed. Measurements have been done at CEA [Antoine et al. 1999].

opened up the discussion again whether oxygen diffusion can be the reason for this effect.

A tool for investigations of the chemical composition is XPS (X-ray Photoelectron Spectroscopy) where energetic photons impinge on the surface and liberate electrons whose energy is measured. The energy depends on the chemical bonds of the elements in the surface. The advantage of this method is that the chemical state of the surface is investigated. The disadvantage is the rather low penetration depth of a few nm so that for obtaining a depth profile layer by layer has to be removed by ion sputtering. Unfortunately, the sputtering can lead to a reduction of the surface oxides [Grundner 1977, Choudhury et al. 1989]. It is therefore difficult to determine the chemical composition as a function of depth.

XPS on niobium has been done by several authors[2]. If one looks at the typical niobium lines in the energy spectrum of the photoelectrons one sees the niobium metal state and the niobium pentoxide. These are shown for example in figure 4.16.

The measurements often were done while a thermal treatment to over 1000°C of the sample took place. The results show that during heating a decomposition of the natural Nb_2O_5 layer takes place at around 300°C. This decomposition results in a NbO layer, which will only be dissolved into the niobium lattice or evaporated from the surface at temperatures above 700°.

[2]See [Grundner 1977, Grundner and Halbritter 1980, Palmer 1988a, Dacca et al. 1998, Antoine et al. 1999]

The temperature region between 150 - 250°C is not as well studied as the high temperature region. Still, in several studies the dissolution of the Nb_2O_5 layer can be seen, as the photoelectron energy spectrum attributed to the fully oxidized state of niobium corresponding to Nb_2O_5 is reduced in intensity (see figure 4.16) [Palmer 1988a, Grundner and Halbritter 1980, Antoine et al. 1999, Daccà 2000, Ma 2000, Kowalski 2001]. The formation of an intermediate oxidation state of the niobium between the fully oxidized Nb_2O_5 state and and the metallic state can be seen. The detailed nature of these intermediate oxidation states is not very clear.

Several different lower oxidised niobium states can exist under rather special conditions. For example, Nb_2O_{5-y} ($y \ll 1$) has been described [Sayagués et al. 2001] where the crystalline modification in some cases has metallic properties [Cava et al. 1991]. Other authors claim the existence of NbO_2 [Grundner 1977, Grundner and Halbritter 1980, Hulm et al. 1972, Palmer 1988a], $NbO_{0.2}$ [Daccà 2000] or $NbO_{0.02}$ [Grundner and Halbritter 1980].

The superconducting properties of some of these niobium oxides were investigated [Hulm et al. 1972]. NbO was found to be a weak superconductor with $T_c \approx 1.4$ K. A two-phase system of niobium and NbO for ratios of O/Nb from 0.5 to 0.95 show a $T_c \approx 6.5$ K. For ratios of O/Nb in the range from 1 - 1.5 the $T_c \approx 1.4$ K which is probably due to the NbO in the two-phase system of NbO/NbO_2.

Several studies focused on the difference in the oxide layer produced by etching, electropolishing, oxipolishing, high pressure water rinsing and high temperature heat treatment e.g. [Grundner 1977, Antoine et al. 1999]. A SIMS[3] study has shown that the oxide layer from electropolishing is thinner (2.5 nm) than the layer produced by chemical etching ($\approx$ 5 nm) [Antoine et al. 1999]. The oxide layer of the electropolished sample reached the thickness of the etched sample only after 2 days of air exposure (4.6 nm). High pressure water rinsing can lead to a further oxidation [Knobloch and Freyman 1998, Antoine et al. 1999].

Another XPS study found that the oxide layer of electropolished samples is rather inhomogeneous and thicker (6nm) than the oxide layers produced in high temperature heat treatments above 1000°C (3nm) [Grundner 1977].

Further complications arise from the fact that niobium well annealed in an oxygen atmosphere yields a Nb-O system where the oxygen is interstitially dissolved in the lattice. The O/Nb ratio is smaller than 0.1 for these mixtures. Most prominently, the critical temperature T_c is reduced by 0.93 K per at.% oxygen dissolved in the lattice [de Sorbo 1963], while B_{c2} is increased

[3]Secondary Ion Mass Spectrometry

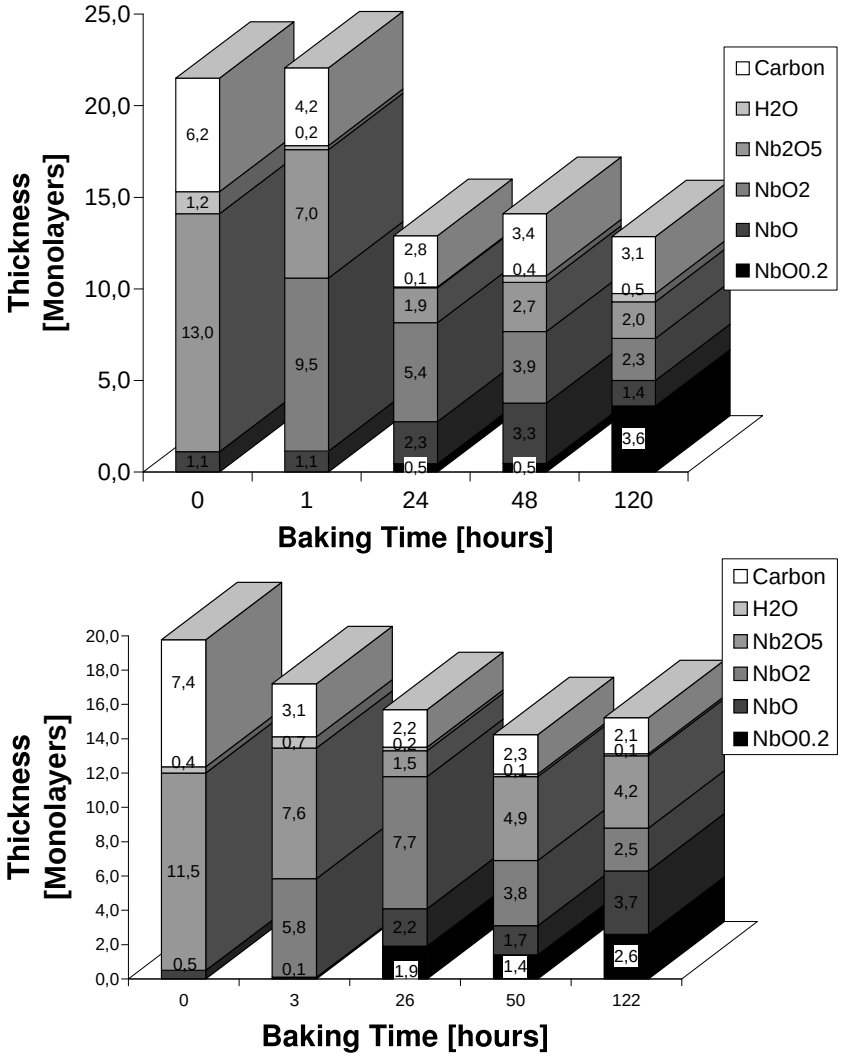

Figure 4.17: Composition of the surface layer deduced from angular resolved XPS during different stages of the baking. Measurements done by A. Daccà at INFN Genoa [Daccà 2000].

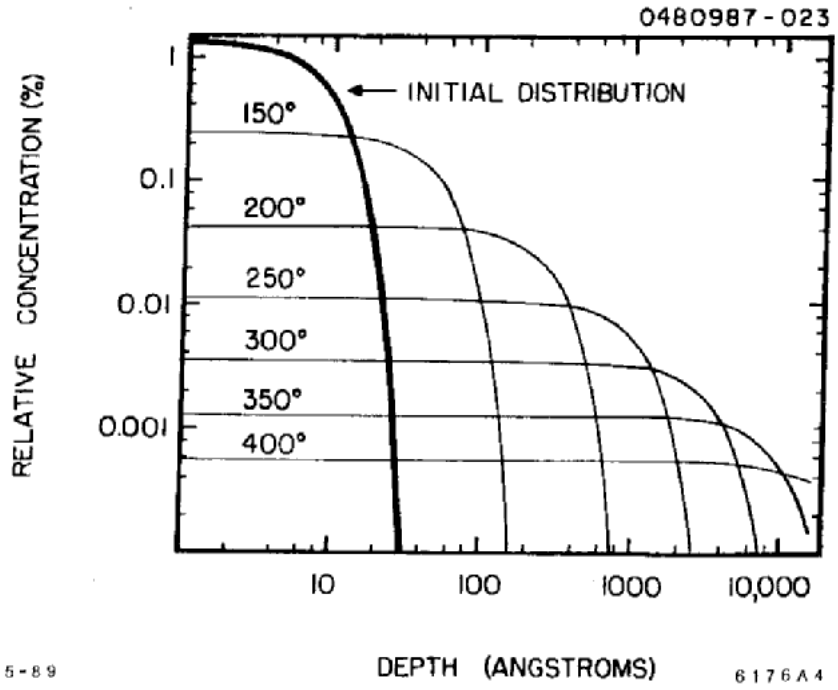

Figure 4.18: Calculated diffusion of oxygen in niobium as a function of temperature [Palmer et al. 1990]. It has been assumed that number of oxygen atoms in the metal does not change i.e. that the heating takes place under vacuum. Evaporation of oxygen into the vacuum is neglected.

[Koch et al. 1974]. Of course, the RRR decreases with a larger amount of oxygen as mentioned already in section 1.5.2. The diffusion of oxygen in niobium has been calculated (see figure 4.18) [Palmer et al. 1990].

A recent study using an X-ray diffraction technique has looked at the atmospheric oxidation of high-quality niobium films with (110) crystal orientation on sapphire substrates [Hellwig 2000, Hellwig and Zabel 2000]. It was found that the oxidation in air inevitably leads to the formation of amorphous oxide layers and the interstitial solution of oxygen in the niobium lattice. Subsequent annealing in UHV leads to the dissolution of the Nb_2O_5 layer by diffusing more oxygen into the niobium lattice. At 300°C with a pressure of 10^{-3} mbar in oxygen atmosphere the formation of NbO was observed and no interstitial solution of oxygen was observed. The formation of NbO was also observed in another study at higher temperatures in UHV [Sürgers et al. 2001]. The formation of NbO due to segregation of oxygen to the surface has also been reported for another crystal orientation (001) [Uehara et al. 2001], and poly-crystalline niobium after the niobium was annealed at high temperatures above 1000 K [Halbritter 1987].

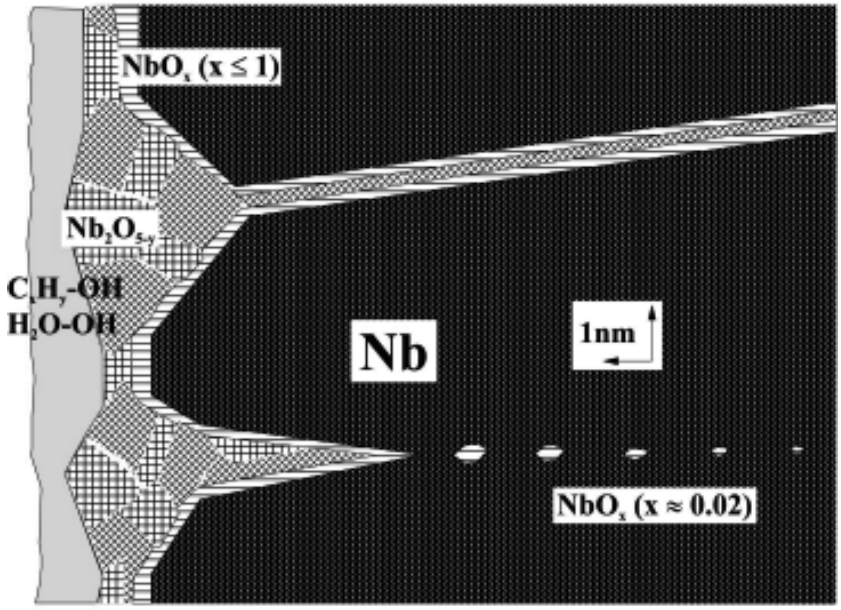

Figure 4.19: Model for the oxide structure of niobium due to strain caused by oxide growth [Grundner and Halbritter 1980, Halbritter 1987].

Some authors have argued that the surface is not a system of homogeneous layers but that oxidation leads also to geometrical defects due to the different lattice structure [Halbritter 1987]. The surface is claimed to be serrated as indicated by angular resolved XPS measurements (see figure 4.19). A more recent study by A. Daccà did not confirm this result [Dacca et al. 1998].

In conclusion, the niobium pentoxide at the surface seems to be reduced by the low temperature 'in-situ' baking. Partly, the oxygen is diffusing into the niobium lattice. Another part of the available oxygen produces other oxides, most notably NbO. The detailed composition of the composition of these other oxides is not yet well understood.

4.3.1.2 Other contaminants

The surface studies mentioned above have revealed a number of other contaminants. Carbon in the form of graphite and also as NbC has been found in nearly every study, especially after baking [Ma 2000] and when sputtering was used for depth profiling e.g. [Kowalski 2001]. Most likely this contamination is due to the residual gases in the XPS measurement system, see e.g. [Dacca et al. 1998]. Further contaminants include fluorine, sulphurus and phosphorus coming from from the different surface treatments (etching and electropolishing).

4.3.2 The role of surface contaminants on the low field performance

A quality factor degradation at high field is observed for chemically etched and electropolished resonators. Assuming that chemical residues from chemical processes play a role in the effect of the bakeout, one might expect to see some evaporation of the substances involved. Only fluor and water are common ingredients for the acid mixtures used for these processes. However, the mass spectrometers on the pump stands used to evacuate the cavity do not show any significant contribution to the residual gas from any other substance than water and hydrogen. Therefore it is difficult to allege the chemical residues on the niobium surface as the reason for this behaviour. If one assumes oxygen diffusion as the driving process behind the 'in-situ' bakeout effect, it is possible to explain some of the observations in the low field behaviour of superconducting niobium cavities.

First of all, the growth in the residual resistance can be attributed to the increased number of impurities in the metal. In this case it would be the interstitially dissolved oxygen atoms. It was calculated that the diffusion of oxygen atoms is in the order of 100-200 nm [Saito and Kneisel 1999] for a typical bakeout (140°C, 40 hours), which corresponds qualitatively to the depth of the layer changed by the bakeout as measured by Kneisel (300 nm) [Kneisel 1999]. The influence of oxygen is to shorten the mean free path ℓ of the electrons. The normal resistivity increases by about 4.5 $\mu\Omega$ per atomic percent oxygen [Schulze 1981].

This has also an influence on the BCS part of the surface resistance because it depends on the normal state conductivity 1.31. Since the niobium used in the cavity is very pure, it is expected that a small reduction in the mean free path of the electrons results in a reduced R_{BCS} as shown in figure 1.4. However, it is unclear whether the mean free path of the electrons is sufficient to explain this dependence. At most a reduction factor of 1.6 can be expected from the BCS theory due to the change in the mean free path. Larger reduction factors $\approx$2 have been observed. K. Saito and P. Kneisel fitted the data and obtained a good fit only after the superconducting energy gap Δ is taken into account [Saito and Kneisel 1999].

Higher baking temperatures above 200°C eventually will enhance oxygen diffusion into the material reducing the thermal conductivity, so that the quench limit can be reduced [Visentin et al. 2001] and the residual resistance growth [Palmer 1988a] (see also section 22). Only higher temperatures around 300°C will allow the surface layer to be purified again as described by [Palmer 1988a] and [Visentin et al. 2001], while the thermal conductivity is further reduced due to the oxygen diffusion.

Chapter 5

Discussion of the high surface field behaviour

5.1 Open questions

The results presented in this thesis pose two fundamental questions: Why does electropolishing allow for higher surface fields? And why is a low-temperature bakeout needed to avoid the quality factor degradation at high surface fields? Several effects can influence the RF losses in superconductors at very high surface fields. In this section some models are presented which address these questions.

5.2 Delayed flux entry into type-II superconductors

Some continuous wave measurements at 2 K on electropolished cavities have reached magnetic fields that are above $B_{c1} \approx 160$ mT corresponding to accelerating fields of 38 MV/m. In electropolished cavities at KEK have also shown the same behaviour has been seen, while etched cavities have achieved these field levels only in a few cases [Kneisel et al. 1995][1]. Apparently B_{c1} is not the limiting field for niobium cavities. So far, none of the cavities has exceeded the thermodynamical critical field $B_{c,th}(2\text{K}) = 190\text{mT}$ which corresponds to 45 MV/m. Due to these results in excess of the first critical field of niobium it is important to look at the effects of delayed flux entry into type-II superconductors.

[1] Pulsed measurements on chemically etched 1.5 GHz single cell resonators have shown even higher values for the critical field [Graber et al. 1993] at 1.5 K.

5.2.1 Bean-Livingston surface barrier

In 1964, Bean and Livingston [Bean and Livingston 1964] have proposed the existence of a surface barrier[2] for the penetration of magnetic flux into a type-II superconductor. They consider a superconductor in the half space $x \geq 0$ whose boundary to vacuum is a perfect plane. A flux quantum in the superconductor oriented along the y-axis will be attracted by the boundary since it experiences an image force by an "image" fluxon of opposite orientation. This is analogous to the image charge method in electrostatics. Hence, if no or only a weak external magnetic field is present, the fluxon will be driven out of the superconductor which means in thermal equilibrium that the type II superconductor is in the Meissner phase.

When an external field is applied in y-direction it will penetrate into the superconductor with a exponential attenuation and exert a force on the flux quantum in positive x-direction. The potential energy is given by[3]:

$$E(x) = \Phi_0 \left(H_{c1} - \frac{1}{2} \frac{\Phi_0}{2\pi\mu_0\lambda^2} K_0 \left(\frac{2x}{\lambda} \right) + H \cdot e^{-\frac{x}{\lambda}} \right) \tag{5.1}$$

The condition that the two energy terms in the above formula are equal at the boundary ($x = 0$) and deep inside the superconductor defines the lower critical field H_{c1}. However, due to the different x dependencies in the two terms, there is a potential barrier which inhibits flux entry at $H \geq H_{c1}$. This barrier vanishes only at significantly larger field. The potential has been calculated and is shown in figure 5.1(Bottom).

5.2.2 Bean-Livingston barrier and geometrical distortions

By using a null-deflection torque magnetometer, it was found that the field of first flux penetration of Pb-Tl films was substantially higher (up to a factor 3) than the lower critical magnetic field [Joseph and Tomasch 1964]. After the film was scored the field of first flux penetration was reduced to values nearly equal to the first critical magnetic field (see fig. 5.2). The larger penetration field in this measurement was attributed to the presence of the Bean-Livingston barrier. After the introduction of defects on the surface, the barrier was assumed to be destroyed, so that the penetration of flux can be facilitated by the irregularities.

[2] There exist several types of surface barriers for superconductors. For a comprehensive overview see [Brandt 1995].

[3] For a detailed derivation see [de Gennes 1966].

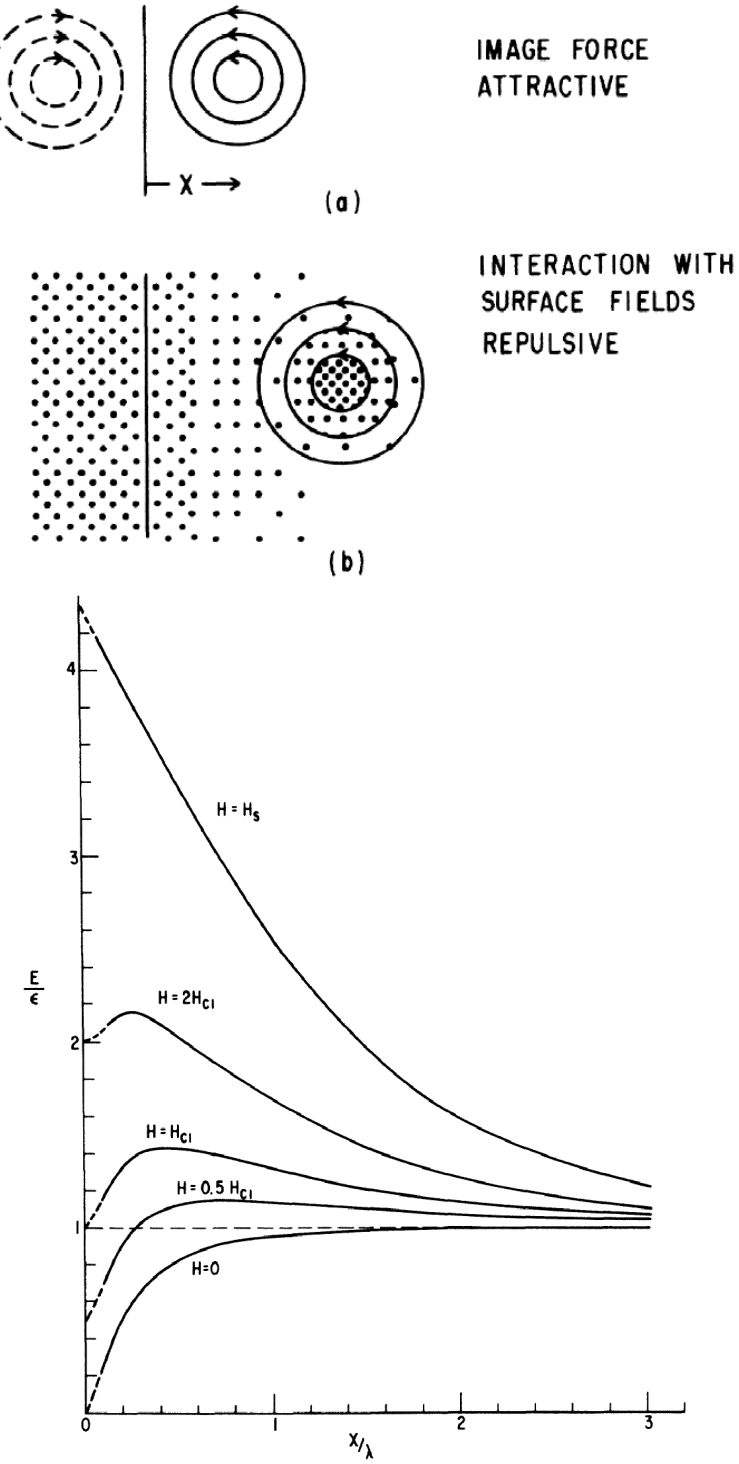

Figure 5.1: Top: (a) A fluxon sees an attractive potential due to its image vortex. (b) Due to the magnetic field changes within the penetration depth, the vortex experiences a force. Dots represent the magnetic field strength. Bottom: Calculated repulsive for various magnetic field values [Bean and Livingston 1964].

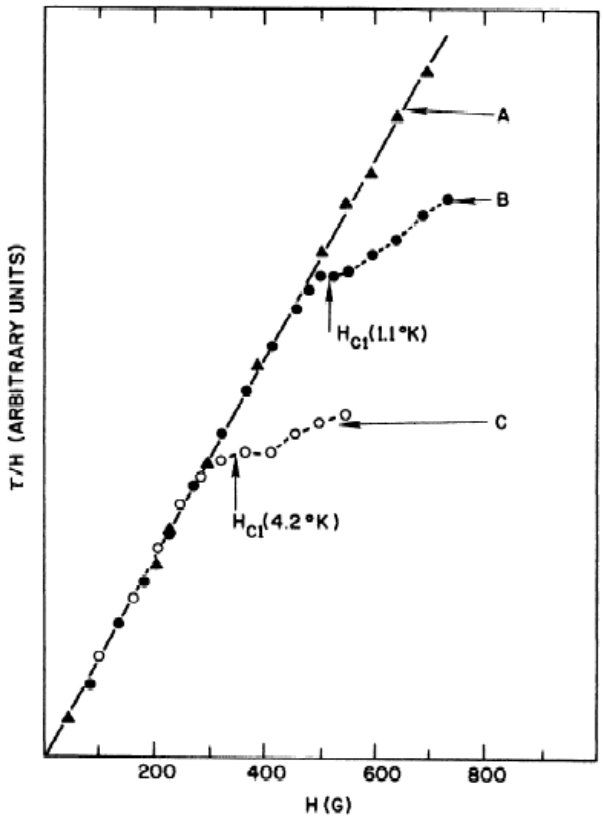

Figure 5.2: Experimental evidence for the Bean-Livingston barrier. The graph shows for a unscored Pb-Tl film (A) the field of first flux penetration at 1.1 K is much larger (730 G) than the lower critical magnetic field (420 G) indicating the existence of a surface barrier. When the film was scored (B) first flux penetration was observed at the first critical field at 1.1 K. For 4.2 K the field of the flux penetration is also consistent with first critical magnetic field (C) [Joseph and Tomasch 1964].

A study on electropolished $Nb_{0.993}O_{0.07}$ wires [Blois and de Sorbo 1964] is also consistent with the existence of the Bean-Livingston surface barrier. In this study a lower magnetic penetration field was found when the surface was scratched. In addition a number of grain boundaries on the sample have shown a lower penetration field. Only very few grain boundaries show high penetration fields comparable to defect-free regions on the sample (figure 5.3). In high temperature superconductors structural defects are known to influence the pattern of the flux penetration [Koblischka 1996][4].

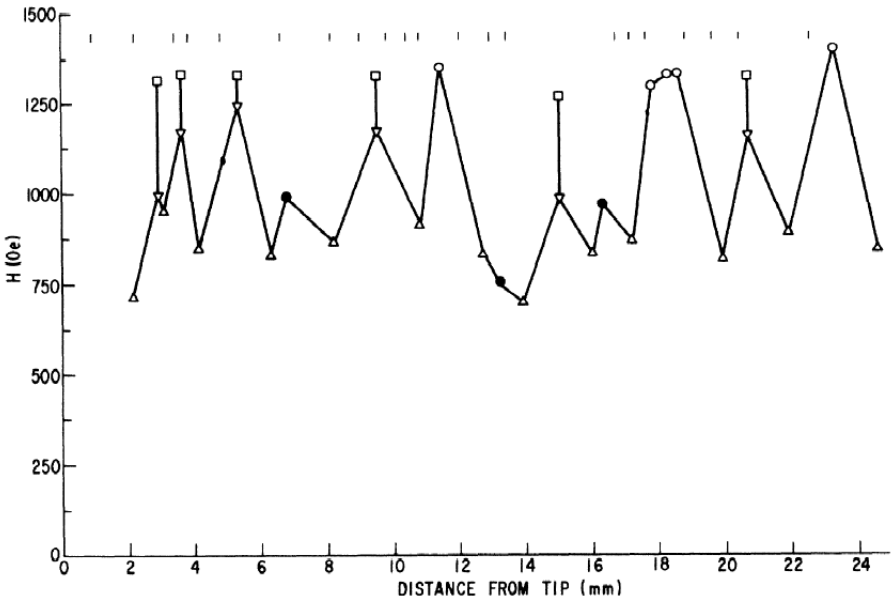

Figure 5.3: Magnetic penetration field into a superconductor as a function of the position along a $Nb_{0.993}O_{0.07}$ wire. Open circles (○) indicate an abrupt onset of field penetration. Squares (□) also indicate an abrupt penetration. The inverted triangles (▽) indicate a first partial penetration of flux into the sample probably due to flux penetration at imperfections in the sample. Dots (•) and triangles (△) mark the field of a gradual flux penetration of the complete sample. H_{c1} is 580 Oe and $H_{c,th}$ is 1360 Oe for this material. The marks on the top of the graph indicate the position of the grain boundaries [Blois and de Sorbo 1964].

[4] A theoretical approach to the reduction of the Bean-Livingston barrier due to surface roughness is given in [Bass et al. 1996].

5.2.3 Surface pinning

The pinning of magnetic flux in the surface can lead to hysteresis in a type-II superconductor. The surface condition can strongly influence the pinning of fluxons. Strong oxidation of the surface has been used to reduce this effect in several experiments [Sekula and Kernohan 1972, Auer and Ullmaier 1973, Weber et al. 1991]. An example of the hysteresis of a niobium single crystal before and after oxidation is shown in figure 5.4. After the oxidation in oxygen atmosphere of 760 Torr at 400°C for 1.5 minutes the hysteresis has been reduced to a much lower value. Such a strong oxidation will produce a 1 μm thick layer of oxygen[5] impurities with steep concentration gradient. It is argued that the surface pinning is reduced in this way [Sekula and Kernohan 1972].

A possible explanation for the reduction of the quality factor at high fields due to surface pinning would then be as follows: Before bakeout, the magnetic flux enters the sample, is pinned in the surface due to impurities and the inhomogeneities in the oxide surface layer. Therefore the flux will not leave the sample. Half an RF period later, flux of the opposite field direction enters the surface layer and annihilates with pinned flux and therefore dissipates energy. After bakeout, the impurity content is smeared out and better homogeneity leads to an improved reversibility of the surface layer so that

[5] Oxygen and nitrogen in the case of oxidation in air.

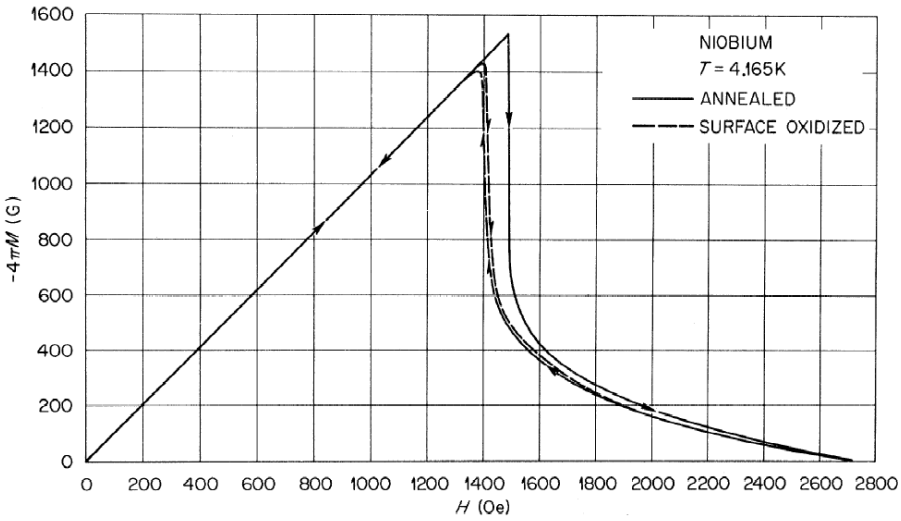

Figure 5.4: Magnetization curve of a niobium single crystal before and after oxidation in oxygen atmosphere of 760 Torr at 400°C for 1.5 minutes [Sekula and Kernohan 1972].

the surface pinning is reduced. The degradation of the quality factor would not be observed.

Measurements on niobium film microstrip resonators at 1.5 GHz showing enhanced losses at higher surface fields have been interpreted to be due to an increased dissipation caused by geometrical defects [Golossovsky et al. 1995]. The results on a subsample of these resonators have shown a nonlinearity in the dependence of the quality factor on the magnetic fields starting at a certain magnetic field H_{fp} where flux penetration starts. The authors claim that magnetic flux can enter the sample and dissipate energy in the films showing a strong nonlinear behaviour. This field is smeared out by the rougher surface. The resonators not showing this nonlinearity are assumed to have smoother edges.

An additional effect is that the penetration depth increases with the surface roughness as proposed by Strongin et al.[6]. These results are compatible with scanning Hall probe microscope images of the field penetration into niobium films [James et al. 2000]. Irregular patterns of the field penetration in the form of dendritic fingers have been observed. For higher quality films (RRR = 30) the flux front is smoother than for lower quality ones (RRR = 3) which the authors attribute to the smaller number of pinning centers in the higher quality film.

5.2.4 Velocity of flux penetration

An uncertainty for the possibility of the flux penetration during an RF period arises from the measurements with pulsed magnetic fields done on niobium tubes with pickup coils in between [Flippen 1965]. The time needed to fully penetrate a niobium tube of 0.85 mm wall thickness was measured to be in the order of 20 μs. The speed of flux penetration in niobium is hence in the order of 42.5 m/s. The rise time of the pulsed magnetic field is in the order of 10^5 T/s.

The long penetration time has been used as an argument that flux penetration is too slow to be relevant for microwave fields [Padamsee et al. 1998]. We do not share this point of view. Using the speed of 40 m/s magnetic flux would penetrate a depth of about 30 nm within a period of the 1.3 GHz radiofrequency in TESLA cavities. This is already in the order of λ_L, and moreover the time derivative of the radiofrequency magnetic is 10^8 T/s, hence a penetration seems plausible.

[6] See [Varmazis and Strongin 1974],[Varmazis et al. 1975],[Varmazis and Strongin 1975], [Varmazis et al. 1976].

5.3 Magnetic field enhancement due to grain boundaries

The remarkable difference between electropolished and etched resonators in terms of the maximum achievable surface field can be taken as evidence that surface roughness plays an important role. On an etched surface the grain boundaries are much more pronounced as shown in figure 2.7. Magnetic field enhancement near the grain boundaries would cause the niobium to become normalconducting at fields below the critical magnetic field. A detailed model was developed by [Knobloch et al. 1999] to describe the gradually decreasing quality factor with an increasing number of grain boundaries becoming normalconducting. In the following this model will be described.

The basic idea is that the roughness of the surface leads the niobium to become normalconducting at a lower than the critical field due to magnetic field enhancement. The magnetic field enhancement factor can be defined as

$$\beta_m = \frac{B_{enh}}{B} \tag{5.2}$$

where B is the magnetic field in the absence of surface roughness. For a hemisphere on a planar superconductor one can calculate the field enhancement analytically ($\beta_m = \frac{3}{2}$).

More power will be dissipated in the normalconducting niobium of the grain boundary, hence the quality factor of the cavity is reduced. The number of normalconducting grain boundaries will increase with larger fields, so that the dissipated power increases and the quality factor decreases. In the model a distribution function $n_{gb}(\beta_m)d\beta_m$ of the field enhancement is introduced. This is needed to describe a gradual increase in the number of normalconducting grain boundaries. In addition the distribution function should allow to describe the magnetic field level where the cavity shows a thermal breakdown [7]. Finally, the distribution function should be adjustable for the field level at which the quality degradation starts.

The model assumes steps of 10 μm height and 100 μm width with an inclination angle of the step corner of 30 - 40° with respect to the cavity surface (see figure 5.5). Thermal simulations show that a grain boundary with a field enhancement $2.1 < \beta_m < 2.9$ will lead to a thermal breakdown of the whole cavity at 30 MV/m. A grain boundary with infinite length and the value of $\beta_m = 2.1$ would still be thermally stable up to 30 MV/m although it becomes normalconducting. To allow for the onset of the degradation at

[7] This assumes of course that there are no other inclusions like tantalum grains in the material.

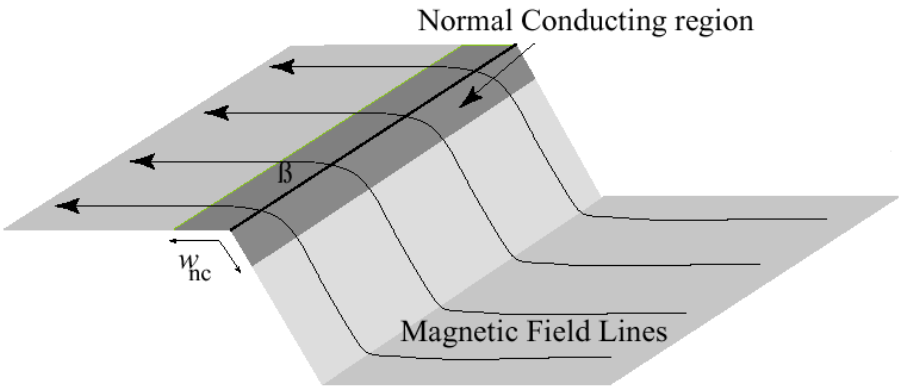

Figure 5.5: Geometry of the modeled grain boundaries in the model of [Knobloch et al. 1999]. A grain boundary becomes normalconducting due to field enhancement in a width w_{nc}.

20 MV/m a $\beta_m = 2.5$ is needed. The simulation assumes a width $w_{nc} = 1\mu$m and a magnetic field penetration due a skin depth of 1 μm (see figure 5.5).

For a continuous decrease of the quality factor, a continuously decreasing distribution of field enhancement factors with larger β_m is assumed. To increase the number of grain boundaries gradually to field values corresponding to 30 MV/m a $\beta_m = 1.6$ is needed. From a consideration of the total area of the grain boundaries in the cavity it is important to have the majority of grain boundaries at $\beta_m < 1.5$ as otherwise the microwave losses in the normalconducting material would become too high to describe the cavity behaviour correctly.

Measurements on samples in combination with electromagnetic field calculations indicated that these field enhancement factors are typical for etched surfaces [Geng et al. 1999]. On electropolished samples step heights are at least a factor of 2 smaller. Therefore this model predicts that electropolished surfaces should quench at higher fields.

The surface roughness model is incapable to describe why the degradation of the quality factor is cured by the low temperature bakeout. The bakeout cannot possibly change the geometry, but rather the chemical composition of the surface. This can only be introduced via a change of the critical magnetic field due to the bakeout.

5.4 Chemical composition of the surface layer

As shown in the previous chapter, the low field behaviour and the temperature dependence of the bakeout are at least qualitatively understandable with the diffusion of oxygen. The fundamental questions remaining is why the high field behaviour is dramatically improved. Above a magnetic surface field of 100 mT the bakeout reduces the microwave surface resistance.

It has been mentioned that the electron mean free path is shortened after baking [Saito and Kneisel 1999, Visentin et al. 2001], but also the penetration depth is influenced by the diffusion of impurities as observed already by Pippard [Pippard 1953]. λ increases with a shorter mean free path ℓ. Therefore a deeper layer of the surface is probed after the bakeout.

The detailed influence of the chemical composition on the superconducting properties of niobium is not well understood. Up to now the formation of other oxides than Nb_2O_5 was thought to result in bad cavity performance see e.g. [Halbritter 1987]. Apparently this is not the case as a change in the oxide composition due to the bakeout as described in section 4.3.1 shows an enhancement of lower oxides. [Halbritter 1999] has proposed that the changes in the oxide layer by the low temperature baking smear out the BCS density-of-states and that the number of localized states in the Nb_2O_{5-y} is reduced, thus reducing inelastic surface scattering and interface tunnel exchanges.

The role of other contaminants remains unclear. An electropolished surface is easier to clean, so it might be expected that less residues remain on the surface after the final high pressure water rinsing [Visentin 2001]. Therefore higher breakdown fields in electropolished cavities might be due to the cleaner surface.

5.5 Weakly coupled grains

Another model to describe a field dependent of the surface resistance is based on the idea of weakly coupled grains (see e.g. [Bonin and Safa 1991]). The grain boundaries are treated as of Josephson junctions with a critical current I_c and a specific resistance

$$G = R_{gb}a^2 \tag{5.3}$$

where R_{gb} is the normal state resistance of the grain boundary and a^2 the area of a grain boundary. For small frequencies $\omega \ll \omega_c = 2eI_cG/\hbar$ and zero temperature a junction can be looked at like it were in the static case: For $I < I_c$ it dissipates no energy, while for $I \gg I_c$ it behaves like a pure resistor. One can relate this to an RF field at which the resistance is turned on:

$$H_{gb} = I_c d \tag{5.4}$$

with d being the penetration depth in the grain boundary. As shown in [Bonin and Safa 1991] for large grains and the low temperature normal state resistivity is very low $G = 2 \cdot 10^{-16} \Omega m^2$ [Schulze 1981]. With a typical width of a grain boundary of 10 μm one would get $H_{gb} = 10^8$ Am^{-1} or $B_{gb} = 125$ T. This is of course much higher than the bulk critical field, so that in principle for polycrystalline niobium sheets there should be no problem.

In a more realistic model, contaminants in the grain boundaries have to be taken into account. They would reduce I_c and cause losses at much lower magnetic field. A possible temperature dependence due to the heating with the RF current is neglected completely.

If one assumes that the bakeout at 100 - 150°C removes part of these contaminants by diffusion or evaporation, the quality factor improvement is qualitatively understandable. A surface analysis with special emphasis on the grain boundary appears highly desirable to decide whether this grain boundary effect is relevant. It will be also difficult to describe the positive effect of the bakeout for both - electropolished and etched - surfaces within this model, although the grain boundaries are of course a much more serious problem in etched cavities.

A better application for this model are superconductors like niobium sputtered films or Nb_3Sn material[8]. These superconductors typically show a strong dependence of the surface resistance on the RF magnetic surface field and are limited to 23 MV/m in one-cell cavities [Arbet-Engels et al. 2001].

5.6 Global thermal instability

[Haebel 1998], [Visentin et al. 1999] considered the thermal feedback mechanism. The temperature dependence of the surface resistance is taken into account via:

$$R_s = R_0 + \frac{\delta R_s}{\delta T} \Delta T \tag{5.5}$$

R_0 represents the surface resistance at low field. ΔT is the temperature increase on the inner cavity wall due to the dissipated RF power.

$$\Delta T = R_{thermal} \cdot P_{diss} \tag{5.6}$$

R_{therm} is the thermal resistance which gives rise to the temperature difference between outer and inner surface. It depends on the thickness d and the

[8] This is also true for other Niobium-based films (NbN) and high temperature superconductors. Of course, there are also other models which try to describe the limiting effects in these superconductors.

thermal conductivity $\lambda_{thermal}$ of the niobium and the Kapitza resistance h_K of the niobium-helium interface. This can be expressed as:

$$R_{therm}\Delta P = \left(\frac{d}{\lambda_{thermal}} + \frac{1}{h_K}\right)\frac{R_s H_s^2}{2} \tag{5.7}$$

This reduces to

$$R_s = \frac{R_0}{1 - CE_{acc}^2} \tag{5.8}$$

where

$$C \approx \frac{1}{2}\left(\frac{4\cdot 10^{-9}}{\mu_0}\right)^2 \frac{\delta R_s}{\delta T}\left(\frac{d}{\lambda_{thermal}} + \frac{1}{h_K}\right) \tag{5.9}$$

A fit of the measured $Q(E_{acc})$ curves is possible, however the proportionality factor describing the dependence of C on $\frac{\delta R_s}{\delta T}$ is one order of magnitude too low [Visentin et al. 1999].

5.7 Field dependence of the energy gap

The electropolished cavities approach the fundamental limit of the superconductor. Therefore one has to take into account the the dependence of the energy gap on the magnetic field. This can be done by using the temperature dependence of the energy gap. For $T = T_c$ the energy gap should be zero. All Cooper pairs have been broken apart due to the thermal excitation. The relation between the energy gap Δ and the temperature T is given in the BCS theory:

$$\frac{1}{N(0)V} = \int_0^{\hbar\omega_{Debye}} \frac{d\epsilon}{\sqrt{\epsilon^2+\Delta^2}}\left[1 - 2f(\sqrt{\epsilon^2+\Delta^2}, T)\right] \tag{5.10}$$

$f(\sqrt{\epsilon^2+\Delta^2}, T)$ is the Fermi-Dirac distribution function, $N(0)$ is the density of states near the Fermi energy, V describes the interaction potential between two electrons in a Cooper pair, ω_{Debye} is the Debye frequency and $\epsilon = (\hbar k)^2/2m - E_{Fermi}$ describes the energy difference of a Cooper pair to the Fermi energy level. The relation 5.10 can be solved numerically.

A good parameterization of the temperature dependence of the superconducting energy gap [Mühlschlegel 1959, Sheehan 1966]:

$$\frac{\Delta(T)}{\Delta(0)} = \sqrt{\left|\cos\left(\frac{\pi}{2}\cdot\left(\frac{T}{T_c}\right)^2\right)\right|} \tag{5.11}$$

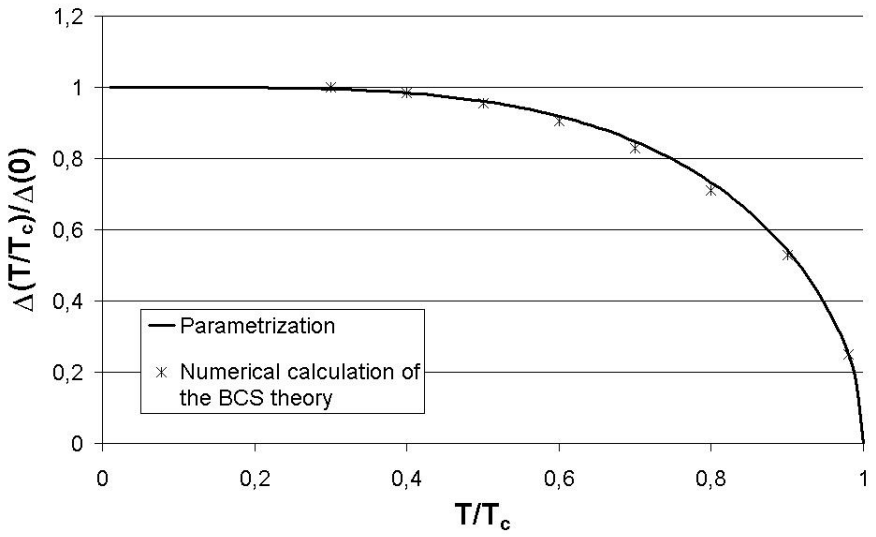

Figure 5.6: Temperature dependence of the energy gap. Dots represent BCS calculation. The line represents the parameterization given in the text (see 5.11) [Schmüser 2001].

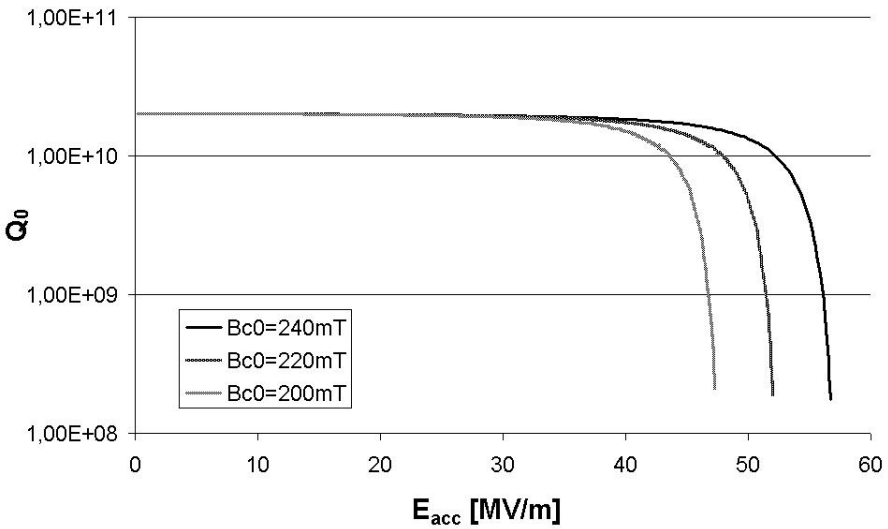

Figure 5.7: Quality factor as a function of the accelerating field for different values of the critical magnetic field. The magnetic field dependence of the energy gap is simulated using equation 5.14 [Schmüser 2001].

The known dependence of the magnetic field on the temperature (see equation 1.11) can be inverted so that the critical temperature is given in terms of the magnetic field:

$$T_c(B) = T_c(B=0) \cdot \sqrt{1 - \frac{B}{B_{crit}}} \tag{5.12}$$

Inserting equation 5.12 in 5.11 gives for a fixed helium temperature T:

$$\frac{\Delta(T)}{\Delta(0)} = \sqrt{\left|\cos\left(\frac{\pi}{2} \cdot \left(\frac{T}{T_c(B=0) \cdot \sqrt{1 - \frac{B}{B_{crit}}}}\right)^2\right)\right|} \tag{5.13}$$

Now one can calculate the BCS surface resistance (see equation 1.29) using the magnetic field dependent energy gap:

$$R_{BCS}(B) = \frac{2 \cdot 10^{-5}}{T} \cdot f^2 \cdot \ln\frac{45.7 \cdot T}{f} \cdot \exp - \left(\frac{1.87 \cdot \Delta(B) \cdot T_c}{\Delta(0) \cdot T}\right) \tag{5.14}$$

With the proper parameters for a typical cavity test ($T = 2$ K, $f = 1.3$ GHz, $T_c(B=0) = 9.2$ K), the dependence of the surface resistance or the quality factor of the cavity can be calculated. A degradation of the quality factor near the critical field can be seen. This degradation depends critically on the choice of B_{crit}. Therefore a measurement of the RF critical field using a high power pulsed measurement on an electropolished cavity are of high interest.

Assuming a reasonable lower limit for $Q_0 > 5 \cdot 10^9$ for cavity in an accelerator, the maximum usable gradient in the machine is about 3 - 4 MV/m lower than the maximum accelerating gradient at the critical magnetic field. If the critical field $B_c = B_{c,th} = 200$ mT the quality drop due to the reduction of the energy gap would be just the limit in the experiment.

Of course, the applicability of this rather simple model is questionable, as the temperature dependence from the Ginzburg-Landau theory of the magnetic field is only correct near T_c.

5.8 Relation of the models to the cavity behaviour

Several points have been addressed in the previous sections. Concerning the two questions brought up in the introduction of this chapter, it is very difficult to attribute the observations in the high field behaviour of cavities to a single effect.

Geometrical field enhancement is probably the best explanation for the difference between etched and electropolished cavities, even though the improvement of the cavities due to the low temperature bakeout is not described very well.

The effects of the surface barriers need to be looked at more closely. So far the results obtained on 1.3 GHz cavities are not conclusive. More defined experimental conditions concerning the surface layer are needed. It would be important to study the influence of oxide layers produced by anodizing using different electrolytes to make a more homogeneous oxide layer and to vary the contaminant in this layer by using different electrolytes.

Chapter 6

Conclusion

Enormous progress in cavity performance has been made in the last 10 years. Today, nine-cell cavities routinely achieve surface fields which exceed 50% of the critical magnetic field of the superconductor. Several single-cell cavities have exceeded 80 % of the critical magnetic field.

An electropolishing system for niobium half cells and a system for single cell niobium cavities has been set up in close collaboration with CERN. A comparison of the cavity performance for different surface treatments of 1.3 GHz niobium single cell resonators was done. The chemically etched resonators reached accelerating gradients of 24 MV/m in continuous wave tests corresponding to magnetic surface fields of 100 mT. The main limitation was a thermal breakdown. These measurements agree well with results on nine-cell cavities at TTF and of other laboratories for the quality of the material used (RRR ≈ 300).

Electropolishing of the niobium surface yields systematically larger surface magnetic fields. The average magnetic field in the electropolished batch was 145 mT. Some resonators exceeded the lower critical field of 160 mT considerably. Fields of up to 180 mT have been measured at a temperature of ≤ 2 K. This is in the order of the thermodynamic critical field $B_{c,th} = 190$ mT. These results are very similar to data obtained on single cells resonators at KEK. The increase of the maximum achievable breakdown field after electropolishing is probably due to the reduction of the field enhancement at the grain boundaries.

First experiments with electropolishing of nine-cell resonators show that the process is technically feasible. In a nine-cell TESLA cavity the accelerating gradient increased from 22 MV/m to 32 MV/m in a continuous wave test. Results on two other resonators are not yet conclusive. More experiments are needed to establish the accelerating gradient of 35 MV/m in a multi-cell structure with electropolishing. DESY sets up an electropolishing facility for multi-cell cavities for this purpose.

A low temperature 'in-situ' bakeout procedure around 120°C for 48 hours was found to be necessary to obtain a quality factor above $5 \cdot 10^9$ at high accelerating fields about 20 MV/m for etched cavities and 30 MV/m for electropolished cavities.

The behaviour at low surface fields (below 10 MV/m) of niobium cavities after bakeout can be understood with a reduction of the dielectric oxide layer due to the diffusion of oxygen into a surface layer of 200 - 300 nm. The increased impurity content of this layer reduces the mean free path of the electrons thus reducing the BCS surface resistance. At most a reduction factor of 1.6 can be expected from BCS theory due to the change in the mean free path. As larger reduction factors ≈ 2 have been observed also other superconducting properties of the niobium are likely to be changed. The oxygen diffusion also can explain slight a increase in the residual resistance.

The high field behaviour is not yet fully understood. Several models have been proposed to describe the degradation of the quality factor. A more detailed analysis of the niobium surface is needed. Cavity measurements on anodized cavities open the possibility to investigate the behaviour of niobium surface which is heavily loaded with oxygen. The thickness of the Nb_2O_5 layer is well defined by the applied voltage. Baking of such a cavity would not lead to a complete dissolution of the dielectric Nb_2O_5, so that it should be possible to distinguish whether the Nb_2O_5 layer has an effect on the high field behaviour or not.

By eliminating many disturbing effects like field emission of electrons or magnetic field enhancement due to the surface roughness electropolishing combined with the clean-room handling allowed to drive microwave cavities close to the physical limit of the superconductor. Although in the past many speculations have been made about the existence of a "superheating" field, the experimental demonstration that the superheating effect exists at 2 K is still missing. High power pulsed measurements should be able to address this questions. Measurements on etched cavities close to T_c [Graber et al. 1993] indicate, that the limiting field is close the superheated field B_{sh} in niobium.

Bibliography

[Antoine et al. 1995]
C. Z. Antoine et al., Evidence for the preferential diffusion and segragation of impurities at grain boundaries in very pure niobium used for radiofrequency cavities, In *Proceedings of the 7th Workshop on RF Superconductivity* [Bonin 1995], p. 647. 78

[Antoine et al. 1999]
C. Z. Antoine et al., Alternative Approaches for Surface treatment of Nb superconducting cavities, In *Proceedings of the 9th Workshop on RF Superconductivity* [Krawcyk 1999]. 35, 38, 40, 79, 80

[Arbet-Engels et al. 2001]
V. Arbet-Engels, C. Benvenuti, S. Calatroni, P. Darriulat, M. Peck, A.-M. Valente, and C. Van't Hof, Superconducting niobium cavities, a case for the film technology, Nucl. Inst. Meth. A, **463**:1, 2001. 95

[Auer and Ullmaier 1973]
J. Auer and H. Ullmaier, Magnetic Behaviour of Type-II Superconductors with Small Ginzburg-Landau Parameters, Phys. Rev. B, **7**:136, 1973. 90

[Aune et al. 2000]
B. Aune et al., The Superconducting TESLA Cavities, PRST-AB, **3**, September 2000, 092001. 14, 20

[Bahte et al. 1997]
M. Bahte, F. Herrmann, and P. Schmüser, Magnetization and Susceptibility Measurements on Niobium Samples for Cavity Production, In *Proceedings of the 8th Workshop on RF Superconductivity* [Palmieri 1997]. 10

[Bahte 1998]
M. Bahte, Materialuntersuchungen an supraleitenden Niob-

Proben mit Magnetisierungs- und Suszeptibilitätsmessungen, Diplomarbeit, Universität Hamburg, 1998, DESY FDET-98-01. 9, 10, 123

[Bardeen et al. 1957]
J. Bardeen, L. Cooper, and J. R. Schrieffer, Theory of Superconductivity, Physical Review, **108**:1175, 1957. 6

[Bass et al. 1996]
F. Bass, V. Freilikher, B. Shapiro, and M. Shvartser, Effect of the surface roughness on the Bean-Livingston surface barrier, Physica C, **260**:231, 1996. 89

[Bean and Livingston 1964]
C. Bean and J. D. Livingston, Surface Barrier in Type-II Superconductors, Phys. Rev. Lett., **12**:14, January 1964. 86, 87

[Bernard et al. 1992]
P. Bernard et al., LEP cavities, in *Proceedings of the 1992 European Particle Accelerator Conference*, edited by E. H. *et al.*, p. 1269, Editions Frontieres, 1992. 20

[Birabeau and Guerin 1974]
J. Birabeau and J. Guerin, Electrolytic polishing of Nb and Ti, Technical Report W 33, CERN, March 1974. 42

[Birabeau and Guerin 1982]
J. Birabeau and J. Guerin, Additif a l'étude de bain du polissage électrolytique du niobium formulé en Juin 1974, Technical Report SB/AC/B/3035/gp, CERN, March 1982. 42

[Bloess 1998]
D. Bloess, Experience on vertical EP at CERN, Private communication, 1998. 37

[Blois and de Sorbo 1964]
R. D. Blois and W. de Sorbo, Surface Barrier in Type-II Superconductors, Phys. Rev. Lett., **12**:499, May 1964. 89

[Bonin and Safa 1991]
B. Bonin and H. Safa, Power dissipation at high fields in granular RF superconductivity, Supercond. Sci. Technol., **4**:257, 1991. 94, 95

[Bonin et al. 1992]
B. Bonin, H. Safa, J. Charrier, et al., Flux trapping in superconducting cavities, in *Proceedings of the 3rd EPAC*, p. 1295, 1992. 13

[Bonin 1995]
P. Bonin, editor, *Proceedings of the 7th Workshop on RF Superconductivity*, volume I+II, Gif-sur-Yvette, October 1995, IN2P3. 103, 105, 110, 115

[Bonin 1996]
B. Bonin, Materials for superconducting cavities, in *Superconductivity in Particle Accelerators*, edited by S. Turner, pp. 191–200, CERN, May 1996, CERN 96-03. 12, 27

[Boucheffa et al. 1995]
A. Boucheffa et al., Kapitza conductance of niobium for superconducting cavities in the temperature range 1,6 , 2 K, In *Proceedings of the 7th Workshop on RF Superconductivity* [Bonin 1995], p. 659. 19

[Brandt 1995]
E. H. Brandt, The flux-line lattice in superconductors, Rep. Prog. Phys., p. 1465, 1995. 86

[Brinkmann et al. 2001]
R. Brinkmann, K. Flöttmann, J. Rossbach, P. Schmüser, N. Walker, and H. Weise, editors, *TESLA - Technical Design Report*, volume II, DESY, March 2001, DESY 2001 - 011, ECFA 2001-209, TESLA Report 2001-23. 1, 15, 19, 21, 24, 60, 119, 123

[Brinkmann et al. 1997]
R. Brinkmann, G. Materlik, J. Rossbach, and A. Wagner, editors, *Conceptual Design Report of a 500 GeV e+e- Linear Collider with Integrated X-ray Laser Facility*, volume I+II, DESY, 1997, DESY 97-048. 1

[Budliger and Laisne 1968]
J. Budliger and A. Laisne, Effet d'Avalanche en Geometrie Plane et Cylindrique, Nuclear Instruments and Methods, **61**:253, 1968. 30

[Cava et al. 1991]
R. Cava, B. Batlogg, J. Krajewski, H. Poulsen, P. Gammel, W. Peck, and L. Rupp, Electrical and magnetic properties of Nb_2O_{5-y} crystallographic shear structures, Phys. Rev. B, **44**:6973, 1991. 80

[Choudhury et al. 1989]
T. Choudhury, S. Saled, J. Sullivan, and A. Abbot, Reduction of oxides of iron, cobalt, tianium and niobium by low-energy ion bombardment, J. Phys. D: Appl. Phys., **22**, 1989. 79

[Citron et al. 1979]
A. Citron, G. Dammertz, M. Grundner, L. Husson, R. Lehm, and H. Lengeler, The Karlsruhe-CERN superconducting RF seperator, Nucl. Inst. Meth., **164**:31 , 1979. 36, 37

[Dacca et al. 1998]
A. Dacca, G. Gemme, L. Mattera, and R. Parodi, XPS analysis of the surface composition of niobium for superconducting RF cavities, Appl. Surf. Sci., **126**:219 , 1998. 34, 79, 83

[Daccà 2000]
A. Daccà, XPS measurements at INFN Genoa on BCP samples during 'In-Situ' bakeout, Private communication, 2000. 80, 81

[de Gennes 1966]
P. de Gennes, *Superconductivity of metals and alloys*, W.A. Benjamin, 1966. 86

[de Sorbo 1963]
W. de Sorbo, Effect of Dissolved Gasses on Some Superconducting Properties of Niobium, Phys. Rev., **132**:107, October 1963. 80

[Diepers et al. 1971a]
H. Diepers, H. Martens, and F. Sun, Improvement of superconducting Nb cavities by anodic oxide films, Physics Letters, **34A**:439, 1971. 38

[Diepers et al. 1971b]
H. Diepers, O. Schmidt, H. Martens, and F. Sun, A new method of electropolishing niobium, Physics Letters, **37A**:139, 1971. 36, 42

[Diepers et al. 1973]
H. Diepers, H. Martens, O. Schmidt, and K. Schnitzke, Superconducting niobium cavities prepared by electropolishing and anodizing, in *Proccedings of the Particle Accelerator conference*, p. 68, 1973. 33

[Doll and Graf 1967]
R. Doll and P. Graf, Superheating in Cylinders of Pure Superconducting Tin, Phys. Rev. Lett., **19**:897, 1967. 10

[Ehmele 2000]
S. Ehmele, Time-table of the EP process of niobium, Private communication, February 2000. 44

[Farnsworth 1934]
P. T. Farnsworth, Multiple Impacting Electron Amplifier, J. Franklin Inst., **218**:411, 1934, nach A. J. Hatch 1966. 30

[Ferreira et al. 1999a]
L. Ferreira et al., SEM measurements on EP samples, Private communication, 1999. 41

[Ferreira et al. 1999b]
L. Ferreira et al., XPS measurements on EP samples, Private communication, 1999. 38, 45

[Ferreira 1998]
L. Ferreira, Surface roughness dependent on amount of niobium material removed, Private communication, 1998. 37

[Flippen 1965]
R. Flippen, The radial velocity of magnetic field penetration in type II superconductors, Phys. Lett., **17**:193, 1965. 91

[Fouaidy et al. 1992]
M. Fouaidy, T. Junquera, and A. Caruette, Surface Temperature Measurements on Superfluid Helium, in *Proceedings of the 5th Workshop on RF Superconductivity*, edited by D. Proch, volume I+II, Hamburg, April 1992, DESY, DESY-M-92-01. 25

[Fuss 1976]
J. Fuss, Diplomarbeit, Universität Stuttgart, 1976. 26

[Geng et al. 1999]
R. Geng, J. Knobloch, and H. Padamsee, Micro-structures of RF surfaces in the electron beam-weld regions of niobium, In *Proceedings of the 9th Workshop on RF Superconductivity* [Krawcyk 1999], pp. 238–245. 38, 93

[Gmelin 1970]
Gmelin, *Handbuch der anorganischen Chemie*, volume 49(Nb), Springer Verlag Berlin, 1970. 34

[Golossovsky et al. 1995]
M. Golossovsky, H. Snortland, and M. Beasley, Nonlinear microwave properties of superconducting Nb microstrip resonators, Phys. Rev. B, **51**:6462, 1995. 91

[Gössel et al.]
A. Gössel et al., TTF Vertical Cavity Test, http://www-mhf.desy.de/desy/ttfadm/doc/vertical/ttf_vertical_test.html. 50

[Graber et al. 1993]
J. Graber, N. Black, H. Padamsee, and M. Pekeler, A New Limit to the Maximum RF Magnetic Field for Niobium, in *Proceedings of the 6th Workshop on RF Superconductivity*, edited by R. Sundelin, volume I+II, pp. 794–801, Newport News, October 1993, CEBAF. 85, 102

[Graber et al. 1994]
J. Graber et al., Reduction of field emission in superconducting cavities with high pulsed power RF, Nucl. Instrum. and Methods A, **350**:572, 1994. 20

[Graber 1993]
J. Graber, High Power RF Processing Studies of 3 GHz Niobium Superconducting Accelerator Cavites, PhD thesis, Cornell University, 1993. 28

[Grundner and Halbritter 1980]
M. Grundner and J. Halbritter, XPS and AES studies on oxide growth and oxide coatings on niobium, J. Appl. Phys., **51**:397, 1980. 34, 79, 80, 83

[Grundner 1977]
M. Grundner, Oberflächenuntersuchungen an Niob für supraleitende Resonatoren mittels der Röntgen-Photoelektronenspektroskopie und der Auger-Elektronenspektroskopie, PhD thesis, Universität Karlsruhe, 1977, KFK 2565. 34, 79, 80

[Guerin 1989]
J. Guerin, Etude du bain de polissage chimique de niobium, Technical Report TE/LC/157/89, CERN, October 1989. 34

[Haebel 1998]
E. Haebel, Thermal feedback to explain the Q-drop, in *R&D issues on superconducting cavities*, number TESLA 98-05 in TTF Meeting, p. 60, DESY, 1998. 95

[Halbritter 1970]
J. Halbritter, Calculation of the BCS surface resistance, Z. f. Phys., **238**:466, 1970. 12, 13

[Halbritter 1987]
J. Halbritter, On the Oxidation and on the Supercondcutivity of Niobium, Appl. Phys. A, **43**:1, 1987. 78, 82, 83, 94

[Halbritter 1999]
J. Halbritter, Rf residual losses, high electric and magnetic rf fields in superconducting cavities, in *Superconducting materials for high energy colliders*, edited by L. Cifarelli and L. Maritato, The science and culture series - Physics, pp. 59–79, World Scientific, 1999. 94

[Hatch and Williams 1954]
A. Hatch and H. Williams, The secondary electron resonance mechanism of low-pressure High-frequency gas breakdown, J. o. Appl. Phys., **25**:417, April 1954. 30

[Hays and Padamsee 1997]
T. Hays and H. Padamsee, Measuring the RF critical field of Pb, Nb and Nb_3Sn, In *Proceedings of the 8th Workshop on RF Superconductivity* [Palmieri 1997], p. 789. 10, 21

[Hellwig and Zabel 2000]
O. Hellwig and H. Zabel, Oxidation of Nb(110) thin films on a-plane sapphire substrates: an X-ray study, Physica B, **283**:228, 2000. 82

[Hellwig 2000]
O. Hellwig, Oxidation of Epitaxial Nb(110) Films: Oxygen Dissolution and Oxide Formation, PhD thesis, Ruhr-Universität Bochum, April 2000. 82

[Hillenbrand et al. 1982]
B. Hillenbrand, N. Krause, K. Schmitzke, and Y. Uzel, Abschlussbericht - Supraleitende Resonatoren, Technical Report NT 2024 7, Siemens AG, Dezember 1982, BMBF Forschungsbericht. 34, 35, 38

[Hörmann 1986]
M. Hörmann, Erstellung von hochwärmeleitfähigem Niob im technischen Massstab für die Hochfrequenzsupraleitung, Z. f. Metallkunde, **77**:338, 1986. 27, 123

[Hulm et al. 1972]
J. Hulm, C. Jones, R. Hein, and J. Gibson, Superconductivity in the TiO and NbO Systems, J. Low Temp. Phys., **7**:291, 1972. 80

[James et al. 2000]
S. James, S. Field, J. Seigel, and H. Shtrikman, Scanning Hall probe microscope images of field penetration into niobium films, Physica C, **332**:445, 2000. 91

[Joseph and Tomasch 1964]
A. Joseph and W. J. Tomasch, Experimental Evidence for Delayed Entry of Flux into a Type-II Superconductor, Phys. Rev. Lett, **12**:219, March 1964. 86, 88

[Kako et al. 1997]
E. Kako et al., Cavity performance in the 1,3 GHz Saclay/KEK cavities, In *Proceedings of the 8th Workshop on RF Superconductivity* [Palmieri 1997], pp. 491–502. 38, 65

[Kako et al. 1999]
E. Kako et al., Improvement Of Cavity Performance In The Saclay/Cornell/Desy's Sc Cavities, In *Proceedings of the 9th Workshop on RF Superconductivity* [Krawcyk 1999], TUP011. 33, 38, 63, 65

[Kako 1998]
E. Kako, Measurement on K-8, remeasurement 14.1.1998, Private communication, January 1998. 67

[Kläui and Lilje 2001]
M. Kläui and L. Lilje, Surface roughness of niobium for different surface treatments, 2001. 38, 39, 40

[Kneisel et al. 1995]
P. Kneisel, R. Röth, and H.-G. Kürschner, Results from a nearly "Defect-Free" Niobium Cavity, In *Proceedings of the 7th Workshop on RF Superconductivity* [Bonin 1995]. 33, 35, 85

[Kneisel 1980]
P. Kneisel, Surface preparations of niobium, in *Proceedings of the Workshop on RF Superconductivity*, edited by M. Kuntze, volume I+II, p. 27, Karlsruhe, 1980, KFK, KFK-3019. 33, 34, 37, 38

[Kneisel 1997]
P. Kneisel, A collection of higher gradient cavity experiments, In *Proceedings of the 8th Workshop on RF Superconductivity* [Palmieri 1997], pp. 830–842. 35

[Kneisel 1999]
P. Kneisel, Preliminary experience with "in-situ" baking of niobium cavities, In *Proceedings of the 9th Workshop on RF Superconductivity* [Krawcyk 1999]. 29, 67, 69, 74, 77, 84, 121

[Kneisel 2000]
P. Kneisel, Messungen an HP1/HP2 nach Ausbacken und Oxipolitur, Private communication, 2000. 77

[Knobloch and Freyman 1998]
J. Knobloch and R. Freyman, Effect on High-Pressure Rinsing on Niobium, SFF Note 980223-01, Cornell University, February 1998. 80

[Knobloch et al. 1997]
J. Knobloch, W. Hartung, H. Padamsee, and F. Newman, Multipacting in 1,5 GHz superconducting niobium cavities of the CEBAF shape, In *Proceedings of the 8th Workshop on RF Superconductivity* [Palmieri 1997], p. 1017. 30

[Knobloch et al. 1999]
J. Knobloch, M. Liepe, R. Geng, and H. Padamsee, High-Field Q slope in Superconducting Cavities Due to Magnetic Field Enhancement at Grain Boundaries, In *Proceedings of the 9th Workshop on RF Superconductivity* [Krawcyk 1999], pp. 77–91. 38, 92, 93, 122

[Knobloch 1997]
J. Knobloch, Advanced Thermometry Studies of Superconducting RF Cavities, PhD thesis, Cornell University, August 1997, CLNS Thesis 97-3. 22, 28, 30, 31, 47

[Koblischka 1996]
M. Koblischka, Analysis of flux distribution of superconductors in the presence of structural defects., Supercond. Sci. Technol., **9**:271, 1996. 89

[Koch et al. 1974]
C. Koch, J. O. Scarbrough, and D. Kroeger, Effects of interstitial oxygen on the superconductivity of niobium, Phys. Rev. B, **9**:888, 1974. 82

[Kojima 1990]
Y. Kojima, editor, *Proceedings of the 4th Workshop on RF Superconductivity*, volume I+II, Tsukuba, 1990, KEK, KEK Report 89-21. 113, 115

[Kowalski 2001]
K. Kowalski, XPS measurements at AGH on EP and BCP samples during 'In-Situ' bakeout, Private communication, 2001. 80, 83

[Krawcyk 1999]
F. Krawcyk, editor, *Proceedings of the 9th Workshop on RF Superconductivity*, volume I+II, Santa Fe, November 1999, LANL. 103, 107, 110, 111, 112, 114, 115, 116, 118

[Lilje et al. 1999]
L. Lilje et al., Electropolishing and in-situ Baking of 1.3 GHz Niobium Cavities, In *Proceedings of the 9th Workshop on RF Superconductivity* [Krawcyk 1999]. 29, 67

[Ma 2000]
Q. Ma, XPS measurements at ANL on EP and BCP samples during 'In-Situ' bakeout, Private communication, 2000. 80, 83

[Matricon and Saint-James 1967]
J. Matricon and D. Saint-James, Superheating fields in superconductors, Phys. Lett., **24A**:241, 1967. 10, 11

[Mittag 1973]
K. Mittag, Kapitza conductance and thermal conductivity of copper, niobium and aluminium in the range from 1.3 to 2.1 K, Cryogenics, p. 94, 1973. 25

[Mühlschlegel 1959]
B. Mühlschlegel, Z. f. Phys., **155**, 1959. 96

[Müller 1988]
G. Müller, Superconducting Niobium in High RF Magnetic Fields, In *Proceedings of the 3th Workshop on RF Superconductivity* [Shepard 1988], pp. 331–358, ANL-PHY-88-1. 20

[Padamsee et al. 1990]
H. Padamsee et al., Superconducting RF activities at Cornell University, In *Proceedings of the 4th Workshop on RF Superconductivity* [Kojima 1990], KEK Report 89-21. 20

[Padamsee et al. 1998]
H. Padamsee, J. Knobloch, and T. Hays, *RF Superconductivity for Accelerators*, John Wiley & Sons, 1998. 3, 9, 22, 27, 47, 60, 91, 123

[Padamsee 1990]
H. Padamsee, editor, *Proceedings of the 1st TESLA WORKSHOP*, Cornell University, 1990, CLNS-90-1029. 14

[Padamsee 2001]
H. Padamsee, The science and technology of superconducting cavities for particle accelerators, Supercond. Sci. Tech., **14**:R28, 2001. 14

[Palmer et al. 1990]
F. L. Palmer, R. Kirby, F. King, and E. L. Garwin, Oxide overlayers and the superconducting rf properties of yttrium-processed high purity niobium, Nuclear Instruments and Methods A, **297**:321 , 1990. 69, 82

[Palmer 1988a]
F. Palmer, Influence of oxide layers on the microwave surface resistance of superconducting niobium, PhD thesis, Cornell University, 1988. 69, 77, 79, 80, 84

[Palmer 1988b]
F. Palmer, Surface resistance of Superconductors - Examples from Nb - O system, In *Proceedings of the 3th Workshop on RF Superconductivity* [Shepard 1988], p. 309, ANL-PHY-88-1. 13

[Palmieri 1997]
V. Palmieri, editor, *Proceedings of the 8th Workshop on RF Superconductivity*, volume I+II, Abano terme, October 1997, INFN. 103, 109, 110, 111, 115, 116

[Pekeler et al. 1995]
M. Pekeler et al., An advanced rotating T-R mapping and its diagnosis of TESLA 9-cell superconducting cavity, in *Proceedings of the Particle Accelerator Conference and International Conference on High Energy Accelerators*, p. 1639, 1995. 22

[Pekeler 1996]
M. Pekeler, Untersuchungen der feldbegrenzenden Mechanismen in supraleitenden Niob-Resonatoren, PhD thesis, Universität Hamburg, August 1996, DESY M 96-16. 22, 24, 47, 48, 49, 50

[Piel 1989]
H. Piel, Superconducting cavities, in *Superconductivity in Particle Accelerators*, edited by S. Turner, p. 149, CERN, May 1989, CERN 89-04. 10, 31

[Piosczyk 1974]
B. Piosczyk, Exerimentelle Untersuchungen an supraleitenden Wendelresonatoren aus Niob im 100 MHz-Bereich, PhD thesis, Universität Karlsruhe, 1974, KFK 1991. 13

[Pippard 1953]
A. B. Pippard, Impurities in superconductors, Proc . Roy. Soc (London), **A203**:98, 1953. 8, 94

[Ponto and Hein 1986]
L. Ponto and M. Hein, Elektropolitur von Niob, Technical Report WUP 86-17, Bergische Universität Wuppertal, 1986. 35, 37

[Proch et al. 1998]
D. Proch, W. Singer, and H. M. Wen, Some Results about RRR Distribution in Nb of Superconducting Cavities for the TESLA Test Facility, TESLA Report TESLA 98-02, DESY, 1998. 60

[Proch 1999]
D. Proch, Which Way to the Frontier? Novel Structures, Materials, and Fabrication Techniques, In *Proceedings of the 9th Workshop on RF Superconductivity* [Krawcyk 1999], Discussion group. 67, 69

[Reece et al. 1995]
C. Reece et al., Performance experience with the CEBAF SRF cavities, in *Proceedings of the Particle Accelerator Conference and International Conference on High Energy Accelerators*, p. 1512, 1995. 14, 28

[Reschke 1995]
D. Reschke, Untersuchungen an 3GHz Niobresonatoren, PhD thesis, Universität Wuppertal, 1995, WUP-DIS 95-5. 13, 28, 78

[Reschke 1997]
D. Reschke, Thermal model calculations for 1,3 GHz TTF accelerator cavities, In *Proceedings of the 8th Workshop on RF Superconductivity* [Palmieri 1997], p. 385. 27, 72

[Reschke 2001]
D. Reschke, Thermal simulations on high RRR niobium, Private communication, 2001. 26

[Röth 1993]
R. Röth, Untersuchungen zu anomalen Verlusten in Niobresonatoren, PhD thesis, Universität Wuppertal, 1993, WUP-DIS 92-12. 34, 35, 52, 54, 78

[Safa et al. 1995]
H. Safa et al., Nb purification by Ti gettering, In *Proceedings of the 7th Workshop on RF Superconductivity* [Bonin 1995], p. 649. 20

[Safa 1997]
H. Safa, High gradients in scrf cavities, In *Proceedings of the 8th Workshop on RF Superconductivity* [Palmieri 1997], pp. 814–821. 35, 65

[Saito and Kneisel 1999]
K. Saito and P. Kneisel, Temperature Dependence of the Surface Resistance of Niobium at 1300 MHz - Comparison to BCS Theory -, In *Proceedings of the 9th Workshop on RF Superconductivity* [Krawcyk 1999]. 12, 13, 84, 94

[Saito et al. 1989]
K. Saito et al., Electropolishing of L-Band cavities, In *Proceedings of the 4th Workshop on RF Superconductivity* [Kojima 1990], pp. 635 – 695, KEK Report 89-21. 36, 42, 60

[Saito et al. 1997a]
K. Saito et al., High accelerating gradients in niobium L-Band cavities, Particle Accelerators, **60**:193, 1997. 33, 63

[Saito et al. 1997b]
K. Saito et al., Superiority of Electropolishing over Chemical Polishing on High Gradients, In *Proceedings of the 8th Workshop on RF Superconductivity* [Palmieri 1997], pp. 759 – 813. 33, 35, 37, 63

[Saito 1999]
K. Saito, Long Term Air Exposure Effect On The Electropolished Surface Of Niobium Superconducting RF Cavity, In *Proceedings of the 9th Workshop on RF Superconductivity* [Krawcyk 1999], p. 270. 76

[Sayagués et al. 2001]
M. Sayagués, F. Krumeich, and J. Hutchison, Solid-gas reactions of complex oxides inside an environmental high-resolution transmission microscope, Micron, **32**:457, 2001. 80

[Schilcher 1995]
T. Schilcher, Wärmeleitvermögen von Niob bei kryogenischen Temperaturen, Diplomarbeit, Universität Regensburg, 1995, TESLA 95-12. 25

[Schmüser 2001]
P. Schmüser, Superconducting energy gap dependence on the magnetic field, Private communication, 2001. 97

[Schulze 1981]
K. K. Schulze, Preparation and Characterization of Ultra-High-Purity niobium, J. Metals, **33**:33, May 1981. 26, 84, 95

[Sciver 1986]
S. Sciver, *Helium Cryogenics*, Plenum Press, 1986. 24

[Sekula and Kernohan 1972]
S. Sekula and R. Kernohan, Superconducting Properties of Vanadium, Phs. Rev. B, **5**:904, 1972. 90

[Sheehan 1966]
T. Sheehan, Phys. Rev., **149**:368, 1966. 96

[Shepard 1988]
K. Shepard, editor, *Proceedings of the 3th Workshop on RF Superconductivity*, volume I+II, Argonne, 1988, ANL, ANL-PHY-88-1. 113

[Silari et al. 1999]
M. Silari, S. Agosteo, J.-C. Gaborit, and L. Ulrici, Radiation produced by the LEP superconducting cavities, Nuclear Instruments and Methods A, **432**:1 , 1999. 28

[Stolzenburg 1996]
C. Stolzenburg, Untersuchung zur Entstehung von Dunkelstrom in supraleitenden Beschleunigungsstrukturen, PhD thesis, Universität Hamburg, Mai 1996. 29

[Sürgers et al. 2001]
C. Sürgers, M. Schöck, and H. Löhneysen, Oxygen-induced surface structure of Nb(110), Surf. Sci., **471**:209, 2001. 82

[Uehara et al. 2001]
Y. Uehara, T. Fujita, M. Iwami, and S. Ushioda, Single NbO nanocrystal formation on low temperature annealed Nb(001) surface, Surf. Sci., **472**:59, 2001. 82

[Varmazis and Strongin 1974]
C. Varmazis and M. Strongin, Inductive transition of niobium and tantalum in the 10 MHz range I. Zero-field superconducting penetration depth, Phys. Rev. B, **10**:1885, September 1974. 91

[Varmazis and Strongin 1975]
C. Varmazis and M. Strongin, Some comments on recent measurements of the penetration depth in niobium, J. Appl. Phys., **46**:1401, March 1975. 91

[Varmazis et al. 1975]
C. Varmazis, M. Strongin, J. Hook, and D. Sandford, Inductive transition of niobium and tantalum in the 10 MHz range II. The peak in the inductive skin depth for T just less then T_c, Phys. Rev. B, **11**:3354, May 1975. 91

[Varmazis et al. 1976]
C. Varmazis, M. Strongin, and Y. Imry, Surface effects at the superconducting phase transition in tantalum and niobium, Phys. Rev. B, **13**:2880, April 1976. 91

[Visentin et al. 1998]
B. Visentin, J. Charrier, and B. Coadou, Improvements of superconducting cavity performances at high gradients, in *Proceedings of the 6th EPAC*, volume III, p. 1885, 1998. 29, 65, 67, 77

[Visentin et al. 1999]
B. Visentin, J. Charrier, B. Coadou, and D. Roudier, Cavity baking: A cure for the high accelerator field Q_0 drop, In *Proceedings of the 9th Workshop on RF Superconductivity* [Krawcyk 1999]. 29, 67, 77, 95, 96

[Visentin et al. 2001]
B. Visentin, J. Charrier, and G. Congretel, Change of RF Superconducting Parameters Induced by Baking on Nb Cavities, in *Proceedings of the PAC2001*, 2001, To be published. 77, 84, 94

[Visentin 2001]
B. Visentin, The role of impurities on the breakdown field, Private communication, 2001. 94

[Waldram 1964]
J. Waldram, Surface Impedance of Superconductors, Adv. Phys., **13**:1, 1964. 8

[Weber et al. 1991]
H. Weber, E. Seidl, C. Laa, E. Schachinger, M. Prohammer, A. Junod, and D. Eckert, Anisotropy effects in superconducting niobium, Phys. Rev. B, **44**:7585, 1991. 90

[Weingarten et al. 1984]
W. Weingarten et al., Electron loading, in *Proceedings of the 2th Workshop on RF Superconductivity*, edited by H. Lengeler, volume I+II, p. 573, Genf, 1984, CERN. 30

[Yogi et al. 1977]
T. Yogi, G. Dick, and J. E. Mercereau, Critical rf Magnetic Fields for some Type-I and Type-II Superconductors, Phys. Rev. Lett., **39**:826, 1977. 11

List of Figures

List of Tables

Acknowledgements

Bedanken möchte ich mich bei allen Kollegen, Freunden und Helfern in allen beteiligten Instituten, die zum Gelingen dieser Arbeit beigetragen haben.

Zuallererst und ganz besonders möchte ich Prof. Dr. Peter Schmüser danken, der mir in allen Phasen der Doktorarbeit als Ansprechpartner zur Verfügung stand. Ohne seine kritische Begleitung, Bereitschaft zu unzähligen Diskussionen und wesentliche Unterstützung in allen Belangen wäre diese Arbeit nicht möglich gewesen.

Durch die Unterstützung des DESY und der dort arbeitenden Kollegen ist ein ganz wesentlicher Teil dieser Arbeit möglich geworden. Für die Hilfe bei der Präparation der Resonatoren und den Messungen an den Kavitäten möchte ich Detlef Reschke, Wolf-Dietrich Möller, Andre Gössel, Denis Kostin, Krzysztof Twarowsky, Michael Lalayan, Guennadi Kreps, Carsten Müller und den Elektronikern, Arne Brinkmann, Jörg Ziegler, Jens Iversen, Svenja Boster und Torsten Büttner aus der Gruppe MHF-SL bedanken. Bei Axel Matheisen und seiner Gruppe MKS3 möchte ich mich für die Hilfe bei den zahlreichen Präparationen der Resonatoren im Reinraum sowie die prompte Hilfe bei mechanischen Problemen bedanken. Rolf Lange und den Kollegen von der Kryogenik möchte ich danken für den Betrieb der Kälteanlage für die Resonatorentests selbst unter schwierigen Umständen. Bei der Vakuumgruppe MVP um Kirsten Zapfe und Georg Wojtkiewicz bedanke ich mich für die sowohl für die Hochtemperaturglühungen als auch für die Ausbackbehandlungen der Resonatoren. Für die Hilfe bei der Bereitstellung des Niobmaterials, der Herstellung der Resonatoren und der Durchführung des ganzen Projekts danke ich Dieter Proch und Martin Leenen. Paul Dieter Gall und Vladimir Gubarev möchte ich für die Hilfe beim Umgang und Einrichten der Datenbank danken. Ingrid Nikodem möchte ich herzlich danken für die Hilfe bei vielen kleinen und größeren administrativen Problemen.

Für die zahllosen hilfreichen Diskussionen zu den Messungen an den Resonatoren möchte ich mich bei Detlef Reschke, Michael Pekeler[1], Matthias Liepe, Jacek Sekutowicz, Wolf-Dietrich Möller, Dieter Proch, Andre Gössel, Axel Matheisen, Rolf Lange, Jürgen Eschke, Waldemar Singer, Siegfried Wolff, Carlo Pagani, Krystof Twarowsky, Denis Kostin, Michael Lalayan und Arne Brinkmann bedanken.

This thesis has allowed me to work within a truly international collaboration where I could learn a lot of things from many people in several laboratories.

Merci à tous mes collegues aux CEA Saclay. En particuliér, je souhaite remercier Bernard Aune qui m'a proposé de faire quelques mesures sur des cavités supra niobium massifs à Saclay. Je souhaite remercier Henri Safa pour m'avoir aidé avec l'organisation de mesure, beaucoup de discussions très intensifes sur les cavités supra et aussi pour son hospitalité. Je remercie également Jean-Pierre Charrier pour ses explications sur les expériences. Je tiens à remercier Bernard Visentin avec qui je pouvais discuter l'effet d'étuvage en détail. Mes remerciments vont aussi à Claire Antoine pour beaucoup de discussions sur l'état de surface de niobium. Que Pierre Bosland soit remercie pour les discussions sur les couches minces de niobium et pour son hospitalité. Merci à Yves Glaser et Jean-Pierre Poupeau pour leur précieuse aide lors des traitements chimiques et pour m'avoir facilité l'accès aux salles blanches du SEA pour le montage des cavités. Jean-Pierre aussi m'a donné les dessins du system de rinçage à haute pression, qui etaient trés valables pour installer une facilité pour les monocellules à DESY. Merci aussi à Michel Bolloré pour avoir facilité les recuits de cavités.

At CERN I would like to thank all the people involved in welding, electropolishing and measuring of the electropolished 1.3 GHz cavities.

The many useful and interesting discussions not only about cavities and physics with Dieter Bloess and Ernst Haebel are gratefully acknowledged. Without their support the results of this thesis would have been quite different. Horst Wenninger's help was crucial to make this project possible.

I would like to thank Enrico Chiaveri and Christoforo Benvenuti for allowing me work within their groups and use the resources which where available and discussing the progress of the project. The welding of the cavities was performed by Bernard Thony, Oliver Aberle and Dominique Deyrail whom I would like to thank also for introducing me into the art of electron-beam welding of cavities. The electropolishing system was set up by Stefan Ehmele, who also brought the high pressure water rinsing at CERN to work again, and Leonel Ferreira, who also studied many samples. Thank you very much!

[1] ACCEL Instruments

The important work of Serge Forel, Guilhelm Preti, Richard Fortin and Alain Lava in the chemistry building is gratefully acknowledged. The support of and the discussions with Alain Lasserre and Jean Guerin were very valuable. Michel Kubly was very helpful in fixing many mechanical problems. The help with the design of the closed electropolishing system by Claude Riuvet, Silvain Girod and Hansuli Preis is gratefully acknowledged. Hansuli's support during the baking with the vacuum people involved and the organization of the cavity transports back and forth between three laboratories was a very important help. The support Albert Insomby and Gabriel Pechaud concerning the cleanroom work was very helpful. I would like to thank also Roberto Losito as he was very important for the setup of the measurement stands for the 1.3 GHz. He also did a lot of the cavity measurements at CERN together Jean-Michel Tessier and Roger Guerin. Thanks!

Without the collaboration of KEK this thesis would not have been possible. I would like Kenji Saito and Eiji Kako very much for the support and their help especially on the electropolishing of nine-cell TESLA cavities. Also, I would thank them for their hospitality during my visits in Japan and introducing me to the japanese way of life. The discussions with Shuichi Noguchi and Yoshishige Yamazaki are gratefully acknowledged. Also the other people working on the 1.3 GHz cavities have made my stay at KEK a very good experience. The friendliness and openness of Nomura Plating is gratefully acknowledged.

Peter Kneisel I would like to thank for the discussions on the superconducting cavities. He also shared some unpublished cavity data with me what I appreciate. Enzo Palmieri I would like to thank for the helpful discussions on spun niobium cavities.

Für die zahlreichen Diskussionen zum Verhalten von supraleitenden Hochfrequenzresonatoren aus Niob möchte ich auch sehr Herrn Dr. habil. J. Halbritter danken. Matthias Kläui möchte ich für die Hilfe bei den AFM Messungen danken. Prof. Dr. K. Scharnberg möchte ich für den Hinweis zur Bean-Livingston Oberflächenbarriere danken. Prof. Dr. J. Kötzler danke ich für die Diskussionen zu den Oberflächenbarrieren aufgrund von Pinning.

Schließlich möchte ich auch die Kaffeerunde erwähnen, die zum Spaß an Physik und dem Rest der Welt wesentlich beigetragen hat. Danke!

Besonders möchte ich vor allem meinen Eltern ein großes Dankeschön sagen. Eure Unterstützung während meines ganzen Studiums war sehr wichtig für mich.

Zum Schluß und ganz besonders danke ich Jeannette für ihr großes Verständnis und auch dafür mir auch immer mal wieder klarzumachen, was wirklich wichtig ist und daß das Leben nicht nur aus hohen Feldstärken und supraleitenden Oberflächen besteht. Ohne Dich wäre ich nicht hier angekommen.